ƒ ‹ F | Œfia‹ ˙'e›ß• |–M^D‹ ª¤s›p e ƒ¤"G‡ł§i

⁄l›p e⁄@:†V fi⁄ ˛O3/UV(' ˛H2O2)‡B†z {§˙„ fił‹ r ˘†£"«ƒ‡
«e‰Ł(¥N" ⁄˘ƒX"«)¥h £‹ ª¤s(3/3)

›p e^ §¡G ªƒX«‹ ›p e

›p e‰ ¸s„¡GNSC94-2211-E-038-001-

ıƒ · ¶¡¡G94 ƒ~08 ⁄°01 ⁄ Ø 95 ƒ~07 ⁄°31 ⁄Ø

ıƒ ‡ ƒ ¡G» O ¥´ ˙⁄j ˙´ ˙¤t

›p e¥ D ø⁄¡HG– i ''

›p e »P⁄H›ß¡G§ ı ' fi ¡ B … B É ¡B»flfl …z

‡ł§i^ «‹¡G§„ ª‡ł§i

‡B†z⁄ ¥Ł¡¡G¥»›p e¥ i ⁄ ‰ ¶‹ d,

⁄⁄ ¥` Œ 95 ƒ~10 ⁄°4 ⁄Ø

Abstract

In water treatment process, the high molecule weight (MW) organic precursors such as humic substances can be removed significantly by the coagulation. However, low-MW organic precursors, i.e., resorcinol, phloroglucinol, and *p*-hydroxybenzoic acid, are not effectively removed by the traditional water treatment process and exhibit high DBP formation potential (DBPFP) during chlorination process. Therefore, the objective in the investigation is intended to evaluate the effect of ozonation of low molecular weight precursors on disinfection by-product (DBP) formation.

The results of the investigation reveal that the destruction of organic precursors by hydroxyl radical exhibits higher DBP formation potential than that by ozone molecule. In the O_3/UV process, the highly hydroxyl radical exposure results in more reduction of DBP formation. The bromate formation concentration increases with increasing ozone dose and reacting time between ozone and bromide. Furthermore, this investigation also focused on aldehyde formation because of its carcinogenic character. According to the carcinogenic risk assessment, the highest and lowest risks were found in the only chlorination process and O_3/UV process, respectively. Therefore, both the ozonation and O_3/UV processes can reduce the DBP formation thereby providing the safety drinking water.

The modified chlorine decay and DBP formation model can predict the chlorine decay and DBP formation data well. In the DBP predictive model, the assumption of the DBP formation corresponded to the second order to chlorine consumption in the rapid reaction and the first order to that in the slow reaction exhibits the high correlation coefficient (good fit) in the study.

Keywords: Low-MW organic precursors, hydroxyl radical, aldehyde, bromate, DBPFP, ozonation, O_3/UV process, risk assessment

″K›n

ƒ b ⁄ ‡ B † z { § ˙ ⁄ ⁄ ¡ A ⁄ j ⁄ ⁄ l ƒ ‡ ‟ « ‰ Ł ¡ A ƒ p » G · ‟«‰Ł¡A,g†‟
ƒ ¡ A ⁄ p ⁄ ⁄ l ƒ ‟«‰Ł¡A,p‟ resorcinol, phloroglucinol, and *p*-hydroxybenzoic acid ƒb¶ † ⁄ B†z
{ §⁄⁄ £ ¥ h£¥Bƒb¥ [· fił‹ r ˉ ª† { , ß ‟ ‟ fił‟«¥ ″ƒ†£ …¶¡Cƒ ƒ„¡A¥ » ‹ ª ¤ ‟ ƒb ‟″
' ß ƒ fl ƒiæ ⁄ ˇ ł ƒ«‡e‰Ł„ fi ł r ‟«¥£ ″ ƒ ¤ ‟…¡C T

‹ ª s †‟ Gª¥ ¡ Ag¥ †Bfiæƒ ¥ fl‟ƒª‡ «e‰ ŁA, ß flfiæ ⁄ l† £ ¥ ″ , ß ‟ ‟ ¥[· fił‹ r ˘
†£‟ « ¡ ƒfb fiæ ¥¥œ { § ˙ ⁄ ¡ ¶q‟″†Bfiæƒ ¥ … ¯ ¶qß fi ˜‟″› §C¥ [· fi ł r‟«‟†¥″
ƒ¤¡ ƒbfl fiæ‡ B † z §˙•⁄ ¡ A ˘Q ″ ¥ƒ¤H • ″ ⁄ l»Pfl fiæ ⁄ ˘ ‡@fi ¶¡‟″…W¥ [ƒ …W¥ [¡C•
⁄ ¯Ø⁄ ⁄ ƒsƒ ‡fi Æfi¡ Afi · Æ»Pƒ,• ˝ ˜¡]HOBr¡ ^‟″⁄ ˘ ‡• | › § C ˝»‟ ″Q¥ƒ¤Cƒ„¥~¡ Aƒ] flfiæ ˘
‡' † £ ¥‟ ″ P ø' ° ‡£‟«‹ ˙ ^ ⁄]¥ O» ‹ ª s ˝ ″«I¡ Cfi › Pø› • I ƒ ⁄ ⁄ ¯ Ø ¡ A‡ ‟' M § C
‟″› • I⁄ § Oo¥ ″ƒb‡ ¿W¥ { § ˙ ' Mfl fiæ ¥¥œ { § ˙ ⁄ ƒ¡ ƒ„¡ Afl fiæ»Pfl fiæ ¥¥œ § ˙ ¥ ¡
⁄ fi ł ‹ r ˘‟‡«‟ ″ ¥ƒ¤A ´ ˙ ƒ„ · £ ¤ ƒ w ¥ ⁄ § ¶¡ C¥ ¸

¥ › ¥¿⁄ §„ w · œ ¥fi¥ H ″ •ƒa„ wœ· ‟fił ' M¥ [· fi ł r‟«‟†£ ¥ƒ¤ C ƒƒ¥b [· fił‹ r
‡£‟«‟″„ w · œ ⁄ ƒ¡ A ‡]fi ł ‹ r ˘‟‡«‟ ″ ¥ƒƒbS ⁄ ˘ ‡‹ Ofl · ¶q‟″⁄ Gƒ,⁄ ˘ ‡¡ Ab″C⁄ ˘ ‡‹ O
fl · ¶q‟″⁄ @ƒ,⁄ ˘ ‡fi ¡ A‹ ^ ' ° « ‟‹ O¤ ƒn‟″„ w · œ ¡ƒC¡

^ ` ƒr: ⁄ p ⁄ ł ƒ«‡e‰Ł¡ F†Bfiæƒ ¥ ¡ F ^ ¡ F• ″ ˝ ˘ ¡ Ffi ł ‹ r ˘‟‡«¥ ″ ƒ ¤ ¡ ¶Ffl fiæ ⁄ ˘ {
§ ˙ ¡ Ffl fiæ ¥¥œ § ˙ ¡ F› • I ƒ

Contents

Abstract.....I

″ Kn.....II

Contents.....III

List of Figures.....V

List of Tables.....VII

I Introduction.....8
II Objective.....8
III Literature Review.....9
3-1 Organic Precursors.....9
3-2 Ozonation and DBP Formation.....9
3-2-1 Ozonation.....9
3-2-2 Free Radicals Scavenger.....13
3-2-3 Ozonation By-Products.....13
3-3 Methods for Hydroxyl Radical Determination.....19
3-4 Chlorination and DBP Formation.....20
3-5 Predictive Model of Chlorine Decay and DBP Formation.....21
IV Materials and Method.....24
4-1 Research flowchart.....24
4-2 Materials.....25
4-2-1 Apparatus.....25
4-2-2 Organic Precursors.....26
4-3 Methods.....26
4-3-1 Experimental Design.....26
4-3-2 Unit Process.....28
4-3-3 Analytical Method for Traditional Method.....31
4-3-4 Analytical Method for DBPs.....32
4-3-5 Hydroxyl Free Radical.....37
4-3-6 Residual ozone.....37
4-3-7 Hydrogen peroxide.....38
V Results and discussion.....39
5-1 Ozonation and O3/UV Processes.....39
5-1-1 Ozonation Process at Different pH Levels.....39
5-1-2 Effect of Alkalinity On Ozonation.....43
5-1-3 Development of Hydroxyl Radical Formation Model.....45
5-1-4 O_3/UV Process.....47
5-1-5 Ozonation (O_3/UV) of Organic Precursors in terms of TOC and UV_{254}.....48
5-1-6 Formation of Ozonation By-products.....50
5-2 The bromate formation in ozonation process.....51

5-2-1 Effect of bromide concentration on bromate formation 51
5-2-2 Effect of ammonia concentration on bromate formation 55
5-3 Chlorine Demand and Chlorine Decay Model 59
5-3-1 Chlorine Demand 59
5-3-2 Chlorine Decay Model 62
5-4 DBP Formation and Predictive Model 62
5-4-1 THM formation 62
5-4-2 HAA formation 67
5-4-3 DBP formation 68
5-4-4 Predictive DBP Formation Model 74
5-5 Comparison of DBPs Formations between with and without ozonation and O_3/UV processes 77
5-5-1 Chlorine Consumption 77
5-5-2 Chlorination Disinfection By-Products Formation 81
5-5-3 Risk Assessment 82
VI Conclusions 85

List of Figures

Figure 3.2.1 Mechanism of ozonation of aromatic ring with — OH group..... 11
Figure 3.2.2 Reaction of hydroxyl radical with organic pollutant (P) leading to a great diversity of oxidized compounds. P: pollutant; Pi: i species of P; oxid: oxidized compounds; NOM: natural organic matter (Hoginé, 1998). 12
Figure 3.2.3 Reaction of O_3 with Br^- and OBr^- in aqueous solutions. 16
Figure 3.2.4 Reaction of bromate formation during ozonation in bromide-containing waters: (a) reactions with ozone (b) reactions with ozone and OH radicals. (von Gunten, 1994) 17
Figure 3.2.5 The oxidation mechanisms of molecular ozone and OH radical. The OH radical oxidation mechanism includes reactions of secondary oxidants as CO_3^- and Br_2^- (von Gunten and Hoigné, 1994). 18
Figure 3.2.6 Bromate formation during ozonation in the presence of ammonia (Pinkernell and von Gunten, 2001)..... 18
Figure 4.3.1 Flowchart of experiments to determine the ozone reaction mechanism and aldehyde formation concentrations in ozonation and O_3/UV processes..... 29
Figure 4.3.2 Flowchart of experiments to determine the residual chlorine, THMs, and HAAs concentrations at various chlorine contact times 30
Figure 4.3.3 The experimental apparatus of the ozone batch reactor: 31
Figure 5.1.1 The ozone decomposition and predictive decay model at different pH levels 40
Figure 5.1.2 The difference in hydroxyl radical formation at pH 7 and 9 in ozonation process 41
Figure 5.1.3 The relationship between ozone and hydroxyl radical concentration at pH 7 and 9 in ozonation process 42
Figure 5.1.4 The formation of H_2O_2 in ozonation process at different pH levels 42
Figure 5.1.5 Alkalinity changes at various pH levels in the ozonation process 43
Figure 5.1.6 The difference in hydroxyl radical at different pH levels by ozonation process 44
Figure 5.1.7 Correlation of the residual alkalinity ratio and the hydroxyl radical concentration during the ozonation process. 44
Figure 5.1.8 The correlation between hydroxyl radical exposure and residual alkalinity ratio at pH 9. .. 44
Figure 5.1.9 The hydroxyl radical formation concentration and predictive model at pH 9 in ozonation. 46
Figure 5.1.10 The hydroxyl radical formation concentration and predictive model at pH 7 in ozonation. 46
Figure 5.1.11 The measured concentration of dissolved ozone and the hydroxyl radical during the O_3/UV process..... 47
Figure 5.1.12 The difference in hydroxyl radical between the ozonation and the O_3/UV processes..... 47
Figure 5.1.13 Decreasing of TOC at various levels of pH and alkalinity in the ozonation and O_3/UV processes for three model compounds. 49
Figure 5.1.14 Reducing of UV254 at various levels of pH and alkalinity in the ozonation and O3/UV processes for three model compounds 49

Figure 5.1.15 SUVA measured at various levels of pH and alkalinity for model compounds treated by the ozonation and O_3/UV processes 50
Figure 5.1.16 The formation of aldehyde for resorcinol, phloroglucinol, and *p*-hydroxylbenzoic acid at the different levels of pH and alkalinity in the ozonation and O_3/UV processes 52
Figure 5.1.17 Correlation between hydroxyl radical and aldehyde formation concentration for three model compounds 53
Figure 5.1.18 Comparison of total aldehyde concentration among three model compounds 53
Figure 5.2.1 The bromide reduction at different levels of bromide concentrations in the ozonation process 54
Figure 5.2.2 Effect of bromide concentration on bromate formation in the ozonation process 54
Figure 5.2.3 The relationship between bromide reduction and bromate formation 55
Figure 5.2.4 The reduction of ammonia concentration at 9.0 mg/L of ozone dose 56
Figure 5.2.5 The reduction of ammonia concentration at 7.0 mg/L of ozone dose 56
Figure 5.2.6 Effect of ammonia concentration on bromide reduction at 9.0 mg/L of ozone dose 56
Figure 5.2.7 Effect of ammonia concentration on bromide reduction at 7.0 mg/L of ozone dose 57
Figure 5.2.8 Effect of ammonia concentration on bromate formation at 9.0 mg/L of ozone dose 58
Figure 5.2.9 Effect of ammonia concentration on bromate formation at 7.0 mg/L of ozone dose 58
Figure 5.3.1. The measured residual chlorine concentration for resorcinol, phloroglucinol, and *p*-hydroxybenzoic acid at various reaction times 60
Figure 5.3.2 Correlation between pH and chlorine demand 61
Figure 5.4.1 THM formation for resorcinol, phloroglucinol and p-hydroxybenzoic acid pretreated by ozonation at different level of pH and alkalinity, and O_3/UV processes 65
Figure 5.4.2 HAA formation for resorcinol, phloroglucinol and p-hydroxybenzoic acid pretreated by ozonation at different levels of pH and alkalinity, and O_3/UV processes 69
Figure 5.4.3 DBP formation for resorcinol, phloroglucinol, and p-hydroxybenzoic acid pretreated by ozonation at different levels of pH and alkalinity, and O_3/UV process 72
Figure 5.4.4 Correlation between DBP formation and pH (chlorine consumption) 73
Figure 5.4.5 Comparison of the measured and predictive THM formation concentration for resorcinol, phloroglucinol and p-hydroxybenzoic acid in the predictive model 78
Figure 5.4.6 Comparison of the measured and predictive HAA formation concentration for resorcinol, phloroglucinol and p-hydroxybenzoic acid in the predictive model 79
Figure 5.4.7 Comparison of the measured and predictive DBP formation concentration for resorcinol, phloroglucinol and *p*-hydroxybenzoic acid in the predictive model 80
Figure 5.5.1 Comparison of aldehyde and DBP formation for resorcinol 83
Figure 5.5.2 Comparison of aldehyde and DBP formation for phloroglucinol 84
Figure 5.5.3 Comparison of aldehyde and DBP formation for p-hydroxybenzoic acid 84

List of Tables

Table 3.2.1 Main reaction involving carbonate species in water during the hydroxyl radical formation process 14
Table 3.2.2 Bromine species formed during bromate formation, oxidation states and important oxidants. 16
Table 4.2.1 Summary of the physical/chemical properties for organic compounds 27
Table 4.3.1 The experimental design in the ozonation/chlorination processes 28
Table 5.1.1 Ozone decomposition constants for parallel first order reaction at different pH levels 40
Table 5.1.2 Hydroxyl radical formation kinetics constants at pH 7 and 9 in ozonation 46
Table 5.1.3 Analysis of variance (ANOVA) — F test for aldehyde formation 53
Table 5.3.1 Analysis of variance (ANOVA) — F test for chlorine demand 61
Table 5.3.2 Chlorine decay constants for parallel first and second order reaction 63
Table 5.3.3 Deviation between the experimental data and predictive model 64
Table 5.4.1 Summary of THM formation of three model compounds pretreated by ozone 66
Table 5.4.2 Analysis of variance (ANOVA) — F test for THM formation 67
Table 5.4.3 Summary of HAA formation of model compounds pretreated by ozone 70
Table 5.4.4 Analysis of variance (ANOVA) — F test for HAA formation 70
Table 5.4.5 Summary of DBP formation of three model compounds pretreated by ozone 71
Table 5.4.6 Analysis of variance (ANOVA) — F test for DBP formation 73
Table 5.4.7 Parameters of the THM predictive model for the model 76
Table 5.4.8 Parameters of the HAA predictive model for the model 76
Table 5.4.9 Parameters of the DBP predictive model for the model 77
Table 5.5.1 Comparison of chlorine consumption for three model compounds 81
Table 5.5.2 Comparison of DBPFP for three model compounds 82
Table 5.5.3 The comparison in D during chlorination 82
Table 5.5.4 The carcinogenic risk in different treatment processes 85

I Introduction

Low-molecular weight organic matters, such as resorcinol, phloroglucinol, and *p*-hydroxybenzoic acid, are considered organic precursors with high DBPs formation potential in the chlorination process. However, the removal efficiency of these low molecular organic matters is insignificant in the traditional water treatment process, such as coagulation. Ozone is a strong oxidant which has been used in water and waste water industries for pathogen control. Taiwan began using ozone for water treatment in 2004.

In order to decrease the THMs and HAAs formation in the chlorination process, ozonation process is employed as an alternating method in the European and American countries. Reports indicate that ozone is effective in reducing THMs and HAAs formation because of its strong oxidative ability. Further, ozone can decompose itself to form hydroxyl radical which is a strong oxidant. However, ozone may produce DBPs while reacting with organic and inorganic matters in water. Bromate, aldehydes, and other DBPs were found and investigated during the ozonation process. The USEPA promulgated drinking water standards to regulate DBPs, and requires that maximum contaminant levels (MCLs) for bromate must be less than 0.01 mg/L. With the above controversy, this study is intended to combine pre-ozonation (O_3/UV) and chlorination technology to achieve the purpose of reducing DBPs formation.

II Objective

1. Determine the hydroxyl radical formation in ozonation and O_3/UV processes and evaluate the effects of hydroxyl radical and ozone molecule on the removal of organic precursor and on the DBP formation.
2. Evaluate the inhibition of alkalinity on indirect ozonation process.
3. Develop the ozone decay model and hydroxyl radical formation model.
4. Assess the effects of bromide and ammonia on bromate formation and develop the bromate formation model.
5. The difference of the chlorine decay rate and DBPs formation potential between pre-ozonation (O_3/UV) and coagulation process was assessed.
6. The predictive model for determining chlorine decay, and THMs and HAAs formation was developed for combining pre-ozonation (O_3/UV) and chlorination.

III Literature Review

3-1 Organic Precursors

The dominant organic precursors of THM formation in the water environment would be considered the aquatic NOMs, mainly consist of humic substance (Bocye et al., 1983 Rook et al., 1976). Therefore, numerous investigators have demonstrated that the THMs formation is due to humic substance in aqueous solution. The components of NOM could be divided into hydrophilic and hydrophobic groups. Marhaba and Van (2000) have found that hydrophilic acid contributes most of THM formation and hydrophobic neutral fraction is related to HAA formation.

Recently, because the aquatic humic substances are complicate by their uncertain structure, many studies have focused on the reaction of chlorine with simple organic species in humic substance. It had been reported that aliphatic carboxylic, hydroxybenzoic acid, phenol, and pyrrole nitrogen derivatives were the main functional group observed in these model compounds such as resorcinol, phloroglucinol, and *p*-hydroxybenzoic acid (Richardson et al., 1999; Bocye et al., 1983).

Some parameters such as total organic carbon (TOC), ultraviolet (UV) absorbance, and specific ultraviolet absorbance (SUVA) are commonly application to representation for water quality and assessment of disinfection by-product formation. SUVA is a ratio of ultraviolet absorbance (UV_{254}) to the concentration of TOC in water, i.e., UV_{254} (m^{-1})/TOC (mg/L) and is commonly used to indicate the nature and molecular weight distribution of NOMs, and the component of natural water exhibit the high $SUVA_{254}$, e.g., ¡ 4 L/mg-m (Edzwald and Tobiason, 1999; Karanifil et al., 2002). According to the Reckhow (1990) study, the value of SUVA is corresponded to dissolved organic matter (DOM) reactivity and DBP formation. Therefore, it was reported that the high SUVA results in more DBP formation (Kitis et al., 2001).

3-2 Ozonation and DBP Formation

3-2-1 Ozonation

Overall ozone consumption during the ozonation process is caused by its autocatalytic self-decomposition and other complex reactions including direct (ozone) and indirect (hydroxyl radical) ozone process, which are affected by different pH levels (Paul et al., 1998; Daniel et al., 1999; von Gunten, 2003(a)). The ozone self-decomposition reaction was reported as different orders (n) of reaction ranging from 0 to 2 shown in Equation 3.2.1 (Slawomir et al., 1999). The representation of an ozone consumption rate r_{O_3} was expressed as follows:

$$-r_{O_3} = \frac{d[O_3]}{dt} = K_D[O_3]^n \qquad (3.2.1)$$

Where

K_D: ozone self-decomposition coefficient

$[O_3]$: concentration of ozone

n: the number of reaction order

According to Yurteri and Gurol study (1988), the reasonable value of the self-decomposition coefficient (K_D) at pH 7 is between 0.16 and 0.36.

In the reaction between NOMs and ozone, the reaction rates for individual compounds were reported as first order with respect to the concentrations of ozone ($[O_3]$) and organic matter ([M]) shown in Equation 3.2.3 (Langlais et al., 1991).

$$-\frac{d[M]}{dt} = k[O_3][M] \qquad (3.2.2)$$

Organic compounds react with ozone molecules, in addition to hydroxyl radical generated by the decomposition of ozone at different operation condition. The reaction mechanism can be summarized by four main reactions listed below (Guittonneau et al., 1996):

$$M_d + O_3 \xrightarrow{k_1} products + O_2 + H_2O_2 \qquad (3.2.3)$$

$$M_i + O_3 \xrightarrow{k_2} \cdot OH \qquad (3.2.4)$$

$$M_p + \cdot OH \xrightarrow{k_3} products + O_2^- \cdot \qquad (3.2.5)$$

$$M_s + \cdot OH \xrightarrow{k_4} products \qquad (3.2.6)$$

This reaction mechanism mainly involves direct ozone reaction (M_d), initiator matter reaction (M_i), promoter matter reaction (M_p) and scavenger matter reaction (M_s). According to these equations, the Equation 3.2.3 could be rewritten as Equation 3.2.8.

$$-\frac{d[M]}{dt} = (k^* + k^{**}\Psi)[O_3][M] = k[O_3][M] \qquad (3.2.7)$$

Where

$$k^* = k_1 + k_2$$

$$k^{**} = k_3 + k_4$$

$$[\cdot OH] = \Psi[O_3] \quad (\Psi = \frac{\sum_i k_{2i}[M_i] + 2k_1'[OH^-]}{\sum_i k_{si}[M_{si}]})$$

Where k_1' is the initial reaction constant with ozone and hydroxyl radical; k_{si} is the reaction constant with hydroxyl radical and its scavenger.

Direct Ozone Process

At acidic condition, the predominance of ozonation is due to molecular ozone (Wei Chu et al., 2000). It was reported that ozone preferentially oxidizes electron-rich portions such as carbon-carbon double bonds and aromatic alcohols (Paul et al., 1998). Due to the electronic configuration, ozonation reaction can be divided into two categories: cycloaddition and substitution reactions.

The different substituting groups in the aromatic molecule would strongly affect the reactivity of the aromatic structure with electrophilic agents (such as ozone molecule). Thus, the different substituting groups would activate or deactivate the aromatic ring in the electrophilic substitution reaction. Generally, the activating groups promote the substitution of hydrogen atoms from their ortho- and pata- positions, but the deactivating groups promote the substitution in the meta-positions (Fernando, 2004).

The aromatic ring with 2-OH and 3-OH phenolic groups under the attack of ozone would lead to ring cleavage and to the formation of organic products such as formic acid, C_2-C_6 dicarboxylic acid, and aldehyde shown in Figure 3.2.1 (Gilbert, 1978).

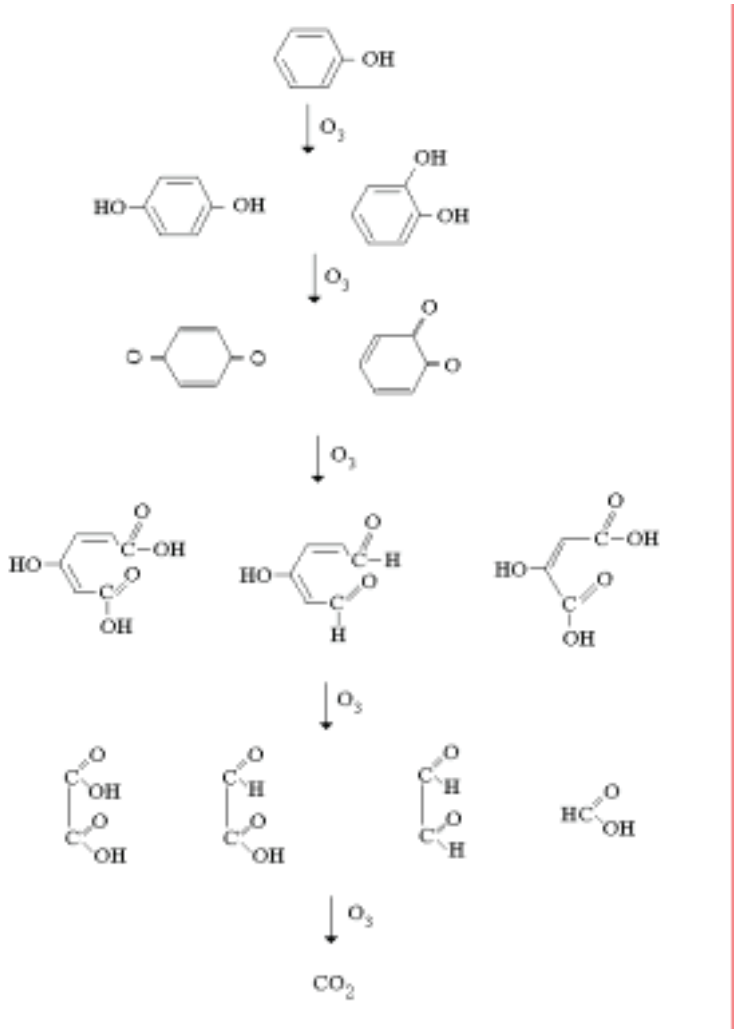

Figure 3.2.1 Mechanism of ozonation of aromatic ring with — OH group.

Indirect Ozone Process

At higher pH, ozone reacts with hydroxyl ions (OH^-) as a catalyst and yields many kinds of free radicals such as $^{\cdot}OH$, $O_2^{-\cdot}$, and $HO_2^{-\cdot}$ etc., which is called indirect ozone process. The most commonly reported radicals in indirect ozone process was hydroxyl free radical ($^{\cdot}OH$) (Staehelin and Hoigné, 1982). The characters of higher oxidative ability and nonselective reaction property result in a faster reaction rate and a higher removal efficiency of organic matters by ozonation.

The substitution and addition reaction in the reaction of ozone with aromatic ring are found in direct ozone process. But because of the nonselective attack of hydroxyl radical the reaction of hydroxyl radical with aromatic ring is random. The aromatic ring with —OH groups under the attack of hydroxyl radical would lead to ring cleavage and to the formation of organic products such as formic acid, C_2-C_6 dicarboxylic acid, and aldehyde (Gilbert, 1978). The reaction between hydroxyl radical and organic compounds could be divided into three different mechanisms including hydroxyl addition, hydrogen abstraction and electron transfer (Huang et al., 1993) shown in Figure 3.2.2.

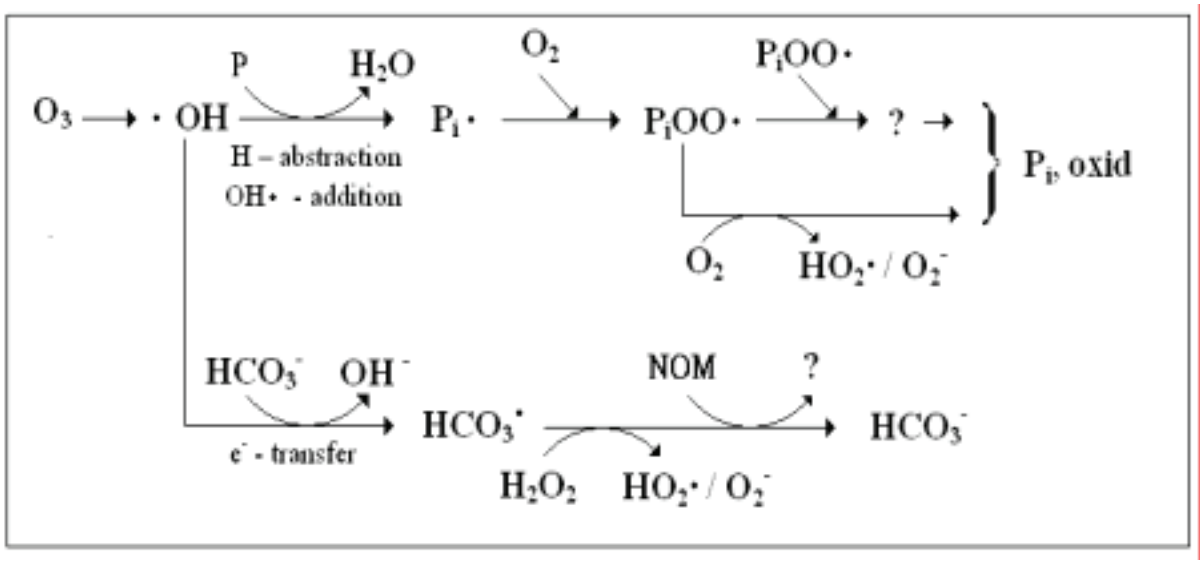

Figure 3.2.2 Reaction of hydroxyl radical with organic pollutant (P) leading to a great diversity of oxidized compounds. P: pollutant; Pi: i species of P; oxid: oxidized compounds; NOM: natural organic matter (Hoginé, 1998).

O_3/UV Process

The advanced oxidative processes (AOPs) are an oxidative process based on the generation of powerfully reactive and oxidative free radical, especially hydroxyl radicals. These free radicals are highly effective for removing refractory organics from water and wastewater (Patrik et al., 2000; Tezcanli-Guyer and Ince, 2004). Generally, the advanced oxidation processes (AOPs) induced free radicals reaction including the use of ultraviolet light (UV) in the presence of hydrogen peroxide (H_2O_2) and ozone, fenton's reagent and a semi-conductor surface (Keiichi et al., 1996; N.H. Ince et al., 1999). Recently, ozone and other AOPs, such as O_3/UV process, have been investigated to reduce the total organic carbon (TOC) concentration and trihalomethane

formation potential (THMFP) in raw source water (Amirsaedari et al., 2000; Chin and Bérubé, 2005).

The reaction mechanism of O_3/UV system is represented as follows (Mirat and Vasistas, 1987):

$$O_3 + H_2O + h\nu \rightarrow H_2O_2 + O_2 \quad (3.2.8)$$

$$H_2O_2 + h\nu \rightarrow 2(\cdot OH) \quad (3.2.9)$$

According to Equations 3.2.8 and 3.2.9, the UV illumination transforms ozone completely into the hydroxyl radicals. In principle, the amount of the hydroxyl radical formed in the O_3/UV system is more than that of the indirect ozone process. As a result, the oxidative ability and removal efficiency of NOMs by the O_3/UV process are both higher than these of the indirect ozone process.

3-2-2 Free Radicals Scavenger

In the O_3/UV or indirect ozone process, the formation of hydroxyl free radicals is the predominant mechanism. There are some species which are inhibitors of O_3/UV or indirect ozone process would terminate the radical chain reaction. These inhibitors, i.e. free radical scavenger, include *tert*-butanol, *p*-chlorobenzoate, carbonate, and bicarbonate ions or some humic substances, which could limit and inhibit the hydroxyl radical formation resulted in reducing the performance of ozonation (Jan et al., 1998; Staehelin et al., 1984).

Among those free radicals scavengers, the commonly found scavengers in natural water are carbonate and bicarbonate ions, which are main components of forming alkalinity and are also called “natural scavengers” (Fernando, 2004).

In the presence of carbonate and bicarbonate ions, the hydroxyl radicals react with these species and yield inactive carbonate and bicarbonate ion radicals ($CO_3^{\cdot-}$ and $HCO_3^{\cdot-}$) in the hydroxyl radical formation process shown in Table 3.2.1. The main reaction involving carbonate species in water during the radical formation process is shown in Table 3.2.1.

3-2-3 Ozonation By-Products

Aldehyde

In order to reduce the THMs and HAAs formation in chlorination, ozonation process can be introduced before chlorination to remove DBP precursors. But many studies were also conducted to investigate the concern of the DBP formation during ozonation process including aldehyde, ketones, ketoaldehydes, carboxylic acids, aldo acids, keto acid, hydroxyl acids, esters, and alkanes (Miltner et al., 1992; Schechter and Singer, 1995; Richardson SD et al., 1999). Among these by-products, aldehyde is the mostly concerned and investigated because it is harmful and carcinogenic to human beings.

Table 3.2.1 Main reaction involving carbonate species in water during the hydroxyl radical formation process

Reaction	Rate Constant	Reaction No.
$HCO_3^- + HO\cdot \rightarrow HCO_3\cdot + OH^-$	8.5×10^6 $M^{-1}sec^{-1}$	3.2.10
$CO_3^{2-} + HO\cdot \rightarrow CO_3^-\cdot + H^+$	4.2×10^8 $M^{-1}sec^{-1}$	3.2.11
$HCO_3^- \rightarrow H^+ + CO_3^{2-}$	2.2 sec^{-1}	3.2.12
$CO_3^{2-} + H^+ \rightarrow HCO_3^-$	5×10^{10}	3.2.13
$H_2CO_3 \rightarrow H^+ + HCO_3^-$	2.25×10^4	3.2.14
$HCO_3^- + H^+ \rightarrow H_2CO_3$	5×10^{10}	3.2.15
$HCO_3\cdot \rightarrow CO_3^-\cdot + H^+$	500 sec^{-1}	3.2.16
$CO_3^-\cdot + H^+ \rightarrow HCO_3\cdot$	5.0×10^{10} $M^{-1}sec^{-1}$	3.2.17
$CO_3^-\cdot + H_2O_2 \rightarrow HCO_3^- + HO_2\cdot$	4.3×10^5 $M^{-1}sec^{-1}$	3.2.18
$CO_3\cdot + HO_2^- \rightarrow CO_3^{2-} + HO_2\cdot$	5.6×10^7 $M^{-1}sec^{-1}$	3.2.19
$CO_3^-\cdot + O_2^-\cdot \rightarrow CO_3^{2-} + O_2$	7.5×10^8 $M^{-1}sec^{-1}$	3.2.20
$CO_3^-\cdot + O_3^-\cdot \rightarrow CO_3^{2-} + O_3$	6.0×10^7 $M^{-1}sec^{-1}$	3.2.21
$CO_3^-\cdot + B \rightarrow CO_3^{2-} + products$		3.2.22

According to Schechter and Singer study (1995), the hydrophobic organic matters exhibit higher aldehyde formation potential than hydrophilic matters in ozonation. Generally, the common aldehydes found in ozonation are including formaldehyde, acetaldehyde, glyoxal, and methyl glyoxal (Weinberg et al., 1993; Gracia et al., 1996). It has been reported that the order of aldehyde formation concentration in the reaction between ozone and organic matter is: formaldehyde > glyoxal > acetaldehyde > methyl glyoxal > C_3-C_{10} monoaliphatic aldehyde (Weinberg and Glaze, 1996).

The formation of aldehyde is caused by the reaction between ozone and the unsaturated organic matters in ozonation. The formation mechanism is via the additional reaction on unsaturated bonds of organic matters as shown in Equation 3.2.23.

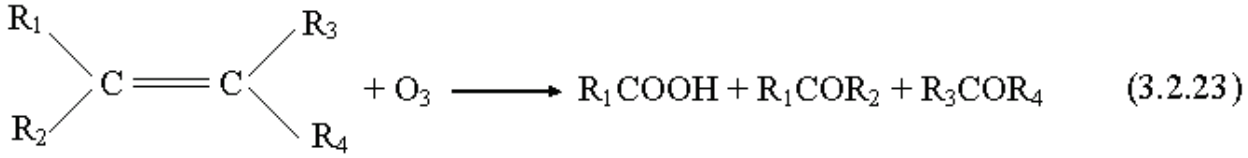

Two important factors affecting the aldehyde formation in ozonation process are pH and TOC. According to Equation 3.2.23, treated water in the presence of higher TOC would result in more aldehyde formation. In addition, the high pH induces the hydroxyl radical formation, and aldehyde is further oxidized to corresponding organic acids such as acetic acid and oxalic acid, which reduces the aldehyde concentration during the ozonation process (Weinberg et al., 1993). For instance, the further oxidation of methyl glyoxal and glyoxal acid could result in the formation of pyruvic acid and oxalic acid, respectively shown in Equations 3.2.24 and 3.2.25. Therefore, the aldehyde decreases with the increasing pH. Moreover, the presence of inorganic carbon and bromide would not affect the aldehyde formation in ozonation.

$$CH_3COCHO + \cdot OH \rightarrow CH_3COCOOH \qquad (3.2.24)$$

$$OHCCOOH + \cdot OH \rightarrow HOOCCOOH \qquad (3.2.25)$$

Bromate

Bromate formation has been of great concern since bromate was classified as a potentially carcinogenic by the IARC (International Agency for the Research on Cancer) (WHO, 1990). Bromate is formed in the ozonation process from the oxidation of bromide through a combination of O_3 and OH radicals (Legube et al., 2004). The mechanism for bromate formation includes both molecular ozone (Haag and Hoigné, 1983) and OH radical reactions, where OH radicals are formed from the natural ozone decomposition in aqueous solutions (von Gunten et al., 1994; von Gunten et al., 1998). Table 3.2.2 shows the bromate formation during ozonation of bromide-containing waters. This process includes up to six oxidation states of bromine (von Gunten, 2003 (b)).

Haag and Hoigné (1983) were the first to investigate the oxidation of bromide during the ozonation processes. Further, Haag and Hoigné (1983) studied the bromate formation mechanism which involved the reaction of O_3 with Br^- and OBr^- in aqueous solutions. Figure 3.2.3 shows the results of this study relating to the reaction of ozone with Br^- and OBr^-. von Gunten (2003 (b)) also studied bromate formation by using different approaches. The first approach involved the reaction of bromate with ozone, and the other approach involved the reaction of bromate with ozone and OH radicals. The oxidation of bromide by ozone in the first approach involved an oxygen atom transfer to produce hypobromite (Figure 3.2.4 a). The second approach involved an extended reaction which included direct ozone reactions and secondary oxidants (OH radicals and carbonate radicals) (Figure 3.2.4 b).

Table 3.2.2 Bromine species formed during bromate formation, oxidation states and important oxidants.

Species	Chemical formula	Oxidation state	Controlling oxidizing species
Bromide	Br^-	-I	$O_3, OH\cdot$
Bromine radical	$Br\cdot$	0	O_3
Hypobromous acid	$HOBr$	+I	$OH\cdot$
Hypobromite	OBr^-	+I	$O_3, OH\cdot, CO_3^-\cdot$
Bromine oxide radical	$BrO\cdot$	+II	
Bromite	BrO_2^-	+III	O_3
Bromate	BrO_3^-	+V	

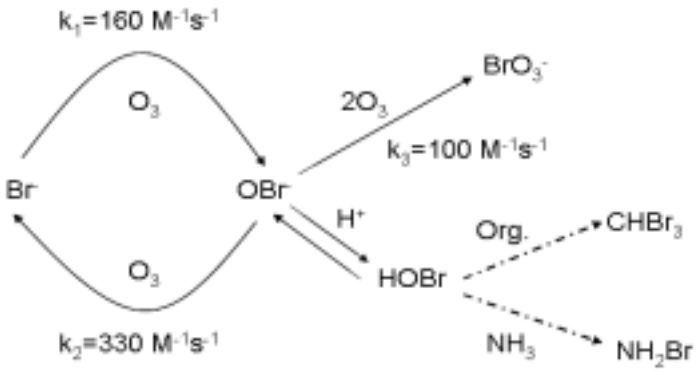

Figure 3.2.3 Reaction of O_3 with Br^- and OBr^- in aqueous solutions.

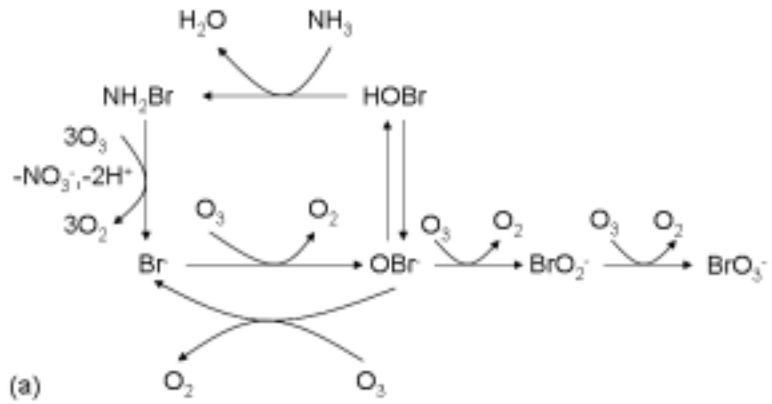

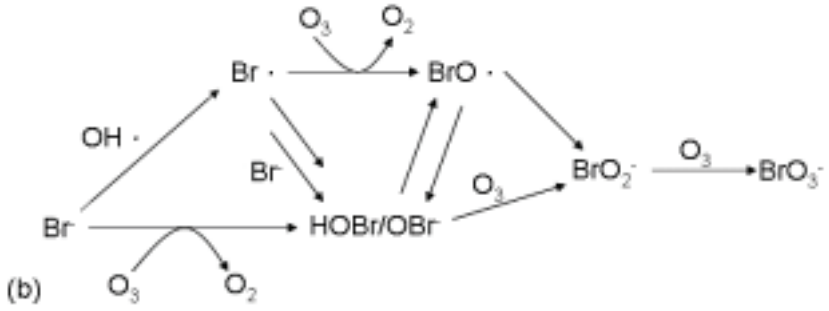

Figure 3.2.4 Reaction of bromate formation during ozonation in bromide-containing waters: (a) reactions with ozone (b) reactions with ozone and OH radicals. (von Gunten, 1994)

There are many factors affecting bromate formation-including pH, Br^- concentration, ozone residual concentration, ammonia, Cτ(ozone concentration and contact time), OH radicals, alkalinity, and NOM. The oxidation mechanisms of ozone and OH radical are shown in Figure 3.2.5 and the bromate formation with ammonia are shown in Figure 3.2.6. The factors affecting bromate formation are explained below:

(1) pH

Previous studies indicate that most OH radicals are formed in high pH and most ozone molecules are formed in low pH. Reaction 3.2.37 is independent of pH, but the overall rates of reactions 3.2.38 and 3.2.39 decreases with decreasing pH because of the masking of hypobromite through protonation. Only 1-10% of $[HOBr]_{tot}$ (in the form of OBr^-) takes part in reactions with molecular ozone. (von Gunten et al., 1994)

$$O_3 + Br^- \rightarrow O_2 + OBr^- \quad (3.2.37)$$

$$O_3 + OBr^- \rightarrow 2O_2 + Br^- \quad (3.2.38)$$

$$O_3 + OBr^- \rightarrow BrO_2^- + O_2 \quad (3.2.39a)$$

$$O_3 + HOBr \rightarrow BrO_2^- + O_2 + H^+ \quad (3.2.39b)$$

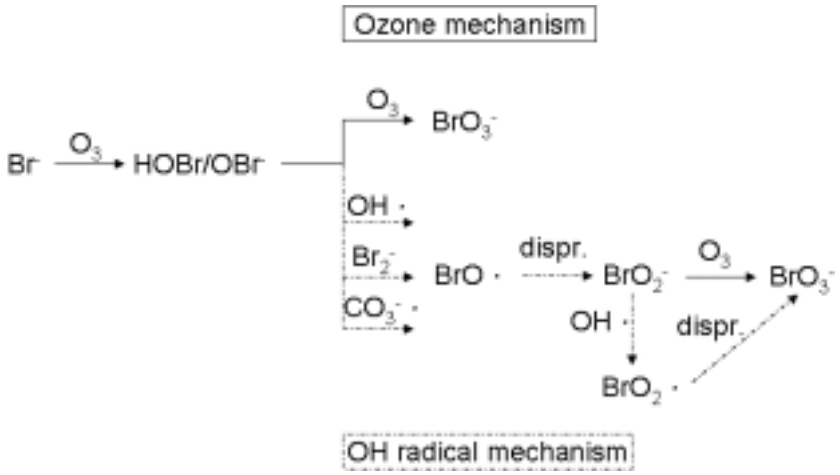

Figure 3.2.5 The oxidation mechanisms of molecular ozone and OH radical. The OH radical oxidation mechanism includes reactions of secondary oxidants as CO_3^- and Br_2^- (von Gunten and Hoigné, 1994).

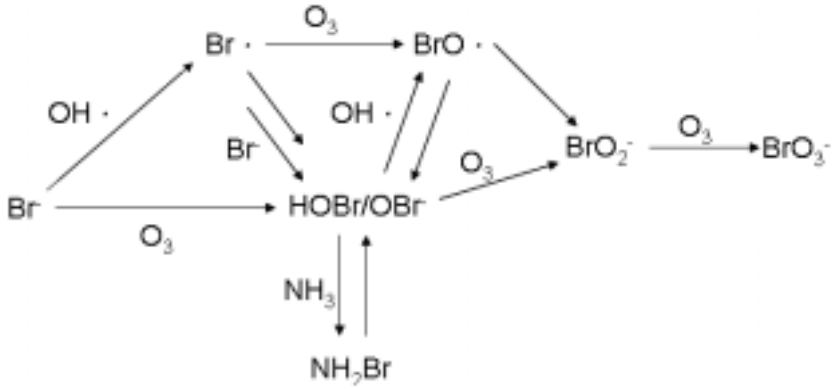

Figure 3.2.6 Bromate formation during ozonation in the presence of ammonia (Pinkernell and von Gunten, 2001).

(2) Ammonia

The presence of ammonia during the ozonation process reduces the formation of bromate. In general, source water often contains low ammonia concentration. Therefore, many scholars discuss and experiment on the level of ammonia concentration affecting bromate formation. (von Gunten et al., 1994; Song et al., 1997)

To treat ozonated drinking water with ammonia to form bromamine (NH_2Br) is a good strategy (Haag and Hoigné, 1985; Siddiqui et al., 1995). In principle, the addition of ammonia prevents bromate formation by two pathways: First, ammonia reacts with OH radicals (OH radicals are formed from ozonation) at a faster rate than bromide, thus minimizing the formation of OBr^-. Second, when the bromide-containing water is treated with ozone, free available bromine (FAB) species such as bromine, hypobromous acid, and hypobromite ion are formed (Gordon et al., 2002).

Ammonia may be added to water by ozonation which may react with FAB to form NH_2Br

species. The efficiency of ammonia in reducing bromate formation appears to be correlated with pH and the initial bromide concentration. Siddiqui et al. (1993) reported that a decrease in bromate formation is found with increasing bromide concentration. For minimizing bromate formation, the addition of ammonia is one of the feasible approaches before ozonation of drinking water.

(3) NOM

Natural organic matter in water includes many types of compounds that affect the reaction of ozone and bromate formation. The hydrophobic or hydrophilic nature of natural organic matter is an important parameter in ozonation processes. Hydrophilic NOM is a better terminology of hypobromite than hydrophobic NOM, because hydrophilic fractions of NOM include more amino groups in their structure than hydrophobic fractions (Legube et al., 2004).

Hydroxyl radical pathway is the predominant pathway for bromate formation in water containing NOM. The reactions between ozone and NOM may produce many ozonation byproducts, including formate, acetate, oxalate, and etc. Therefore, a high level of NOM may reduce the formation of bromate formation because of the predominance of hydroxyl radical pathway in NOM water (Xie, 2004).

3-3 Methods for Hydroxyl Radical Determination

Because of the high activity and short-lived character of hydroxyl radical, the quantitative analysis of hydroxyl radical is difficult and complex. The general principle for hydroxyl radical determination is based on the characters of the unpaired electron and high activity. Methods commonly used for the analysis of the hydroxyl radical are discussed as follow:

1. Electron Spin Resonance (ESR)

   ESR methodology is considered to be the least ambiguous method for the detection of free radical (Tomasi and Lannone, 1993). ESR is based on the reaction between spin trapping agent (STA) and free radical to form stable free radical products. Using ESR proceeds to quantitative analysis of free radical as soon as possible to contribute the spectrum of the stable product. According to the spectrum, the hydroxyl radical formation concentration can be determined. Generally, the common use of STA includes DMPO (5,5-dimethyl-1-pyrroline-N-Oxide), PBN (o-phenyl N-tertbutyl nitrone) and N-tertbutyhydroxylamine (Zhiru, 1999).

2. Hydroxyl Radical Scavenger Analysis Method

   This method is based on the reaction between the hydroxyl radical and its scavenger to forms a stable product. The hydroxyl radical formation concentration is confirmed via the formation product analysis such as GC (Richmond, 1981) and LC (Radzik, 1983). For example, Fridorich proposed to analyze the product ethylene in the reaction between

methional and hydroxyl radical by GC and determine the hydroxyl radical formation concentration.

3. Fluorescence Method

This fluorescence method is based on the hydroxylation of coumarin-3-carboxylic (3-CCA) and produces 7-hydroxyl- coumarin-3-carboxylic acid (7-OHCCA), a fluorescent, stable and specific product. Based on the fluorescence of 7-OHCCA, the hydroxyl radical formation concentration can be calculated accordingly (Karin and Stefan, 2002).

4. Vivo Method

The salicylic acid is commonly used to the hydroxyl radical trapping reagent in vivo. The resulting stable products include 2,5 dihydroxybenzoic acid (2,5-DHBA), 2,3-dihydroxybenzoic acid (2,3-DHBA) and catechol analyze in HPLC-ECD. Given these products concentrations, the hydroxyl radical formation concentration can be determined (Wu, 2002).

3-4 Chlorination and DBP Formation

Chlorination

Because of its effectiveness in oxidation and disinfection, chlorine is a popular disinfectant in water treatment plant, especially in Taiwan. While chlorine dissolves in aqueous solution, it would undergo a rapid hydrolysis reaction to form two products, i.e., hypochlorous acid (HOCl) and hypochlorite (OCl^-). The speciation of chlorine in aqueous solution is governed by following three principal reactions. (Cotton et al, 1972)

$$Cl_2 + H_2O \xrightarrow{K_1\,(3.94\times10^{-2}\,M^2)} HOCl + Cl^- + H^+ \qquad (3.4.1)$$

$$HOCl \xrightarrow{K_2\,(3.2\times10^{-8}\,M)} H^+ + OCl^- \qquad (3.4.2)$$

$$Cl_2 + Cl^- \xrightarrow{K_3\,(0.18\,M^{-1})} Cl_3^- \qquad (3.4.3)$$

From the above equations, the composition of HOCl and OCl^- of chlorinated solution varies as a function of pH and the concentration of Cl^-. At low Cl^- concentration, hydrolysis reaction of Cl_2 goes on completely and produces more HOCl, OCl^- and less Cl_3^-. However, HOCl is a major component in acidic and neutral solutions, and OCl^- exists in a basic solution. These two species (HOCl and OCl^-) would proceed to addition and substitution reaction with organic precursor to form chlorination by-products such as THM and HAA because of their electrophilic character (Boyce et al, 1983).

Disinfection By-Products (DBPs) Formation

Chlorinated disinfection by-products are a general term used to describe a group of organic compounds formed during the chlorination process (Krasner et al, 1994). The major DBPs are characterized as trihalomethanes (THMs) and haloacetic acids (HAAs). These DBPs (THMs and HAAs) are potential carcinogens and health risks, and are regulated by United State Environment Protection Agency (USEPA) under the Disinfectant- Disinfection By-Product Rule (D/DBP Rule). According to D/DBP rule, the maximum contaminant levels (MCLs) of THMs and HAAs are limited at 0.08 mg/L and 0.06 mg/L, respectively (Mohamed et al., 1997).

The complex reaction between chlorine and NOMs in raw water is illustrated in Equation 3.4.4.

$$NOM + chlorine + bromide \rightarrow THMs + HAAs + other\ chlorinated\ compounds \quad (3.4.4)$$

The THMs include four chlorinated products they are chloroform ($CHCl_3$), dichlorobromomethane ($CHCl_2Br$), chlorodibromomethane ($CHClBr_2$), and Bromoform ($CHCl_3$) (APHA, 1998). The formation mechanism of THMs can be described by the reaction of propanone and chlorine. As shown in Equation 3.4.5, propanone would be oxidized readily by chlorine to form trichloropropanone which further undergoes a hydrolysis reaction to contribute THM formation, especially at high pH (Xie, 2004).

$$CH_3COCH_3 + HOCl \rightarrow CH_3COCl_3 \quad (3.4.5)$$

$$CH_3COCl_3 + H_2O \rightarrow CH_3COOH + CHCl_3 \quad (3.4.6)$$

The USEPA has proposed a maximum contaminant levels for the sum of five HAAs including monochloroacetic acid (MCAA), dichloroacetic acid (DCAA), trichloroacetic acid (TCAA), monobromoacetic acid (MBAA), and dibromoacetic acid (DBAA). The formation mechanism of HAA is demonstrated by the reaction equations of propanone and chlorine shown below. According to Equation 3.4.7, trichloropropanone was formed in the chlorinated water. Moreover, trichloropropanone can be further oxidative to form tetra-, penta- and hexchloropropanone, and undergoes a hydrolysis to contribute HAA, especially at low pH (Xie, 2004).

$$CH_3COCH_3 + HOCl \rightarrow CH_3COCl_3 \quad (3.4.7)$$

$$CH_3COCl_3 + HOCl \rightarrow CHCl_2COCCl_3 \quad (3.4.8)$$

$$CHCl_2COCHCl_3 + H_2O \rightarrow CHCl_2COOH + CHCl_3 \quad (3.4.9)$$

The distribution and concentration of various compounds in chlorinated products would depend on water quality parameters and operating conditions including pH, temperature, relative concentration of chlorine, bromide concentration, reaction time, and the NOM concentration and nature.

3-5 Predictive Model of Chlorine Decay and DBP Formation

Chlorination of NOMs is divided into two stages: rapid reaction and slow reaction. The

kinetics of both reactions is shown in Equations 3.5.1 and 3.5.2 (Gang et al., 2002).

$NOM_R + Cl_2 \rightarrow Chloro-byproducts$ (rapid)

$$\frac{dC_R}{dt} = -K_R \cdot C \qquad (3.5.1)$$

$NOM_s + Cl_2 \rightarrow Chloro-byproducts$ (slow)

$$\frac{dC_S}{dt} = -K_R \cdot C \qquad (3.5.2)$$

Where C_R is the chlorine consumption in a hypothetical separate rapid reaction, C_S is the chlorine consumption in a hypothetical separate slow reaction.

Hass and Karra (1984) proposed a model parallel first-order reaction model to evaluate the chlorine decay shown in Equation 3.5.3.

$$C(t) = C_0\{f \cdot e^{-K_R \cdot t} + (1-f) \cdot e^{-K_s \cdot t}\} \qquad (3.5.3)$$

Where C (t) is the chlorine concentration at time t (mg/L); C_0 is the initial chlorine concentration (dose) in chlorination; *f* is the fraction of the chlorine demand attributed to rapid reaction; K_R is the first-order rate constant for rapid reactions (h^{-1}); and, K_S is the first-order rate constant for slow reactions (h^{-1}).

According to the earlier studies, DBPs formation was corresponding to chlorine demand. Therefore, the rate coefficients determined from chlorine decay model were used to predict the DBPs formation. As shown in Equation 3.5.4, assuming the DBPs formation is direct proportion of the chlorine demand (Gang et al., 2003).

$$DBP = D(C_0 - C),\ [\ D = \frac{DBPFP\ (\mu g / L)}{Chlorine\ Demand\ (mg / L)}\ ] \qquad (3.5.4)$$

According to Equation 2.5.3, the Equation could be rewritten as Equation 3.5.5.

$$DBP = D \cdot C_0 \cdot \{1 - f \cdot e^{-K_R \cdot t} - (1-f) \cdot e^{-K_S \cdot t}\} \qquad (3.5.5)$$

The predictive DBP formation models for THM and HAA are described as follows :

$$THM = \alpha \cdot C_0\{1 - f \cdot e^{-K_R \cdot t} - (1-f) \cdot e^{-K_S \cdot t}\} \qquad (3.5.6)$$

$$HAA = \beta \cdot C_0\{1 - f \cdot e^{-K_R \cdot t} - (1-f) \cdot e^{-K_S \cdot t}\} \qquad (3.5.7)$$

The definitions of these coefficients are listed below:

α = THM yield coefficient, defined as the ratio of the THM concentration (μg/L) formed to the concentration of chlorine demand (mg/L).

β = HAAs yield coefficient, defined as the ratio of the HAA concentration (μg/L) formed to the concentration of chlorine demand (mg/L)

D= DBPs yield coefficient, defined as the ratio of the DBP concentration (μg/L) formed to the concentration of chlorine demand (mg/L).

The parameters of *f*, K_R, K_S, and yield coefficients of α, β, and *D* were determined by non-linear regression software (SYSTAT 5.0).

However, several studies reported that the above-mentioned THMs kinetics model was not in agreement with their experiments because of the $THMFP_i$ (initial THMFP corresponded to fast reacting THM precursors) and $THMFP_f$ (final THMFP) showing different kinetics for the formation of THM (Clark, 1998; Gallard et al., 2002). Therefore, a modified predictive model which is modified as the parallel first-order (slow reaction) and second-order (rapid reaction) reactions. The kinetics of both reactions can be described as follows (Chang et al., 2006):

$$C(t) = [-K_R \cdot t \cdot (-n+1) + f \cdot C_0^{\,-n+1}]^{\frac{1}{-n+1}} + [-K_S \cdot t \cdot (-m+1) + f \cdot C_0^{\,-m+1}]^{\frac{1}{-m+1}}$$

in which $C(t)$ is the chlorine concentration at any time t (mg/L), C_0 is the initial chlorine concentration (dose), f is the fraction of the chlorine demand attributed to rapid reactions, k_R is the rate constant for rapid reactions, and k_S is the rate constant for slow reactions. The value n and m are determined by the best fit as compared with the suggested reaction orders.

The rate coefficients determined from the Equation 3.5.10 are used to predict THM formation. Equation 3.5.11 assumes that the THM formation is a function of the chlorine demand with respect to the rapid and slow reaction:

$$THM = A \times (C_{R0} - C_R)^n + B \times (C_{S0} - C_S)^m \qquad (3.5.11)$$

Where A is the THM yield coefficient for rapid reaction, and B is the THM yield coefficient for slow reaction.

With the above observation of the chlorine decay model (Equation 3.5.10), Equation 3.5.11 can be simplified as follows:

$$THM = A \cdot \{f \cdot C_0 \left[1 - \frac{1}{f \cdot C_0 \cdot K_R \cdot t + 1}\right]\}^n + B \cdot \{(1-f) \cdot C_0 \cdot (1 - e^{-K_s \cdot t})\}^m \quad (3.5.12)$$

The corresponding HAA and DBP predictive kinetics model are described as follows:

$$HAA = C\{f \cdot C_0 \left[1 - \frac{1}{f \cdot C_0 \cdot K_R \cdot t + 1}\right]\}^n + D \cdot \{(1-f) \cdot C_0 \cdot (1 - e^{-K_s \cdot t})\}^m \quad (3.5.13)$$

$$DBP = E\{f \cdot C_0 \left[1 - \frac{1}{f \cdot C_0 \cdot K_R \cdot t + 1}\right]\}^n + F\{(1-f) \cdot C_0 \cdot (1 - e^{-K_s \cdot t})\}^m \quad (3.5.14)$$

Where C and D are the HAA yield coefficient for rapid and slow reactions, respectively. E and F are the DBP yield coefficient for rapid and slow reactions, respectively. The parameters of f, K_R, K_S, and yield coefficients of A, B, C, D, E and F were determined by non-linear regression software (SYSTAT 5.0).

IV Materials and Method

4-1 Research flowchart

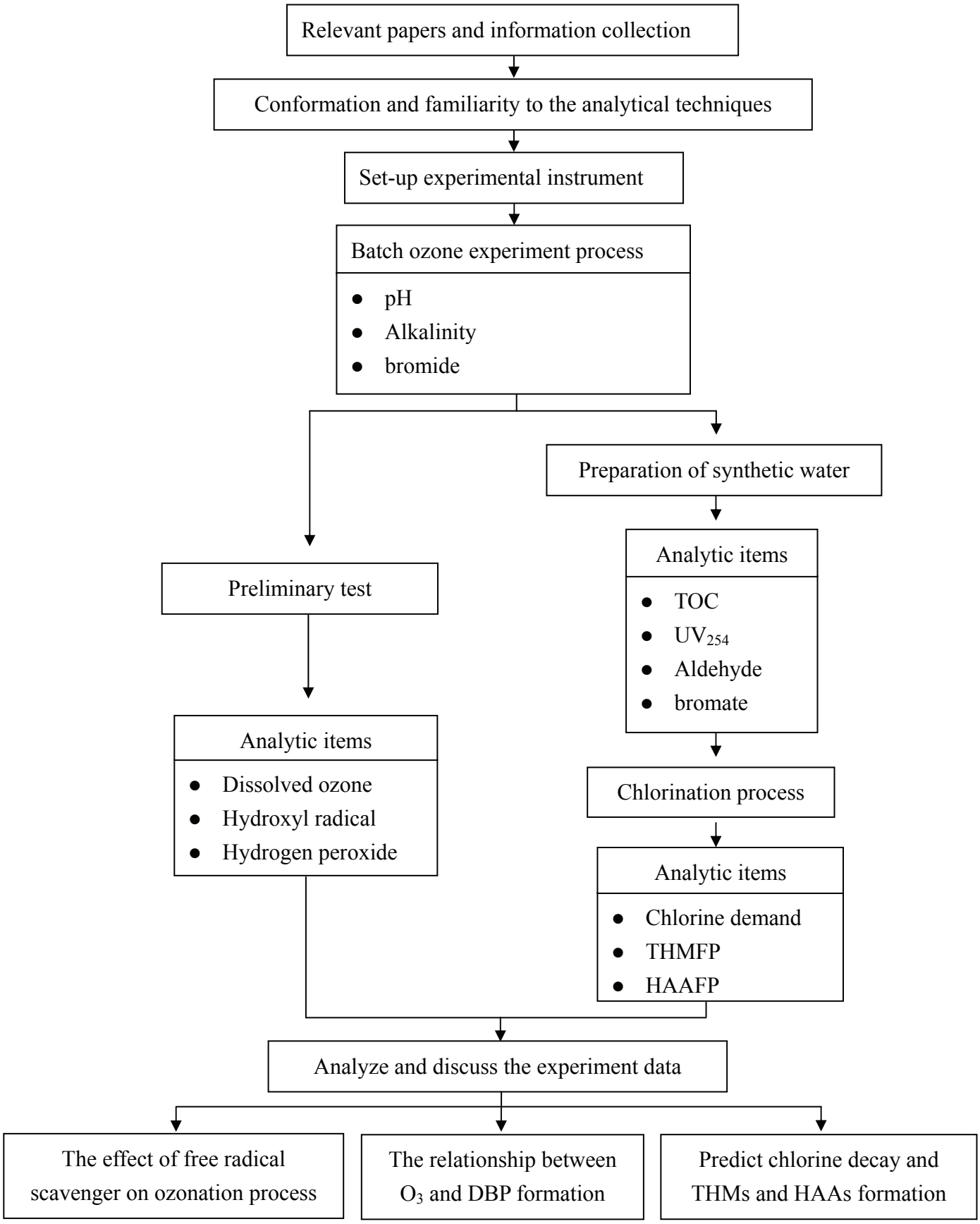

4-2 Materials

4-2-1 Apparatus

Ozonation process

(1) Ozone generator

Model	Ozonizer SG-01A
Specification	Operation voltage: 205 Volts Maximum electric current: 2.5 A Inner pressure: 0.9 ~ 1.1 Kg/cm^2
Functional Performance	Normal quantity of output: 25 g/hr Ozone concentration: 0 ~ 104 g/Nm^3

(2) Batch reactor

Size
Inner diameter : 18 cm
Outer diameter : 23 cm
Height : 29 cm
Operation condition
Rotation rate : 200 rpm
Control volume : 5 L
Control temperature : 25 ¢J

Analytic apparatus

The apparatus used in the experiments and for the analyses are listed following Table. The model of HP 6890 series and HP 5890 II series are used to determine the THMs and HAAs concentration, respectively. The model of Trace GC is used to determine the aldehyde concentration.

Name	Model
Total organic carbon analyze	O. I. Analytical
Fluorescence spectrophotometer	F2000, Hitachi
UV-visible spectrophotometer	UV-1601, SHIMADZU
Purge & trap autosampler, concentrator, and GC system	HP 6890 series
GC system and autosampler	HP 5890 II series
GC system	Trace GC
Ion chromatography	Dionex

4-2-2 Organic Precursors

The physical and chemical properties of these three selected organic model compounds are listed in Table 4.2.1.

4-3 Methods

4-3-1 Experimental Design

The experiment in the study was divided into two stages. The experimental detail design is shown in Table 4.3.1. In stage 1, take 5 liters Milli-Q water in a 25 ^{o}C bath and the ozone gas introduced to the water through a bubble diffuser bottom of the reactor for 2 hours before reaching an equilibrium concentration. The saturated ozone concentration in aqueous solution is about 18 mg/L.

The preliminary test is conducted to add the blank water in the experiment and takes sample with following reaction time until 40 minutes to determine concentration of dissolved ozone, hydroxyl radical, and hydrogen peroxide. In addition, by adding the selected compounds of different pH levels, alkalinity, and bromide concentration changes the experimental conditions (pHs 5, 7 and 9) and maintains 40 minutes reaction time. The purpose of this ozonation process is to evaluate the removal of TOC and UV_{254}, aldehyde, and bromate formation. An additive of alkalinity in ozonation is prepared by $NaHCO_3$ at 60 mg/L as $CaCO_3$ to evaluate the effect of alkalinity on ozonation process (Figure 4.3.1)

It appears that batch ozone reaction is popular application for the reaction of low reactant concentration and fast reaction rate. In addition, it has a benefit to evaluate ozone reaction thoroughly and accurately. Therefore, the batch ozone reaction was chosen instead of the semi-batch ozone reaction for this study.

The purpose of stage 2 (Figure 4.3.2) of this study is to evaluate the chlorine decay and chlorinated by-products formation in the chlorination followed by the ozonation process. A 7-days chlorine demand study was introduced by 10mg/L chlorine dose to determine the chlorine consumption, trihalomethane formation potential (THMFP), and haloacetic acid formation potential (HAAFP). Throughout these chlorination experiments, all samples were chlorinated by 13% free chlorine (sodium hypochlorite) stock solution and add phosphate buffer (pH 7.0). Sample were chlorinated in 300 mL glass bottle and kept headspace free in the dark at room temperature (25±2 ^{o}C) until 168 hours. The samples were collected after 1, 3, 6, 24, 48, and 168 hours contact time.

Table 4.2.1 Summary of the physical/chemical properties for organic compounds

Organic Compounds	Resorcinol	Phloroglucinol	*p*-hydroxybenzoic acid
Molecular Formula	$C_6H_6O_2$	$C_6H_6O_3$	$C_7H_6O_3$
Molecular Weight	110.11	126.11	138.12
Structure	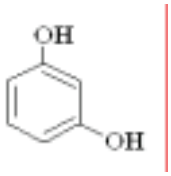	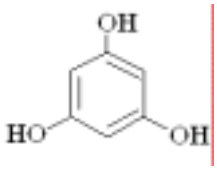	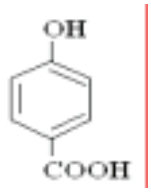
Boiling Point (°C)	280	-	211
Melting Point (°C)	177	218.5	214.5
Density/Specific Gravity	1.27	1.46	1.44
Dissociation Constants	pK = 9.30	pK = 8.45	pK = 4.54
Water Partition Coefficient	$pK_{ow} = 0.80$	$pK_{ow} = 0.16$	$pK_{ow} = 1.58$
pH	5.2	-	2.4
Solubility	0.717 g/L	10.6 g/L	5 g/L
Vapor Density (air = 1)	3.79	4.3	4.8
Vapor Pressure (mmHg)	4.89×10^{-4}	1.6×10^{-4}	8.2×10^{-5}

4-3-2 Unit Process

Ozonation

1. Procedure

   a. Fill 5 L Milli-Q water in batch reactor (shown in Figure 4.3.3) at 25 ¢J and set up ozone experiment instrument.

   b. Ozone gas introduced to Milli-Q water through a bubble diffuser for 2 hours before reaching an equilibrium concentration.

   c. Adjust the specific pH of synthetic water with NaOH and H_2SO_4 to maintain pH of saturated ozone water at 5, 7, and 9.

   d. Let stand for 40 minutes.

   e. Take sample and analyze for TOC, UV_{254}, alkalinity, and aldehyde.

   f. Proceed to chlorination process.

Table 4.3.1 The experimental design in the ozonation/chlorination processes

Model compounds	mg O_3/mg C	Alkalinity* (mg/L as $CaCO_3$)	Analytic items	
			Ozonation (40 mins)	Chlorination
Blank pH = 5 pH = 7 pH = 9	6	0 / 60	˙OH Ozone H_2O_2 TOC UV_{254} Alkalinity Aldehyde bromate	Residual Cl_2 THMFP HAAFP DBPFP
Resorcinol (R) pH = 5 pH = 7 pH = 9	6	0 / 60		
Phloroglucinol (P) pH = 5 pH = 7 pH = 9	6	0 / 60		
***p*-hydroxybenzoic acid (PHBA)** pH = 5 pH = 7 pH = 9	6	0 / 60		

* Alkalinity: An additive quantity of alkalinity

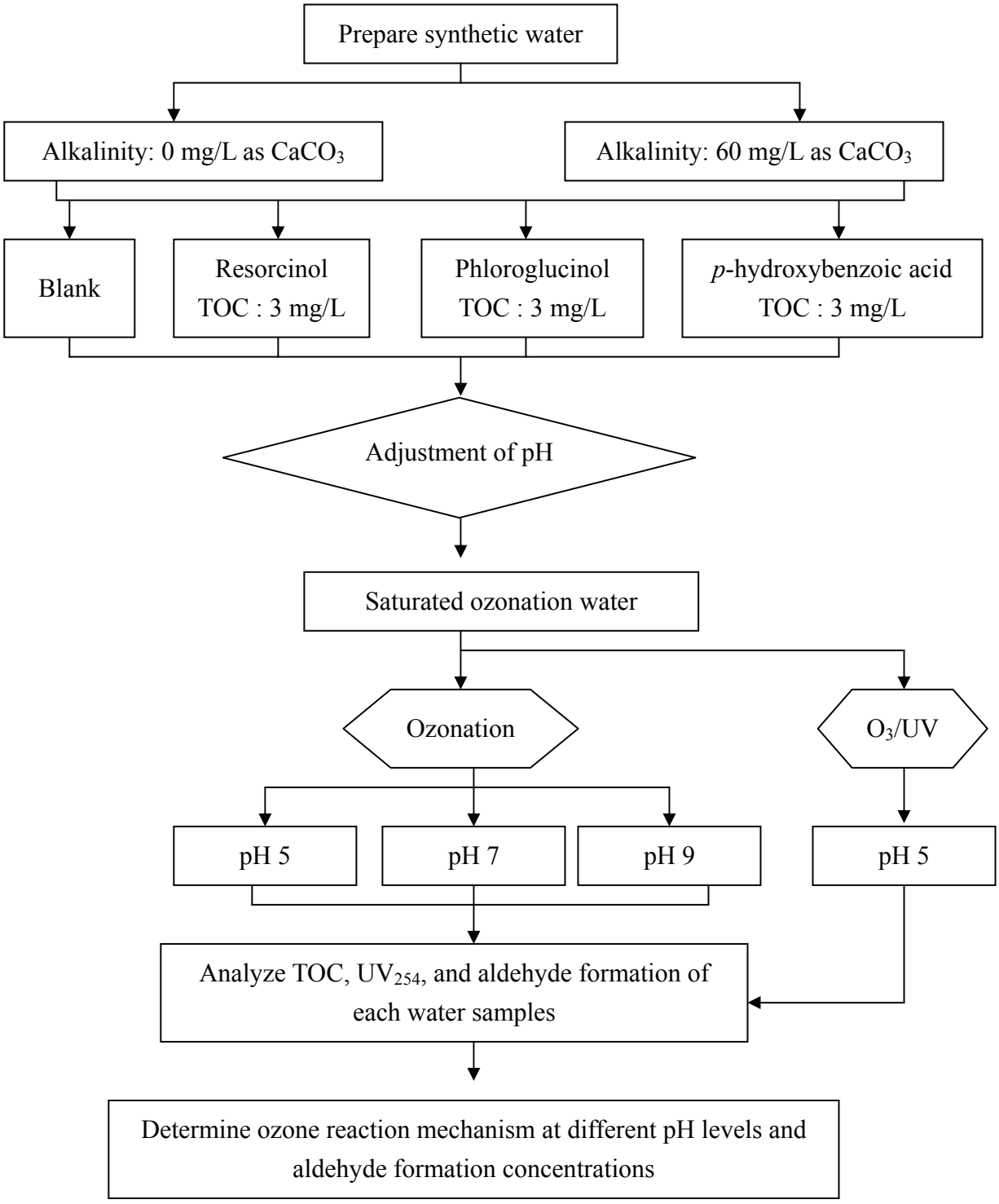

Figure 4.3.1 Flowchart of experiments to determine the ozone reaction mechanism and aldehyde formation concentrations in ozonation and O_3/UV processes

Chlorination

1. Procedure

   a. Take 300 mL ozonated water and place in a bottle.

   b. Inject standard chlorine solution formulated by NaOCl in the bottle to reach the initial chlorine dose of 10 mg/L.

   c. Store the chlorinated water in dark place in specific contact time (1, 3, 6, 24, 48, and 168 hours).

   d. Analyze residual chlorine concentration, THMFP, and HAAFP.

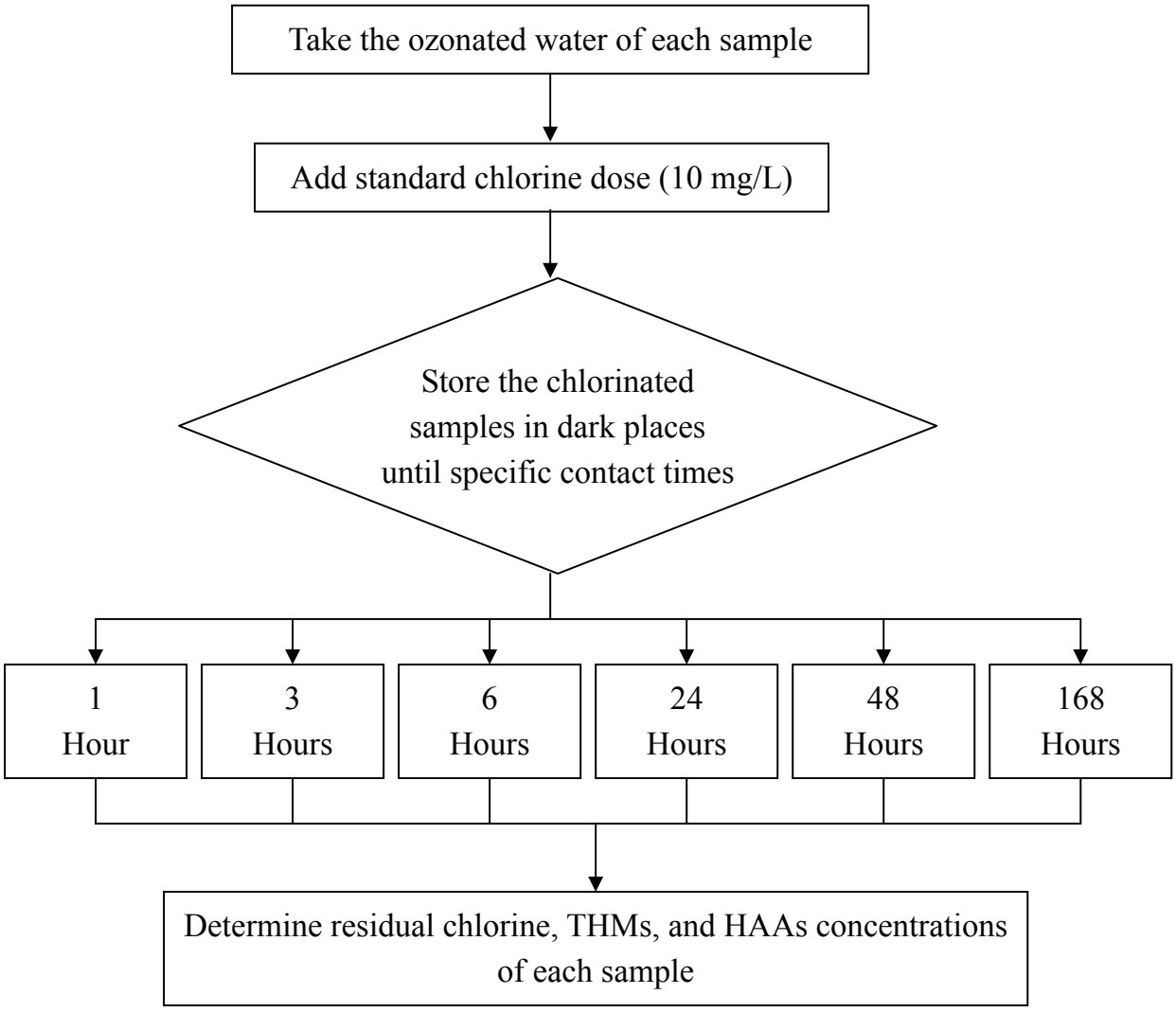

Figure 4.3.2 Flowchart of experiments to determine the residual chlorine, THMs, and HAAs concentrations at various chlorine contact times

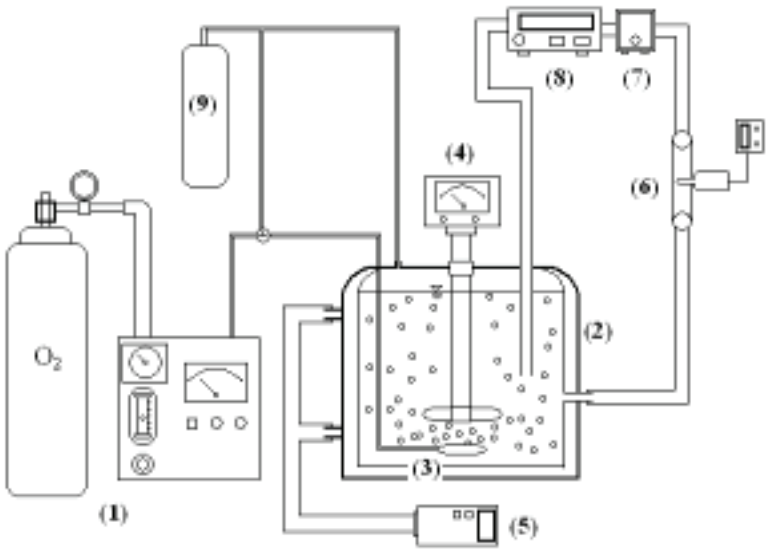

Figure 4.3.3 The experimental apparatus of the ozone batch reactor:

(1) Ozone generator and oxygen cylinder
(2) Batch reactor
(3) Gas distributor
(4) 6-bladed-disk turbine
(5) Thermostat
(6) pH meter
(7) Pump
(8) Liquid ozone sensor
(9) Activated carbon cylinder

4-3-3 Analytical Method for Traditional Method

TOC

Method：NIEA W532.51C, promulgated by EPA, Republic of China.

UV_{254}

Method：Method 5910, Standard Methods 19th edition

Alkalinity

Method：NIEA W449.00B, promulgated by EPA Republic of China.

Residual Chlorine

Method：Method 2350B and 4500-Cl F., Standard Methods 19th edition

Ammonia

Method：NIEA W448.51B, promulgated by the Taiwan EPA

4-3-4 Analytical Method for DBPs

THMs

1. Method

   Method 2350 B and 4500-Cl F, Standard Methods 19th edition

2. Procedure
   a. Warm up GC system for at least 30 minutes, and run blanks until the signal area is lower than 100.
   b. Prepare the standard curve
   c. Inject the sample into the column of purge & trap autosampler. If sample's THM concentration falls out of the range of standard curve, the sample must be diluted to fit within the range.
   d. Chromatographic condition

Column
Type : Fused silica capillary Length : 30 m Inner diameter: 0.25 mm Film thickness : 1.0 μm
Injector
Temperature : 177¢J Split/splitless (using straight open-bore insert) Spilt valve open at 0.5 min
Detector
Type : ECD Temperature : 272 ¢J
Temperature program
35¢J (10 min) → 110 ¢J (9 ℃/min, 1 min) → 220 ¢J (27℃/min, 2 min)
Gas
Carrier gas flow : He 2.0 mL/min Make-up gas flow : N_2 35 mL/min

3. Calibration curve (Range 0.5 ~ 30 μg/L)

	Calibration function	R^2	N
$CHCl_3$	Y=498.87X+906.93	0.9911	7
$CHBrCl_2$	Y=1601.2X+1541.5	0.9992	7
$CHBr_2Cl$	Y=1271.2X+1691.7	0.9989	7
$CHBr_3$	Y=430.61X+1227.9	0.9922	7

X : THM concentration (μg/L) Y : Peak area

HAAs

1. Method

   Method 552.2, USEPA

2. Procedure

   a. Place a minimum of 50 mL sample into the amber glass container with a TFE-lined screw cap, add granular NH_4Cl to the sample container and refrigerate at 4¢J.

   b. Place 40 mL of the water sample into a 60 mL glass vial with a Teflon-lined screw cap.

   c. Add 20 μL of surrogate standard (10.0μg/mL 2,3- dibromopropionic acid in MTBE).

   d. Add at least 2 mL of concentrated sulfuric acid to adjust the pH to less than 0.5.

   e. Add 2 g $CuSO_4 \cdot 5H_2O$ and 16 g Na_2SO_4 quickly, and shake for 3 ~ 5 minutes until almost all solids were dissolved.

   f. Add 4.0 mL MTBE and place the glass vial on the mechanical shaker for 30 minutes.

   g. Wait the phases to separate, and transfer 3 mL of the upper layer to a 15 mL centrifuge tube.

   h. Add 1 mL 10% sulfuric acid in methanol to each centrifuge tube.

   i. Cap the centrifuge tube and place in the constant- temperature water bath at 50¢Jfor 2 hours.

   j. Remove the centrifuge tube from the heating block and allow it to cool before removing the caps.

   k. Add 4 mL saturated sodium bicarbonate solution to each centrifuge tube in 1 mL increments and shake each centrifuge tube for 2 minutes.

   l. Transfer 1.0 mL of the upper MTBE layer to an autosample vial. The excess extract should be duplicated.

   m. Add 10 μL internal standard to the vial (25 μg/mL 1,2,3-trichloropropane in MTBE). Analyze the sample in GC system as soon as possible.

   n. Chromatographic condition

Column
Type : Fused silica capillary Length : 30 m Inner diameter: 0.25 mm Film thickness : 0.25 μm
Injector
Temperature : 200 ¢J Split/splitless (using straight open-bore insert) Spilt valve open at 0.5 min
Detector
Type : ^{63}Ni ECD Temperature : 300¢J
Temperature program
37¢J (21 min) → 136¢J (3 min) → 236¢J (3 min) 11℃/min　20℃/min
Gas
Carrier gas flow : He (1.6 mL/min at 37¢J) Make-up gas flow : N_2 (23 mL/min)

3. Calculation

An injection of each calibration level would provide peak area (A_a)data for each HAA and an internal standard peak area (A_i) for each level; use these peak area to calculate the relative response for each HAA. Moreover, the relative standard deviation (% RSD) of selected experimental data is less than 10 %.

$$\text{Relative response} = A_a/A_i$$

The three major peaks represent the most prominent haloacetic acid, monochloroacetic acid (MCAA), dichloroacetic acid (DCAA), and trichloroacetic acid (TCAA).

4. Calibration curve (Range 0.5 ~ 50 μg/L)

	Calibration function	R^2	N
MCAA	Y=1148.3X+233405	0.9926	6
DCAA	Y=4381.1X+195062	0.9999	6
TCAA	Y=8631.9X+12089	0.9975	6

X: HAA concentration (μg/L)

Y: Relative response

Aldehydes

1. Method

   Method 6252, Standard Methods 19th Edition.

2. Procedure

   a. Remove samples and standard solution from storage and let them equalize with the room temperature.

   b. Take 20 mL samples from sample vials.

   c. Add 10μL surrogate and 1 mL buffer solution using a micro syringes and dispenser.

   d. Add 1 mL fresh PFBHA solution to each vial and swirl to mix gently.

   e. Place all samplers in a constant-temperature water bath set at 45 ± 0.5 ¢J for 1 hour and 45 minutes. Remove vials and cool to room temperature for 15 minutes.

   f. Add 0.05 mL (approximately 2 drops) concentrated H_2SO_4 to quench the derivatization reaction.

   g. Add 4 mL hexane solution containing the internal standard and shake manually for about 3 minutes.

   h. Draw off top hexane layer into a smaller 7 mL vial containing 3 mL 0.2 N H_2SO_4.

   i. Shake for 30 seconds and let it stand approximately 5 minutes.

   j. Draw off top hexane layer and place the sample in a 1.8-mL autosampler vial.

   k. Analyze the sample in the GC system as soon as possible.

   l. Chromatographic condition

column
Type : Fused silica capillary Length : 30 m Inner diameter: 0.25 mm Film thickness : 0.25 μm
Injector
Temperature : 180 ¢J Split/splitless (using straight open-bore insert) Spilt valve open at 0.5 min Spilt flow : 50 mL/min
Detector
Type : ^{63}Ni ECD Temperature : 300¢J
Temperature program
50¢J (1 min) —4℃/min→ 220¢J (1 min) —20℃/min→ 250¢J (1 min)
Gas
Carrier gas flow : He (1.5 mL/min at 100¢J) Make-up gas flow : N_2 (27 mL/min)

3. Calculation

Relative response and concentration can be used calculate a calibration curve for the analysis. Moreover, the relative standard deviation (% RSD) of selected experimental data is less than 10 %.

Relative response = A_a/A_i

Where

Aa = the peak area of sample
Ai = the peak area of internal standard

4. Calibration curve (Range 1 ~ 50 μg/L)

	Calibration function	R^2	N
Formaldehyde	Y=139048X+1000000	0.9732	6
Acetaldehyde	Y=59795X+379270	0.9643	6
Glyoxal	Y=879131X+597866	0.9988	6
Methyl glyoxal	Y=332925X+2000000	0.9331	6

X: aldehyde concentration (μg/L)

Y: Relative response

Bromate

1. Method

NIEA W415.52B, promulgated by the Taiwan EPA

2. Procedures

A. Prepare 0.009 Na_2CO_3 for mobile reagent

B. Open IC and warming

C. Put sample into autosampler

D. Read and analyze data

4-3-5 Hydroxyl Free Radical

1. Method

   Karin and Stefan study (2002).

2. Procedure

   a. Warm up the fluorescence photometer for at least 10 minutes.

   b. Place 30 mL 3-CCA stock solution in a 50 mL volumetric flask and fill Milli-Q water to the 50 mL mark, called blank.

   c. Place 30 mL 3-CCA stock solution in a 50 mL volumetric flask and fill sample to the 50 mL mark, called sample.

   d. Set the excitation wave length at 388 nm to make the emission wave length at 444 nm and read value of blank and sample from the Fluorescence photometer.

   e. Calculate the difference between blank and sample, and substitute the calculation curve.

3. Calibration curve

	Calibration function	Range (mM)	R^2	N
7-OHCAA	$Y = 8\times10^{6}\ X + 129.03$	$2.5\times10^{-6} \sim 5\times10^{-4}$	0.9984	9

X: concentration of 7-OHCAA (mM)

Y: difference fluorescence between sample and blank

4-3-6 Residual ozone

1. Method

   Method 4500-O_3, Standard Methods 19th edition.

2. Procedure

   a. Warm up the photometer for at least 10 minutes.

   b. Add 10 mL indigo reagent to 100 mL volumetric flask. Fill to the 100 mL mark with distilled water, called blank.

   c. Add 10 mL indigo reagent to 100 mL volumetric flask. Fill to the 100 mL mark with sample, called sample.

   d. Measure absorbance of both solutions at 600 ± 5 nm as soon as possible but must be within 4 hours.

3. Calculation

$$mg\ \ O_3 = \frac{100 \times \Delta A}{f \times b \times V}$$

Where

ΔA = Difference of absorbance between sample and blank
b = Path length of cell (cm)
V = Volume of sample (mL)
f = Coefficient (0.42)

4-3-7 Hydrogen peroxide

1. Method

Bader et al. study (1988).

2. Procedure

a. Place 20 mL sample in the 50 mL beaker.

b. Add 3 mL buffer solution and stir.

c. Add 50μL DPD reagent solution and 50μL POD reagent in a rapid succession.

d. Measure absorbance of solutions at 551 nm after at 10 seconds.

3. Calculation

$$[H_2O_2]_{sample} = \frac{\Delta A_t^{551} \times V_{final}}{\varepsilon \times L \times V_{sample}}$$

Where

ΔA_t^{551} : Difference of absorbance between blank and sample

ε : 21000 $M^{-1}cm^{-1}$

L : Path length of cell

V_{final} : Final volume after addition all reagents as buffer

V_{sample} : Volume of original sample

V Results and discussion

5-1 Ozonation and O3/UV Processes

This study of ozonation and O_3/UV process is divided into two phases. The preliminary test was performed to investigate the effects of hydroxyl radical and alkalinity on ozonation. Further, this study focused on ozonation (O_3/UV) of organic precursors and ozonation by-products formation.

5-1-1 Ozonation Process at Different pH Levels

In a batch reactor, ozonation mechanism changes at different pH levels. At pH 5 (acidic condition), ozone self-decomposition reaction is the predominant reaction. This reaction mechanism may be described by the first-order model (Slawomir et al., 1998) shown in Equation (5.1.1), and is called direct reaction. At pH 7 (neutral condition) and pH 9 (basic condition), ozone decomposes rapidly to form hydroxyl radical, and is called indirect reaction.

$$-r_{O_3} = \frac{d[O_3]}{dt} = k_D[O_3] \qquad (5.1.1)$$

In Figure 5.1.1, it was observed that ozone decomposition rate increases with increasing pH. There are more hydroxyl ions (OH^-) at high pH, which promotes ozone decomposition reaction to form hydroxyl radical (Staehelin and Hoigné, 1982). At pH 5, ozone self-decomposition reaction results in high ozone concentration. Further, the highest ozone decomposition rate is at pH 9 and the order of ozone decomposition rate at different pH levels is O_3 (pH 9) > O_3 (pH 7) > O_3 (pH 5).

As shown in Figure 5.1.1, the ozone decomposition reaction may be divided into two stages. Ozone decomposes fast in the first stage (rapid reaction), but the decomposition curve trends to smooth in the second stage (slow reaction). According to the Slawomir study (1998), the theory of ozone decomposition reaction follows the first-order model, but the simply kinetics equations (Equation 5.1.1) does not completely describe the ozone decomposition in both stages. The kinetics constants of both stages are obviously different as indicated by the slop of the curve shown in Figure 5.1.1. The designation k_R and k_S represents the kinetics constants for the first and second stages in this study, respectively. In order to mathematically model the experimental data of ozone decomposition reaction in two stages, the ozone decomposition reaction was modified the parallel first-order reaction model as:

$$[O_3] = [O_3]_0 \cdot \{F \cdot e^{-k_R \cdot t} + (1-F) \cdot e^{-k_S \cdot t}\} \qquad (5.1.2)$$

Where $[O_3]$ is the ozone concentration at time t (mg/L); $[O_3]_0$ is the initial ozone concentration; F is the fraction of the ozone consumption attributed to rapid reaction; k_R is the first-order rate constant for rapid reactions (min^{-1}); and, k_S is the first-order rate constant for slow reactions (min^{-1}).

The kinetics constants for the two stages at pHs 5, 7, and 9 are listed in Table 5.1.1. The higher correlation coefficients (R^2) shown in Table 5.1.1 indicate that Equations (5.1.2) express the ozone decomposition reaction very well. Figure 5.1.1 also presents the ozone decomposition reaction and predictive model at different pH levels, in which the dashed lines and solid lines denote the predictive data determined by the Slawomir model and Equations (5.1.2), respectively. The parameters F, k_R, and k_S were determined by non-liner regression software (SYSTAT 5.01).

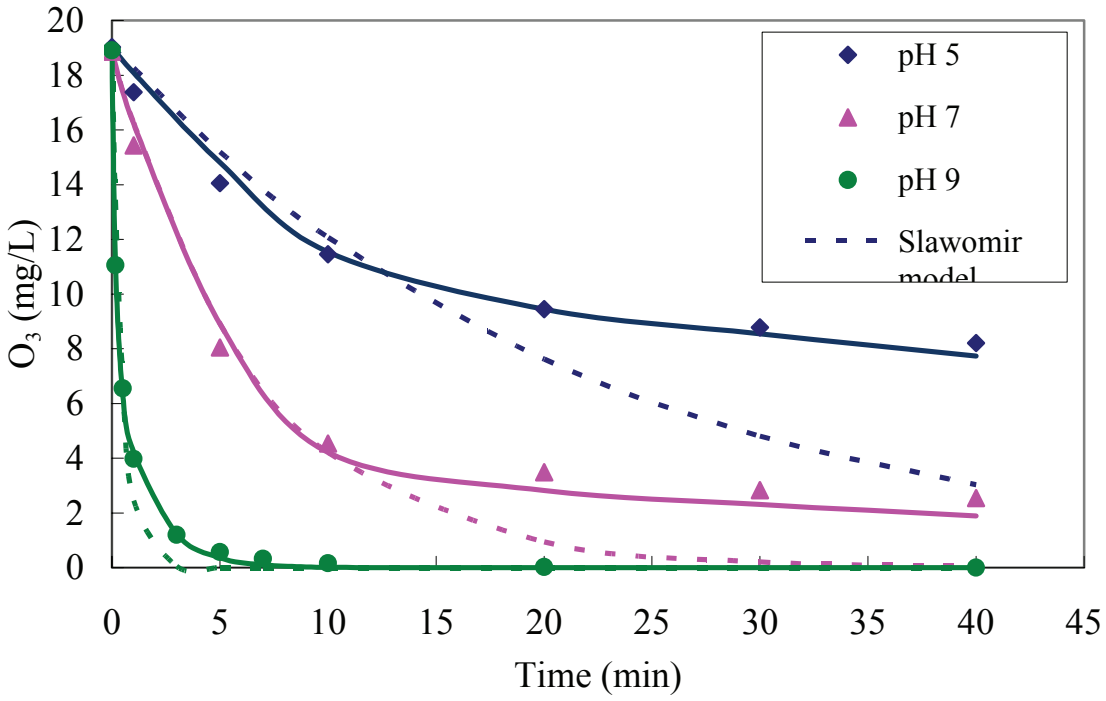

Figure 5.1.1 The ozone decomposition and predictive decay model at different pH levels

Table 5.1.1 Ozone decomposition constants for parallel first order reaction at different pH levels

pH	F	k_R	k_S	R^2
5	0.534	0.005	0.158	0.999
7	0.787	0.256	0.011	0.999
9	0.592	5.892	0.609	0.999

Model: $[O_3] = [O_3]_0 \cdot \{F \cdot e^{-k_R \cdot t} + (1-F) \cdot e^{-k_S \cdot t}\}$

Hydroxyl Radical

At higher pH, the ozone molecule reacts with hydroxyl ions and yields free radical such as $O_2^{\cdot-}$, $HO_2^{\cdot-}$ and $^{\cdot}OH$, which are the main oxidants for the indirect ozone process (Staehelin and Hoigné, 1982). In this study, the characteristics of the hydroxyl radical ($^{\cdot}OH$) affecting the ozonation process was investigated thoroughly.

The formation of hydroxyl radical at pHs 7 and 9 is shown in Figure 5.1.2. According to Figure 5.1.2, hydroxyl radical formation is more significant at pH 9 than pH 7, which indicates that more hydroxyl ions (OH^-) would promote more hydroxyl radical formation, and also affect ozone decomposition rate. The high pH increases the ozone decomposition rate as well as the hydroxyl radical formation.

Figure 5.1.3 presents the linear correlation between ozone and hydroxyl radical concentration at pHs 7 and pH 9 at different ozonation time. Since the high OH^- concentration at pH 9 decomposes ozone completely to form more hydroxyl radical, the residual ozone concentration shown in the y-intercept (O_3) is close to zero. However, the occurrence of less hydroxyl radical formation and high ozone concentration at pH 7 resulted in a residual ozone concentration of 15 mg/L as shown in the y-intercept (O_3). The above evidence suggests that the main oxidants in ozonation at pH 7 are both ozone molecule and hydroxyl radical.

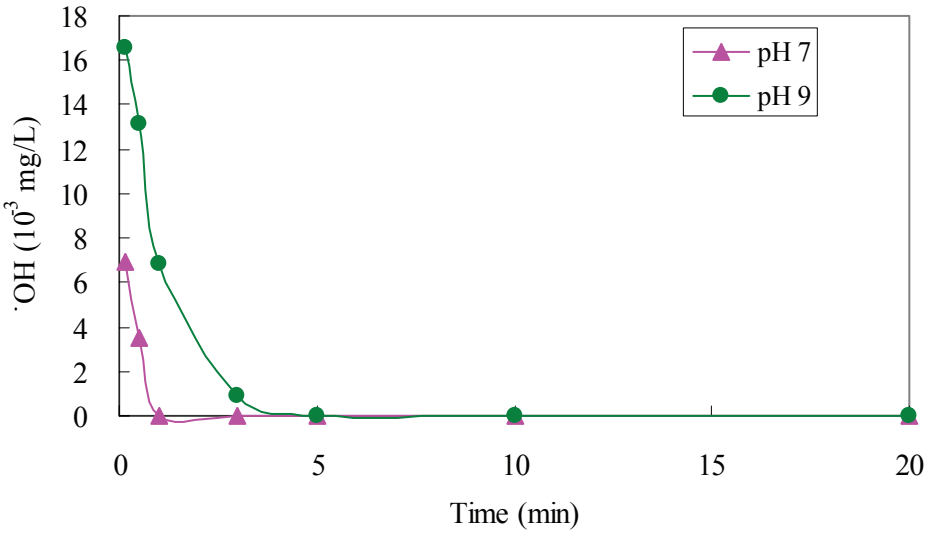

Figure 5.1.2 The difference in hydroxyl radical formation at pH 7 and 9 in ozonation process

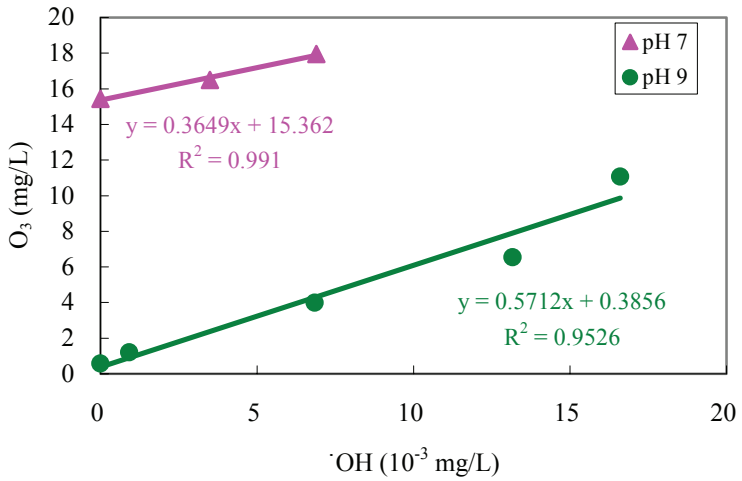

Figure 5.1.3 The relationship between ozone and hydroxyl radical concentration at pH 7 and 9 in ozonation process

Hydrogen peroxide (H_2O_2)

It was reported that hydrogen peroxide (H_2O_2) forms simultaneously in ozone decomposition during the rapid stage of the ozonation process (Buhler et al., 1984). According to the Guittonneau study (1996), low H_2O_2 concentration also increases the organic compound removal efficiency in ozonation. As a result, the effect of H_2O_2 formation was further study in this investigation.

As shown in Figure 5.1.4, the formation of H_2O_2 increases as the reaction time. The formation concentration increases a maximum value within the first 30 minutes and gradually decreases afterwards. However, in the indirect ozonation process, hydroxyl radicals formed and reacted with H_2O_2 as shown in Equation 5.1.3, which results in a lower H_2O_2 concentration than that of the direct ozonation process.

$$HO\cdot + H_2O_2 \xrightarrow{k=2.7\times10^7\ M^{-1}S^{-1}} HO_2\cdot + H_2O \qquad (5.1.3)$$

Therefore, the effect of pH on the ozonation process results in forming different ratios of hydroxyl radical and H_2O_2 formations, and changes the oxidation ability.

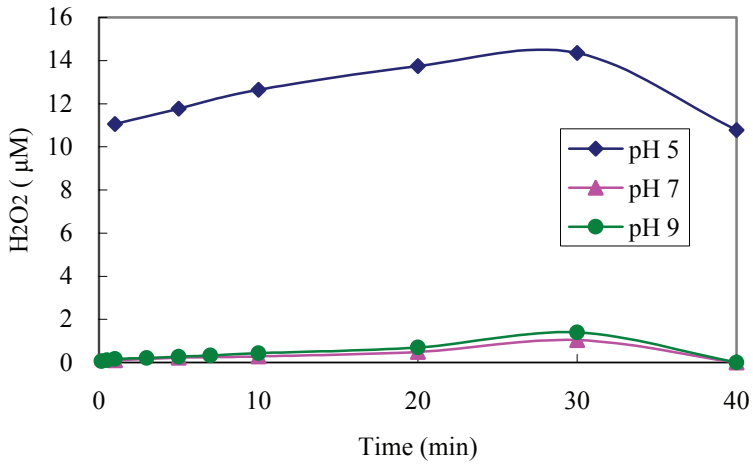

Figure 5.1.4 The formation of H_2O_2 in ozonation process at different pH levels

5-1-2 Effect of Alkalinity On Ozonation

To simulate nature water quality in this experiment, alkalinity is prepared by $NaHCO_3$ at 60 mg/L as $CaCO_3$. Figure 5.1.5 presents the changes of alkalinity at pHs 5, 7, and 9. As shown in Figure 5.1.5, the [Alkalinity/Alkalinity$_0$] represents the ratio between the residual alkalinity and the initial alkalinity. Alkalinity at pHs 7 and 9 decreases rapidly at the beginning and remains constant afterwards. It was reported that the hydroxyl radical reacts with carbonate and bicarbonate ions to leads to the alkalinity decrease at pHs 7 and 9. The reducing degree of alkalinity has a strong correlation with the presence of hydroxyl radical concentration, i.e., pH 9 > pH 7. Since there is no free radical formation at pH 5, constant alkalinity was observed in this experiment.

The hydroxyl radical formation concentration in ozonation at different levels of pH and alkalinity is shown in Figure 5.1.6. As shown in Figure 5.1.6, the amount of hydroxyl radical remaining in the solution of 60 mg/L of alkalinity (as $CaCO_3$) is lower than that of without adding alkalinity at pHs 7 and 9. This observation confirms that carbonate and bicarbonate alkalinities inhibit the hydroxyl radical.

Correlation of radical alkalinity ratio and hydroxyl radical concentration during the ozonation process was shown in Figure 5.1.7. In Figure 5.1.7, alkalinity concentration decreases as hydroxyl radical increase, and maintains constant once the hydroxyl radical disappears. Therefore, the hydroxyl radical is one of the most important chemical elements affecting the alkalinity concentration during the ozonation process.

Further evidence of the effect of alkalinity on ozonation is illustrated in Figure 5.1.8, which presents the relationship between hydroxyl radical exposure and alkalinity reduction. In this study, the exposure represents the multiplication between reactant ($\cdot OH$) concentration and reaction time. The high exposure of hydroxyl radical (10^{-3} mg/L×min) leads to low alkalinity ratio (alkalinity/alkalinity$_0$), which is expressed by the empirical formula: Y = -0.0006 X + 0.8786 (X: hydroxyl radical exposure; Y: alkalinity/alkalinity$_0$) as shown in Figure 5.1.8. Based on the empirical formula, the hydroxyl radical exposure during the ozonation process could be easily calculated by decrease of alkalinity.

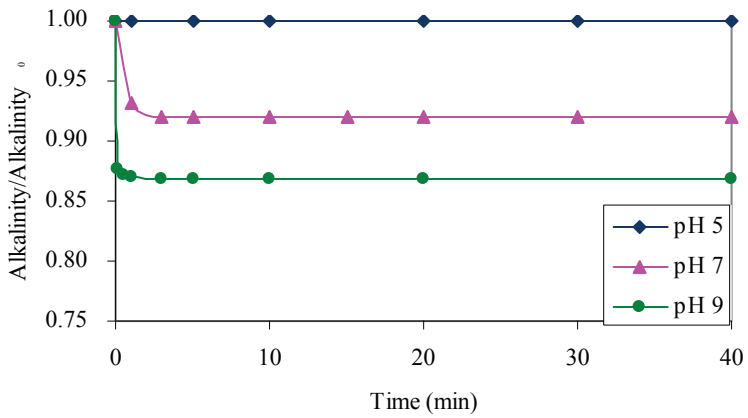

Figure 5.1.5 Alkalinity changes at various pH levels in the ozonation process

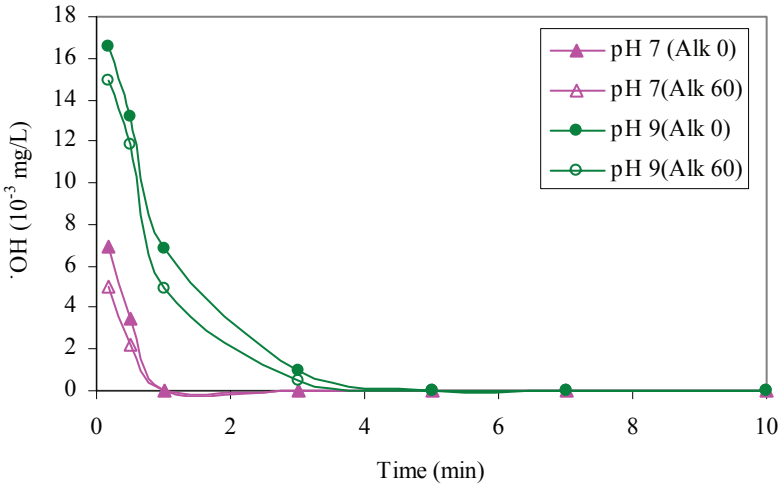

Figure 5.1.6 The difference in hydroxyl radical at different pH levels by ozonation process

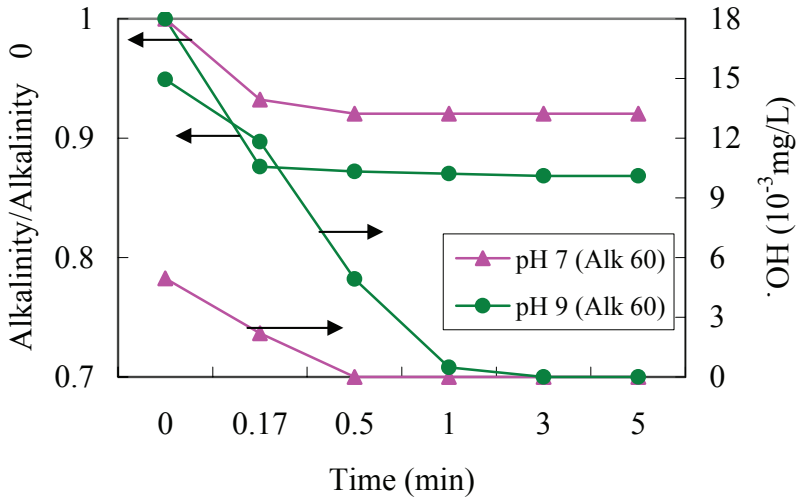

Figure 5.1.7 Correlation of the residual alkalinity ratio and the hydroxyl radical concentration during the ozonation process.

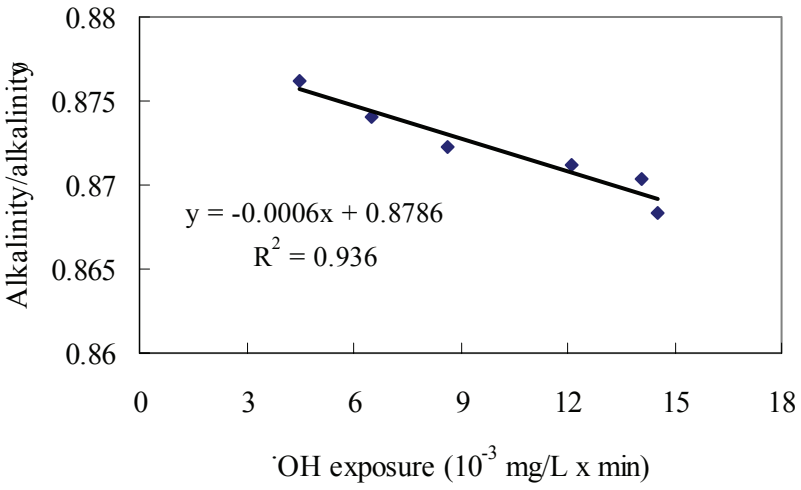

Figure 5.1.8 The correlation between hydroxyl radical exposure and residual alkalinity ratio at pH 9.

5-1-3 Development of Hydroxyl Radical Formation Model

According to hydroxyl radical formation mechanism and the effect of carbonate species in indirect ozonation process, hydroxyl radical formation equation could be simply as:

$$2O_3 + OH^- \rightarrow \bullet OH + O_2^{\bullet -} + 2O_2 \qquad (5.1.4)$$

$$\bullet OH + CO_3^{2-} \rightarrow CO_3^{-\bullet} + OH^- \qquad (5.1.5)$$

Therefore, the hydroxyl radical formation kinetics model could be proposed by Equations 5.1.4 and 5.1.5 as the following:

$$\frac{d[\bullet OH]}{dt} = k_1[O_3][OH^-] - k_2[\bullet OH][CO_3^{2-}] \qquad (5.1.6)$$

in which k_1 represents the rate constant for hydroxyl radical formation, and k_2 is the rate constant for hydroxyl radical inhibition reaction.

Integrating the Equation 5.1.6 (Equation 5.1.7) with assumption of constant carbonate ions concentration, the hydroxyl radical formation concentration is shown in Equation 5.1.8.

$$[\bullet OH] = \int \{ k_1[O_3][OH^-] - k_2[\bullet OH][CO_3^{2-}] \}\, dt \qquad (5.1.7)$$

$$[\bullet OH] \approx k_1[OH^-] \cdot \int [O_3]\ dt - k_2 \cdot [CO_3^{2-}] \cdot \int dt \qquad (5.1.8)$$

Combining the ozone decomposition model $[O_3] = [O_3]_0 \cdot \{F \cdot e^{-K_1 \cdot t} + (1-F) \cdot e^{-K_2 \cdot t}\}$, the hydroxyl radical formation concentration at any time is:

$$[\bullet OH] \approx k_1[OH^-] \cdot [O_3]_0 \cdot \left[F \cdot \frac{e^{-k_R \cdot t}}{-k_R} + (1-F) \cdot \frac{e^{-k_S \cdot t}}{-k_s} \right] - k_2 \cdot [CO_3^{2-}] \cdot t \qquad (5.1.9)$$

The parameters k_1 and k_2 were determined by non-liner regression software (SYSTAT 5.01).

The kinetics constants for hydroxyl radical formation reaction are listed in Table 5.1.2. And the hydroxyl radical formation data and predictive model at pH 9 and 7 are shown in Figure 5.1.9 and 5.1.10, respectively.

In Figures 5.1.9 and 5.1.10, it was observed that the predictive model fits the experimental data at pH 9 is more accurate than at pH 7. It can be attributed that the hydroxyl radical formation concentration is low and the formation time is only lasted for 30 seconds at pH 7. Therefore, the predictive model is not suitable for simulating the hydroxyl radical at pH 7. On the contrary, the high correlation coefficient at pH 9, listed in Table 5.1.2, is evident in Figure 5.1.9.

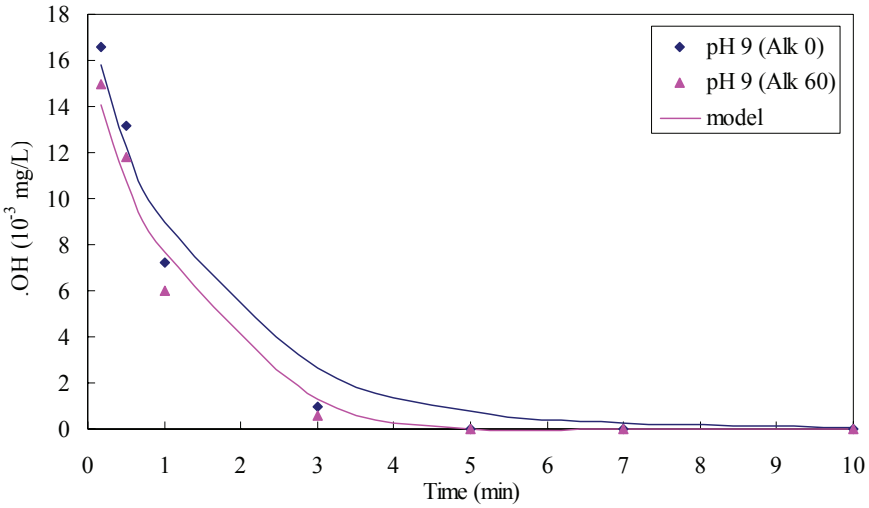

Figure 5.1.9 The hydroxyl radical formation concentration and predictive model at pH 9 in ozonation.

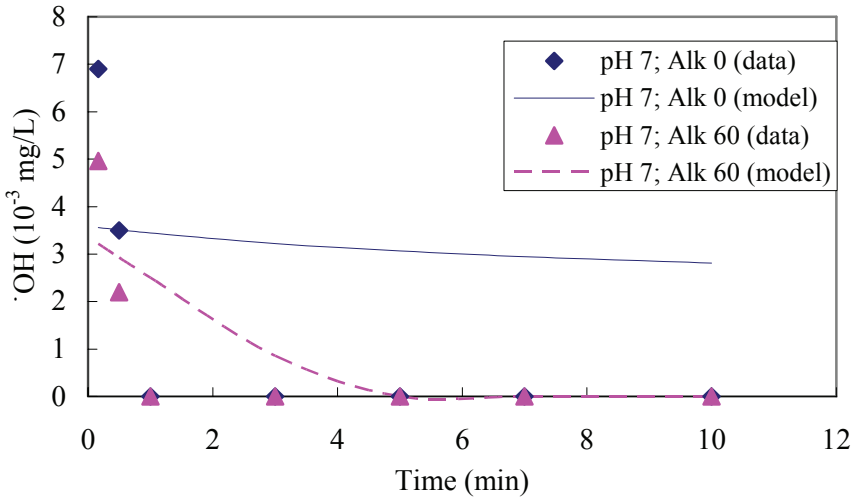

Figure 5.1.10 The hydroxyl radical formation concentration and predictive model at pH 7 in ozonation.

Table 5.1.2 Hydroxyl radical formation kinetics constants at pH 7 and 9 in ozonation

	k_1	k_2	R^2
pH 9 (Alk 0)	-7.640	-	0.981
pH 9 (Alk 60)	-6.843	0.006	0.971
pH 7 (Alk 0)	-4.976	-	0.556
pH 7 (Alk 60)	-4.659	0.012	0.637

5-1-4 O_3/UV Process

The photolysis of the aqueous ozone (O_3/UV process), called the advanced oxidation processes (AOPs) is commonly used in water and wastewater treatment plants. The mechanism of hydroxyl radical formation in the O_3/UV process is expressed as follows:

$$O_3 + H_2O + h\nu \rightarrow H_2O_2 + O_2$$

$$H_2O_2 + h\nu \rightarrow 2(\cdot OH)$$

(Mirat and Vasistas, 1987)

Figure 5.1.11 shows the measured concentration of dissolved ozone and hydroxyl radical during the ozonation and O_3/UV process. The O_3/UV process is operated at 30 Watts (UV light intensity) and saturated ozone concentration in the batch reactor. With increasing illumination time by UV light, the ozone concentration decreases rapidly and forms more hydroxyl radical.

The difference in hydroxyl radical formation between indirect ozonation and O_3/UV processes was clearly shown in Figure 5.1.12. The hydroxyl radical concentration in the O_3/UV process is higher than that in the indirect ozone process, which suggests that oxidation ability in the O_3/UV process is much stronger than that in the indirect ozone process. The order of hydroxyl radical formation concentration is ˙OH (O_3/UV)>˙OH (pH 9; Alk 0)>˙OH (pH 9; Alk 60)>˙OH (pH 7; Alk 0)>˙OH (pH 7; Alk 60).

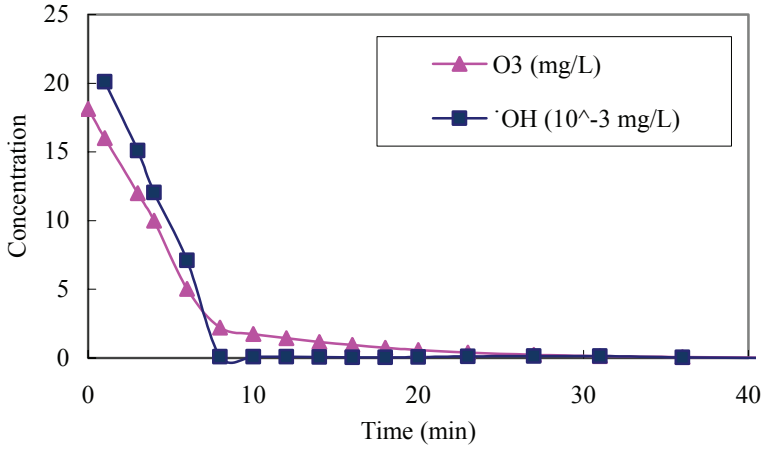

Figure 5.1.11 The measured concentration of dissolved ozone and the hydroxyl radical during the O_3/UV process

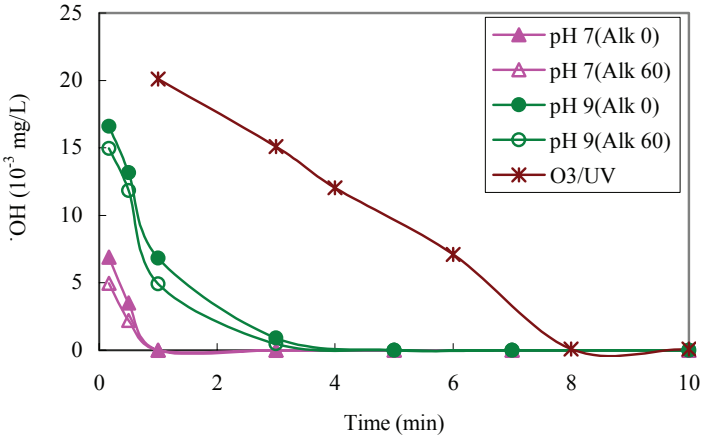

Figure 5.1.12 The difference in hydroxyl radical between the ozonation and the O_3/UV processes.

5-1-5 Ozonation (O_3/UV) of Organic Precursors in terms of TOC and UV_{254}

According to a Symon study (1990), it was suggested that the ratio of ozone dose and organic carbon (mg O_3/mg C) should be maintained between 3~6 to achieve a better removal efficiency of chlorinated by products formation potential. Since the theoretical saturated ozone concentration in 25 ^oC is approximately 18 mg/L (Standard Method 19th) and the influent TOC concentration of three model compounds is at 3 mg/L, the ozone dose of 6 mg O_3/ mg C was chosen for this experiment. Furthermore, the reaction time in ozonation and O_3/UV system is operated for 40 minutes until the ozone concentration disappeared.

Figure 5.1.13 presents the results of TOC removal efficiency in the ozonation and O_3/UV processes. The removal efficiency of TOC for three model compounds in ozonation is below 6 %, especially at pH 9 (closed to zero). This evidence suggests that the electrophilic character of ozone could only oxidize and destroy a small amount of the aromatic structure and unsaturated bond of organic matter without mineralizing the organic carbon to form carbon dioxide as well as the destruction by hydroxyl radical. Therefore, the reduction of these organic precursors in the ozonation process is very limited.

The removal efficiency of TOC for three model compounds was found to be over 40 % in the O_3/UV process, which indicates that the higher hydroxyl radical exposure can mineralize organic carbon to form carbon dioxide. It also suggested that hydroxyl radical exposure is an important factor to evaluate the TOC removal efficiency in the ozonation and O_3/UV processes.

The effect of alkalinity on the removal of TOC also was presented in Figure 5.1.13, which indicates that the natural inhibitor (alkalinity) could be negligible because of the insignificant removal efficiency of TOC in the ozonation process.

Organic compound with aromatic structure or with conjugated double bonds would absorb light in the ultraviolet wavelength range, commonly 254 nm (UV_{254}). Figure 5.1.14 illustrates the removal efficiencies of UV_{254} for the model compounds in the ozonation and O_3/UV processes. The value of UV_{254} decreases below 0.01, which is close to the detection limit of UV_{254} measured by a Spectrophotometer. Therefore, the removal efficiency of UV_{254} is up to 96 % in both the ozonation and O_3/UV processes, which indicates that the ozone and hydroxyl radical would destroy the most aromatic structure and conjugated double bonds to form ozonation by-product such as aldehyde and carboxylic acid resulting in the low value of UV_{254}.

The effect of alkalinity on the removal of UV_{254} is also shown in Figure 5.1.14, which indicates that hydroxyl radical formation concentration in the presence of inhibitor also can destroy the most aromatic structure and conjugated double bonds. Therefore, the effect of alkalinity on UV_{254} removal is negligible.

As shown in Figures 5.1.13 and 5.1.14, the difference in between TOC and UV_{254} removal for three model compounds is insignificant, because of the similar benzene structure in three model compounds, which the attack of ozone following Criegee mechanism and the nonselective reactivity of hydroxyl radical result in having the similar TOC and UV_{254} removal.

The change of the value SUVA is shown in Figure 5.1.15. In Figure 5.1.15, the values of SUVA are below 1.0 L/mg·m because of the low UV_{254} value after the ozonation and O_3/UV process. According to a Edzwald and Van (1990) study, when the value of SUVA is smaller than 2 L/mg·m, the composition in the sample is mostly non-humics, low hydrophilic materials, and low molecular weight. In other words, the sample contains relatively small amount of aromatic moieties. Therefore, the lower SUVA after the ozonation and O_3/UV processes indicates that ozone and hydroxyl radical can effectively destroy the aromatic structure and reduce chlorinated by-products formation potential (Rook et al., 1976).

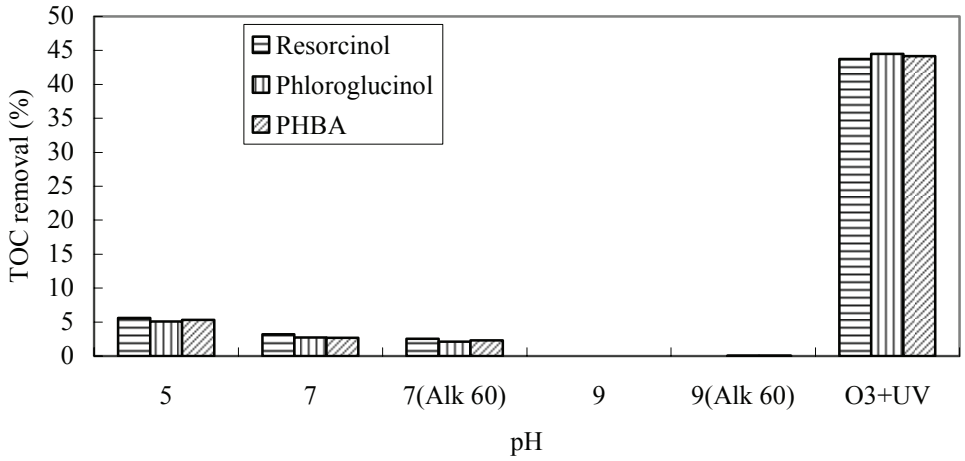

Figure 5.1.13 Decreasing of TOC at various levels of pH and alkalinity in the ozonation and O_3/UV processes for three model compounds.

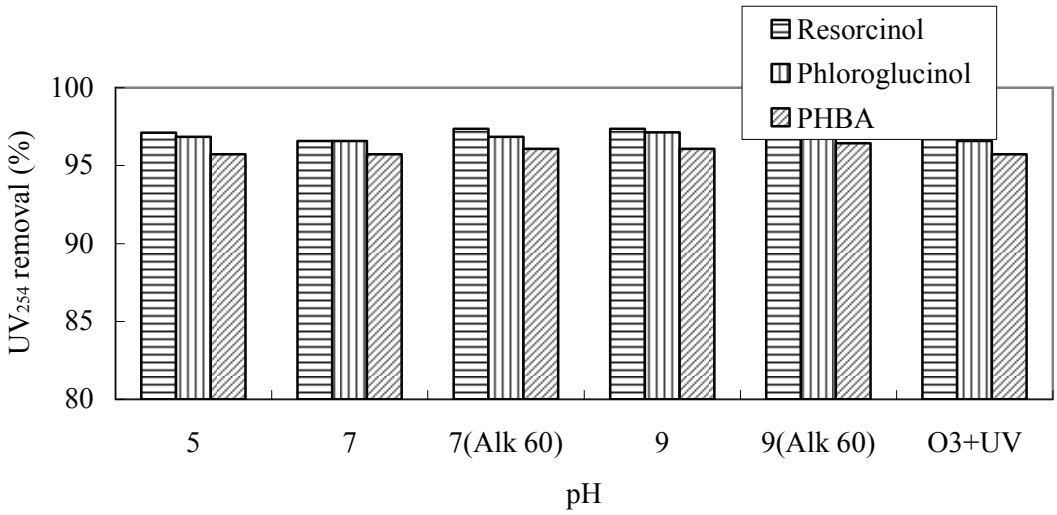

Figure 5.1.14 Reducing of UV_{254} at various levels of pH and alkalinity in the ozonation and O_3/UV processes for three model compounds

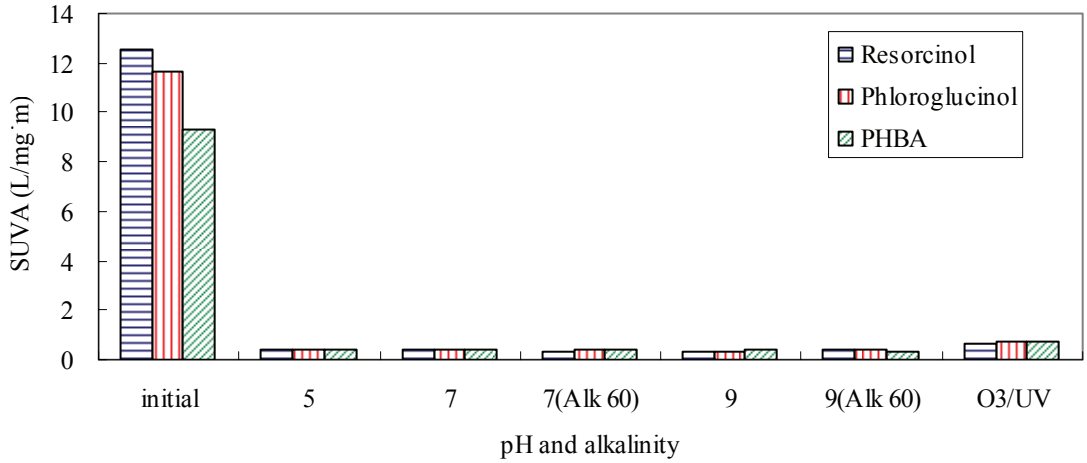

Figure 5.1.15 SUVA measured at various levels of pH and alkalinity for model compounds treated by the ozonation and O_3/UV processes

5-1-6 Formation of Ozonation By-products

According to a Glaze study (1986), the ozonation by-products include aliphatic aldehyde, hydrogen peroxide, organic peroxide, and saturated carboxylic acid. Among them, aldehyde is the most concerned because it is harmful to human health. Aldehyde consists of formaldehyde, acetaldehyde, glyoxal, and methyl glyoxal that are commonly found in ozonation.

Figures 5.1.16 shows the formation of the ozonation by-product (aldehyde) for resorcinol, phloroglucinol and *p*-hydroxybenzoic acid at different levels of pH and alkalinity treated by the ozonation and O_3/UV processes. In this study, the principal aldehyde formation is formaldehyde, especially at high pH. For instance, at pH 9 the ratio of formaldehyde formation in aldehyde formation is up to 70 %, while at pH 7 is 50 %, and pH 5 is 39 % in resorcinol. This formation suggests that hydroxyl radical (formed at pH 9) could destroy organic compound generate shorter chain by-products such as formaldehyde than ozone molecule (formed at pH 5). As shown in Figure 5.1.16, addition of alkalinity would decrease the aldehyde concentration in the indirect ozone process. The phenomenon conforms to previous finding, which state that alkalinity could reduce hydroxyl radical concentration to inhibit oxidation reaction and result in less aldehyde formation.

As shown in Figure 5.1.17, the amount of aldehyde formation is proportionate to hydroxyl radical formation, i.e., hydroxyl radical formation promotes the aldehyde formation. The order of the aldehyde formation concentration is O_3 (pH 9) > O_3 (pH 7) > O_3 (pH 5).

In the O_3/UV process, the higher hydroxyl radical exposure removes TOC by 40 % and further oxidization results in lowering aldehyde concentration to 2 μg/L. Therefore, the O_3/UV process reduces the level of harmful aldehyde in water treatment. In summary, the order of aldehyde formation with respect to the ozonation process is O_3 (pH 9; Alk=0) > O_3 (pH 9; Alk =60) > O_3 (pH 7; Alk=0) > O_3 (pH 7; Alk=60) > O_3 (pH 5) > O_3/UV. It was thus concluded that

the ozone hydroxyl radical could destroy organic precursors resulting in the cleavage of aromatic structure in the ozonation process.

The comparison of total aldehyde concentration for three model compounds at different pH levels is shown in Figure 5.1.18. Resorcinol and phloroglucinol with 2-OH and 3-OH phenolic groups lead to ring cleavage and generate aldehyde formation via the ozone and hydroxyl radical reactions (Gilbert, 1978). In Figure 5.1.18, the difference in aldehyde formation between *p*-hydroxybenzoic acid and resorcinol (or phloroglucinol) is insignificant because of the similar benzene structure characterized by the three model compounds. This hypothesis was confirmed further by analyzing the data presented in Table 5.1.3 throughout the analysis of variance (ANOVA) — F test. The assumption of H_0: difference of aldehyde formation among the three model compounds is insignificant. In Table 5.1.3, F-ratio is $0.008 < F(2, 16) = 2.8068$. Therefore, the assumption is accepted and difference of aldehyde formation among the three model compounds is insignificant.

5-2 The bromate formation in ozonation process

5-2-1Effect of bromide concentration on bromate formation

To assess the effects of the different levels of bromide concentrations on the bromate formation, the bromide concentrations were prepared at 0.25, 0.5, and 1.0 mg/L. In the batch ozonation experiment, the bromide reductions in the absence of ammonia at various reaction times are shown in Figure 5.2.1 under which the ozone doses are 9.0 and 7.0 mg/L. The bromide reductions increased with increasing reaction times and approached to a constant rate after 10 minutes. The effects of different ozone doses on bromide reductions also are shown in Figure 5.2.1 which reveals that the bromide reductions measures at 9.0 mg/L of ozone dose are higher than that at 7.0 mg/L of ozone dose.

The bromate formation with different levels of bromide concentrations is shown in Figure 5.2.2. The bromide concentration influences the bromate formation during the ozonation process. The bromate concentration increased with increasing bromide concentration, but not proportional to the ratio of initial bromide concentration. In Figure 5.2.2, a sharp increase of bromate formation was observed at reaction times from 0 to 10 minutes. After 10 minutes, the bromate formation stabilized because the ozone was mostly consumed in the first 10 minutes.

The effects of different ozone dose on bromate formation also are shown in Figure 5.2.2 which reveals that the bromate formation measured at 9.0 mg/L of ozone dose are higher than that at 7.0 mg/L of ozone dose. Comparing the effect of different ozone dose on bromate formation reveals that bromate formation increased with increasing bromide concentrations.

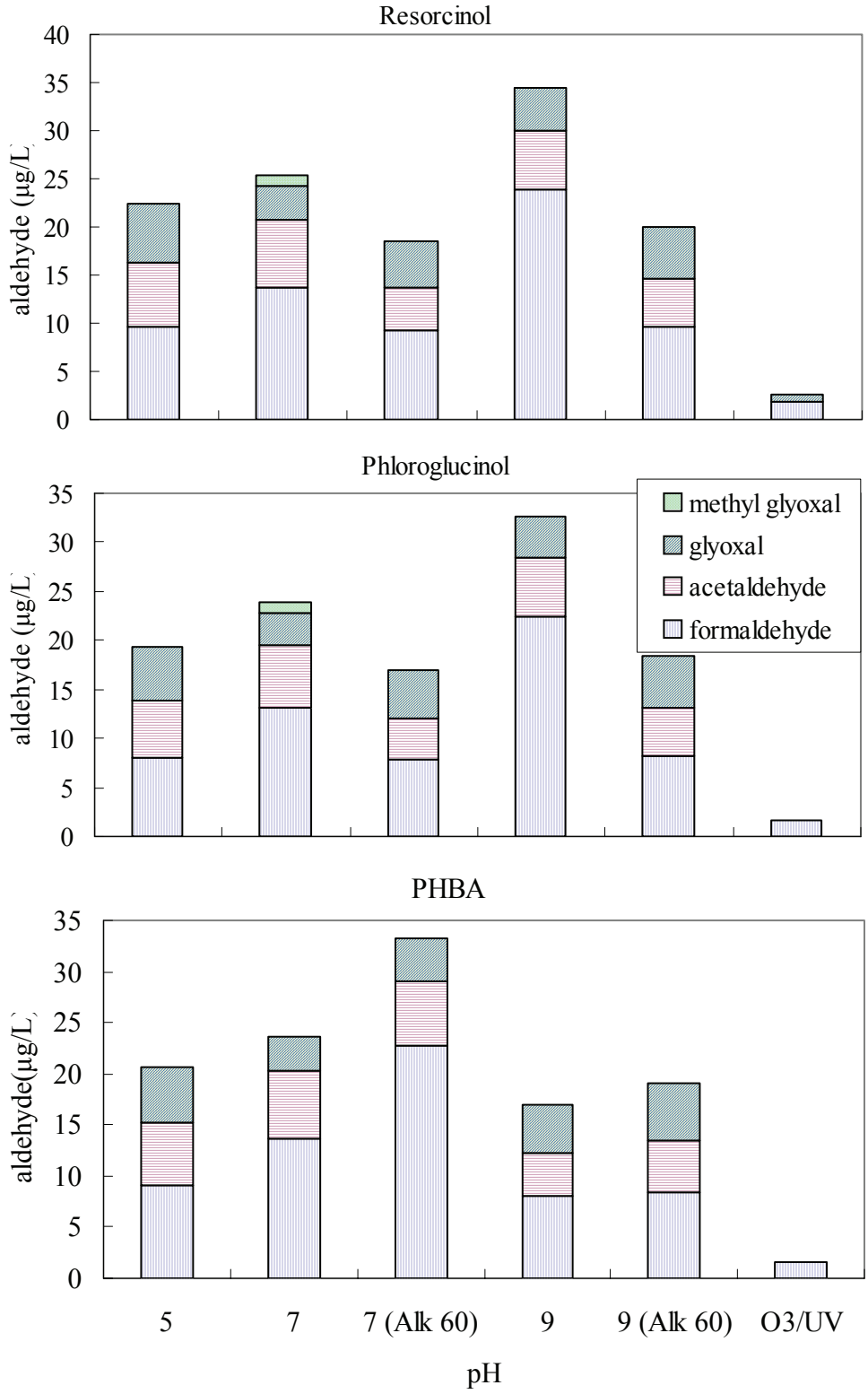

Figure 5.1.16 The formation of aldehyde for resorcinol, phloroglucinol, and *p*-hydroxylbenzoic acid at the different levels of pH and alkalinity in the ozonation and O_3/UV processes

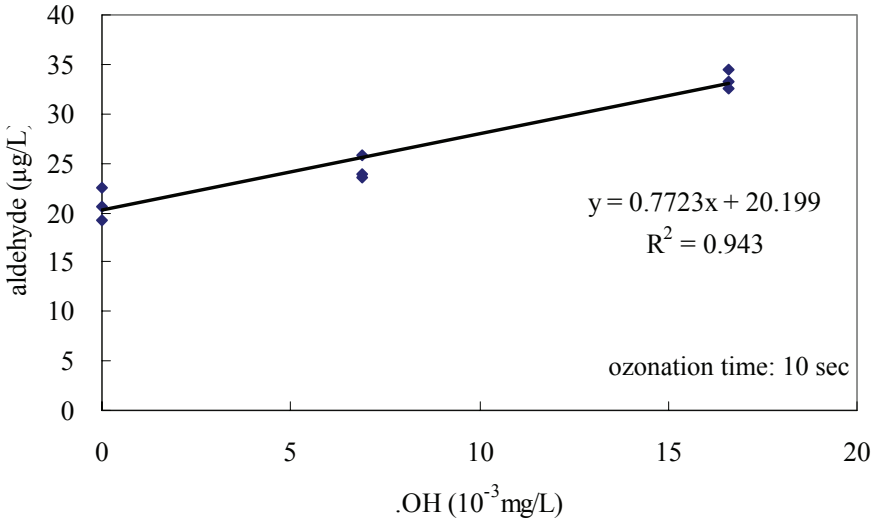

Figure 5.1.17 Correlation between hydroxyl radical and aldehyde formation concentration for three model compounds

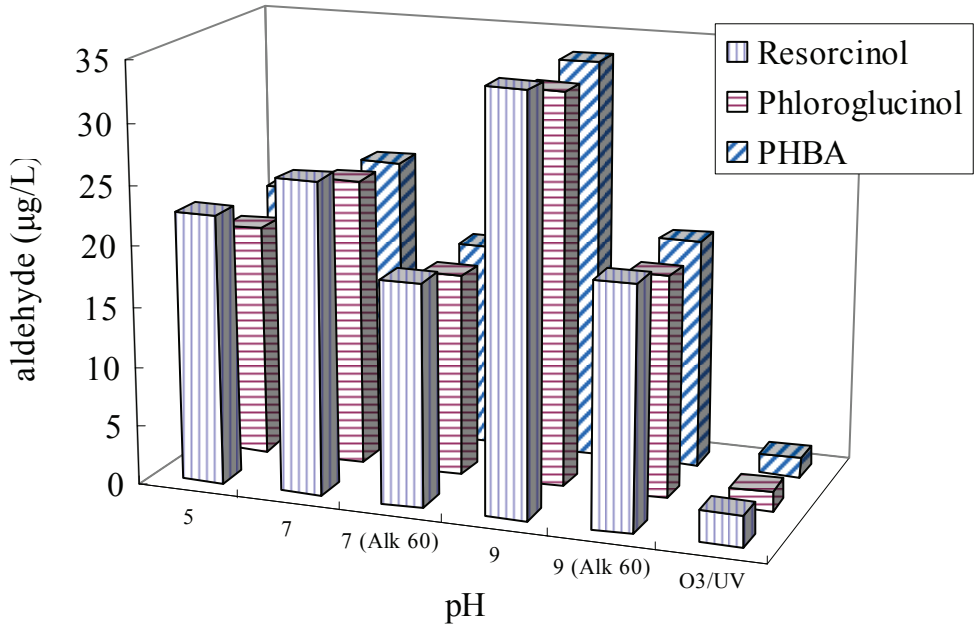

Figure 5.1.18 Comparison of total aldehyde concentration among three model compounds

Table 5.1.3 Analysis of variance (ANOVA) — F test for aldehyde formation

Source of variance	Sum of Square	Degree of freedom	Mean of square	F-ratio	F(2,12)
Between	11.271	2	5.636		
Within	8491.901	12	107.72	0.008	2.8068
Sum	8503.172	14	-		

The relationships between bromide reduction and bromate formation are shown in Figure 5.2.3 which reveals that bromate formation increased with increasing bromide reductions. However, both of the bromate formation and bromide reduction are varied with the ozone doses (9.0 and 7.0 mg/L). Both the bromate formation and bromide reduction measured at 9.0 mg/L of ozone dose are higher than those at 7.0 mg/L. Therefore, the effect of different ozone dose on bromate formation and bromide reduction are significant.

Figure 5.2.3 also shows bromate formation percentages (total bromate formation / total bromide reduction) which reveal that the bromate formation percentages increased with increasing initial bromide concentrations. Therefore, the effect of bromide concentration on bromate formation is significant and the increasing bromide concentration increases the bromate formation.

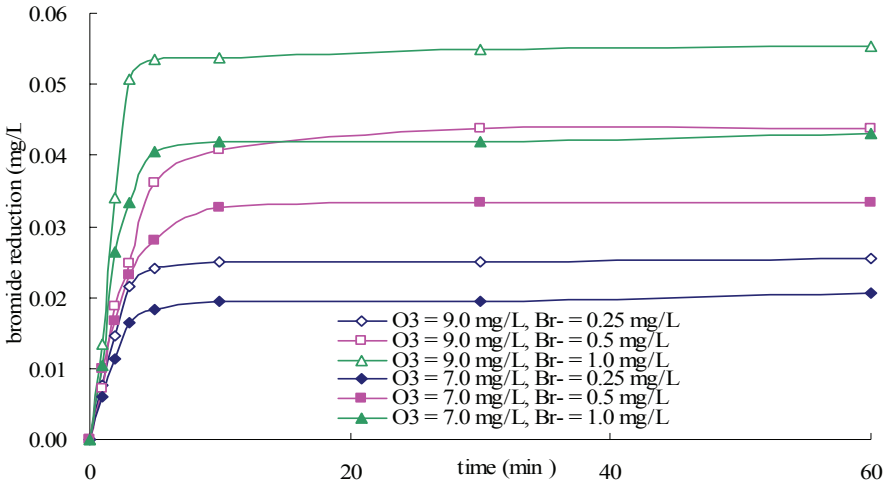

Figure 5.2.1 The bromide reduction at different levels of bromide concentrations in the ozonation process

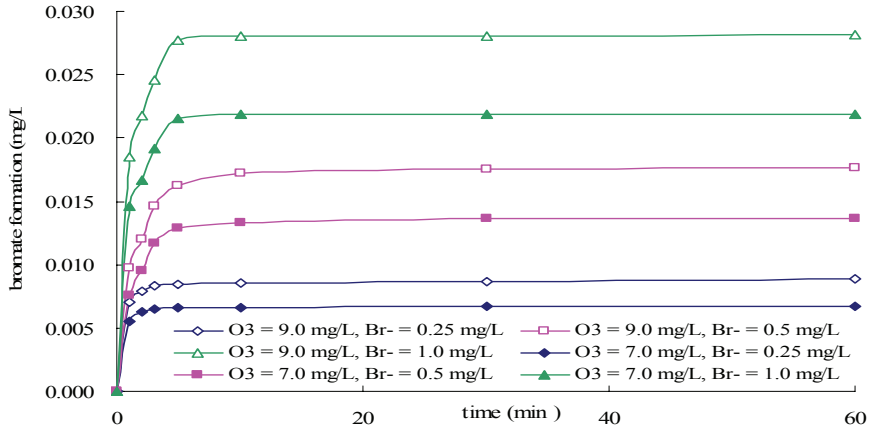

Figure 5.2.2 Effect of bromide concentration on bromate formation in the ozonation process

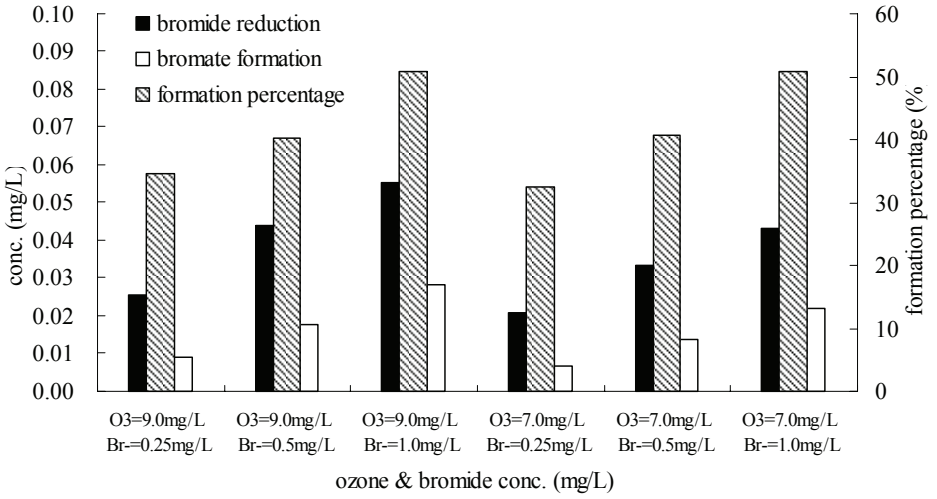

Figure 5.2.3 The relationship between bromide reduction and bromate formation

5-2-2 Effect of ammonia concentration on bromate formation

The ammonia reductions measured at different levels of bromide concentrations are shown in Figures 5.2.4 and 5.2.5 under which the ozone dose are 9.0 and 7.0 mg/L, respectively. The results indicate that most ammonia reductions were observed at reaction time from 0 to 10 minutes. At ammonia concentrations of 0.25 and 1.0mg/L and ozone dose at 9.0 mg/L, the ammonia reduction percentages range from 57 to 58% and 59 to 74%, respectively. When the ammonia concentrations is at 0.25 and 1.0 mg/L and the ozone dose is at 7.0 mg/L, the ammonia reduction percentages range from 60 to 68% and 65 to 74%, respectively. Within this time interval (0 to 10 minutes), ammonia reacts with ozone or reacts with hypobromite (OBr^-) and hypobromous acid (HOBr) resulting in a high ammonia reduction. However, after 10 minutes reaction time, ammonia only reacts with hypobromite and hypobromous acid to form monobromamine. Under this condition, the ammonia reduction approaches a constant rate in the presence of the hypobromite and hypobromous acid.

As shown in Figures 5.2.6 and 5.2.7, the bromide concentration varies with different levels of ammonia concentrations. According to a previous study, ozone reacts with bromide and ammonia which produces bromate and nitrite (nitrate). Adding ammonia to water results in an incomplete reaction between bromide and ozone because the bromide reacts directly with ozone and indirectly with ammonia. As shown in Figures 5.2.6 and 5.2.7, the reduction of bromide in the presence of ammonia is higher than that without ammonia.

At the initial ammonia concentration of 1.0 mg/L and the ozone dose of 9.0 mg/L, the order of bromide reductions are as follows: $Br^- = 1.0 > Br^- = 0.5 > Br^- = 0.25$ mg/L. Under this condition, the order of bromide reductions is the same as when the ozone dose is at 7.0 mg/L. Figures 5.2.6 and 5.2.7 also show the variations of bromide concentrations at different ozone doses. The data indicates that the variation of bromide reduction measures at 9.0 mg/L of ozone dose is higher than that at 7.0 mg/L of ozone dose regardless of the presence of ammonia.

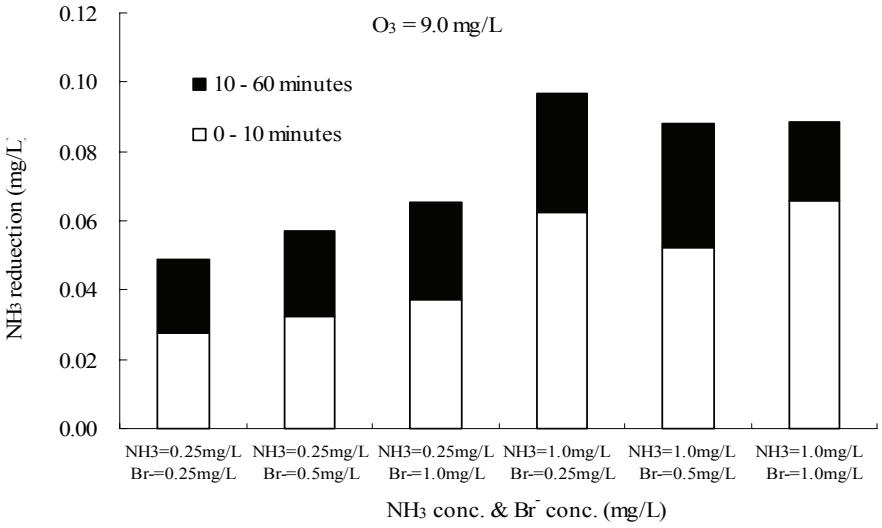

Figure 5.2.4 The reduction of ammonia concentration at 9.0 mg/L of ozone dose

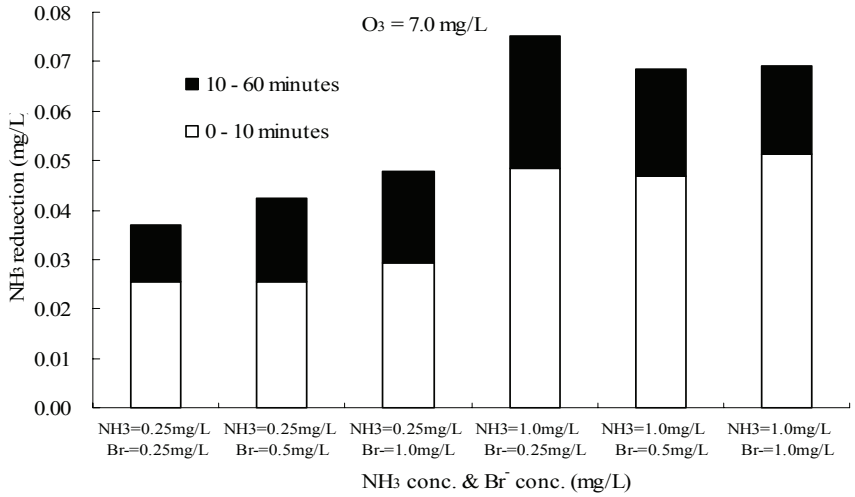

Figure 5.2.5 The reduction of ammonia concentration at 7.0 mg/L of ozone dose

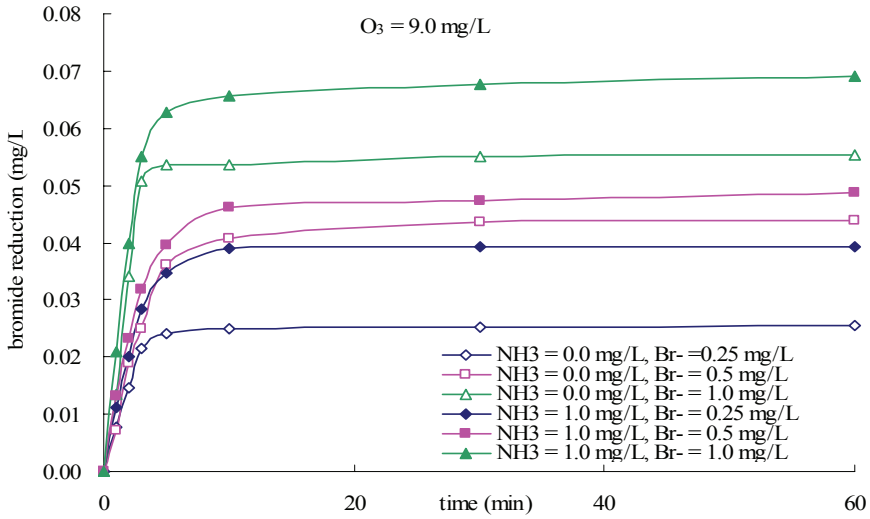

Figure 5.2.6 Effect of ammonia concentration on bromide reduction at 9.0 mg/L of ozone dose

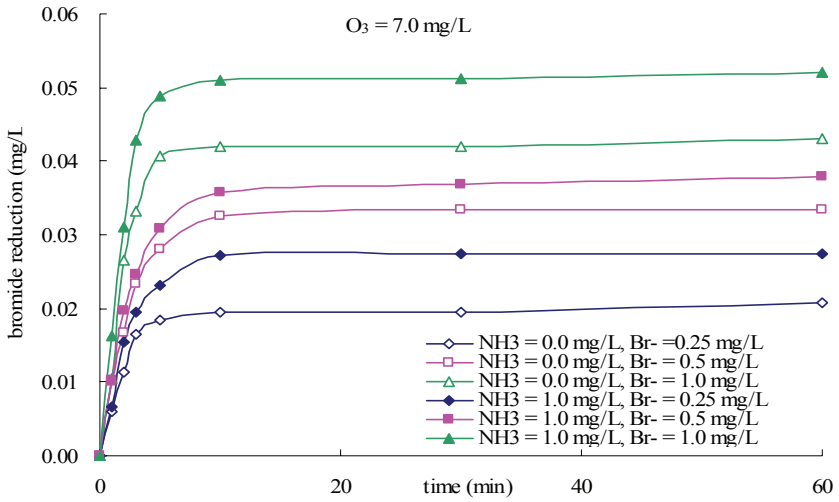

Figure 5.2.7 Effect of ammonia concentration on bromide reduction at 7.0 mg/L of ozone dose

Figures 5.2.8 and 5.2.9 illustrates the effects of ammonia concentrations on bromate formations at various reaction times when the ozone doses are at 9.0 and 7.0 mg/L. Figures 5.2.8 and 5.2.9 also show that the effects of ammonia are insignificant when the bromide concentration is maintained at 0.25 and 0.5 mg/L, indicating that bromide is not easily converted to hypobromite and hypobromous acid to react with ammonia.

When the initial bromide concentration is at 1.0 mg/L, the effect of ammonia on the bromate formation is significant. This observation suggests that at higher bromide concentrations, bromide could react with ozone to form more hypobromite and hypobromous acid and could react with ammonia to form monobromamine. The reaction between ammonia and bromide at reaction time of 0 to 10 minutes results in a significant reduction of ammonia concentration. After reaction times greater than 10 minutes, the residual hypobromite and hypobromous acid were less and the ammonia concentration was reduced slowly. In Figures 5.2.8 and 5.2.9, the data shows that the final bromate concentration may be depressed to 6% and 4% at ammonia concentration of 1.0 mg/L and bromide concentration at 0.25 mg/L. However, if the initial bromide concentration is at 1.0 mg/L, the final bromate concentration may be reduced to 22% and 12%.

Because of the high oxidation power of ozone, ammonia is oxidized to form nitrite and nitrate in ozonation process. In the presence of bromide and ammonia, the hypobromite and hypobromous acid are formed during the reaction between ozone and bromide. Because hypobromite is the major reaction component in the bromate formation, ammonia reacts with hypobromite and hypobromous acid which results in a decrease of bromate formation. The reaction between ozone and ammonia increases the ozone consumption and inhibits the reaction between bromide and ozone. Thus, the presence of ammonia in source water could not only decrease the bromate formation, but also reduce the oxidant ability of ozone.

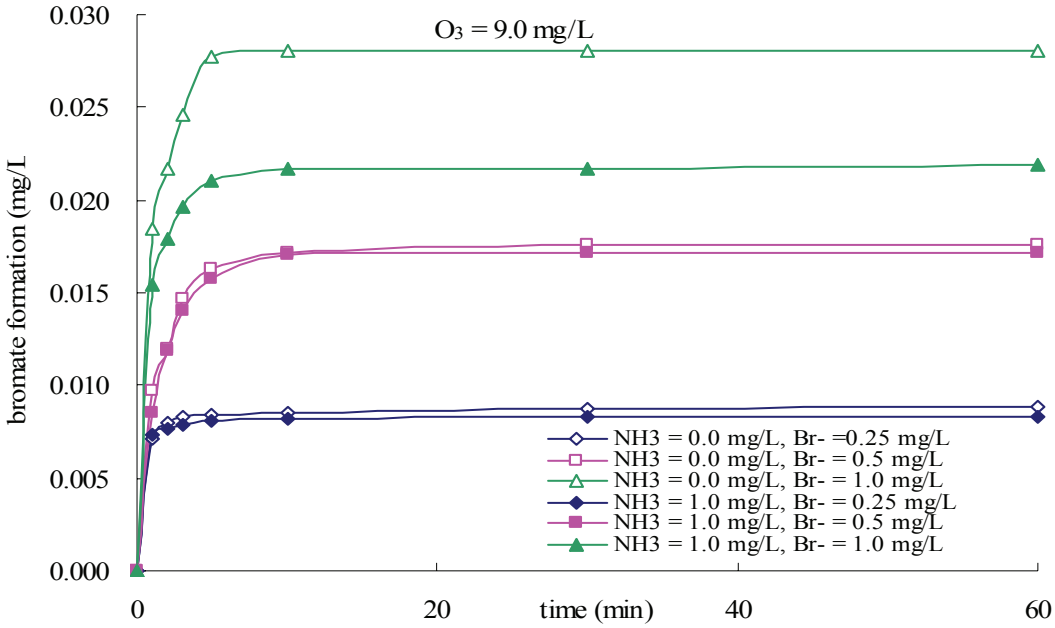

Figure 5.2.8 Effect of ammonia concentration on bromate formation at 9.0 mg/L of ozone dose

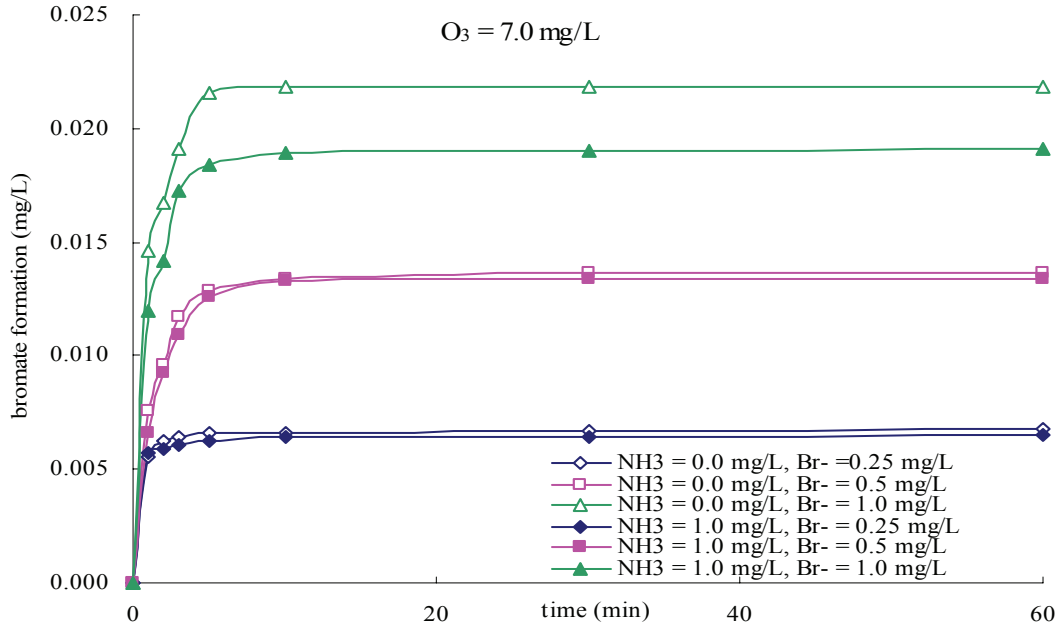

Figure 5.2.9 Effect of ammonia concentration on bromate formation at 7.0 mg/L of ozone dose

5-3 Chlorine Demand and Chlorine Decay Model

In this investigation, these three model compounds were first pretreated by the ozonation and O_3/UV processes and then followed by the general procedure to determine the chlorine demand in chlorination process (APHA, 1998).

5-3-1 Chlorine Demand

Figure 5.3.1 presents the measured residual chlorine concentration for resorcinol, phloroglucinol, and p-hydroxybenzoic acid at various reaction time during the chlorination process. The chlorine demand was increased as the chlorine contact time increased. The chlorine consumption rate is fast during the first 6 hours (rapid reaction) and then the rate gradually slows down (slow reaction).

As shown in Figure 5.3.1, the chlorine consumption increases with decreasing pH. Because the model compounds selectively destroyed by ozone molecule form more complex hydrocarbon compounds than by hydroxyl radical, the more complex compounds would then proceed to the addition, substitution and oxidation reactions by chlorine and result in more chlorine demand. In the presence of alkalinity, hydroxyl radical oxidation reaction would be inhibition, which causes the higher chlorine demand than that of without alkalinity in the indirect ozone process. Further, the negative correlation between pH and chlorine demand (in 168 hours) for three model compounds is shown in Figure 5.3.2, which suggests that the ozone molecule would promote the chlorine demand and hydroxyl radical would reduce the chlorine demand.

Figure 5.3.1 also presents the chlorine consumption of three model compounds after the O_3/UV process which is greatly different from that of the ozonation process. For instance, the residual chlorine concentration after 168 hours in the O_3/UV process is about 1.6 mg/L, which is lower than other experiments conducted during the ozonation process (4.44 ~ 6.27 mg/L). The phenomenon indicates that the high hydroxyl radical exposure ($mg/L \times \min$) in the O_3/UV process would oxidize the organic precursors more completely and further transfer hydroxyl radical electrons to the carbon ions of reactants resulting in the additional electrophilic character on the carbon ions. These specific carbon ions would proceed the intensely addition and substitution reactions by chlorine. Therefore, the chlorine consumption in the O_3/UV system is much higher than that of the ozonation process and the order of chlorine consumption is O_3/UV > O_3 (pH 5) > O_3 (pH 7; Alk=60) > O_3 (pH 7; Alk=0) > O_3 (pH 9; Alk=60) > O_3 (pH 9; Alk=0).

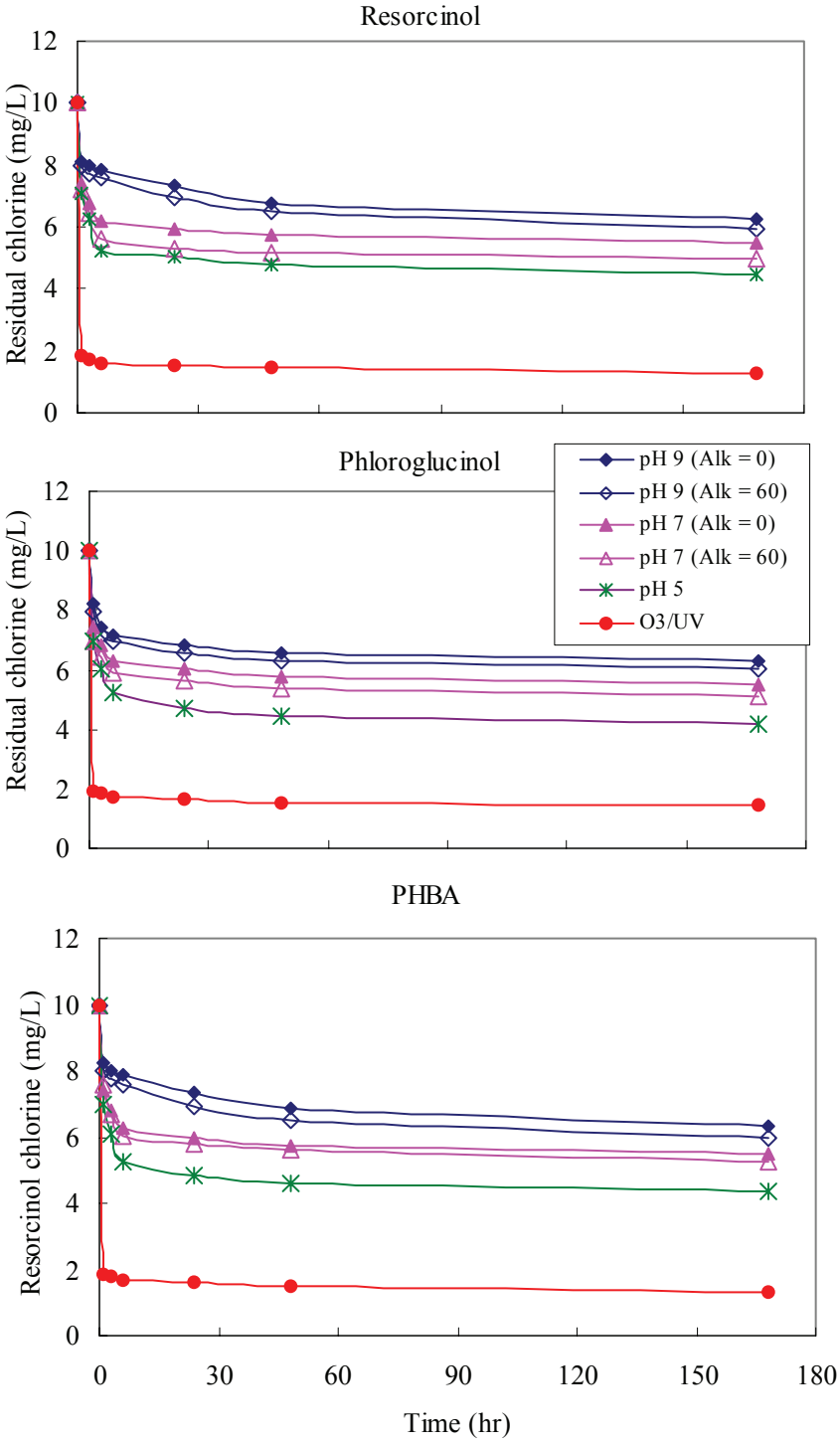

Figure 5.3.1. The measured residual chlorine concentration for resorcinol, phloroglucinol, and *p*-hydroxybenzoic acid at various reaction times

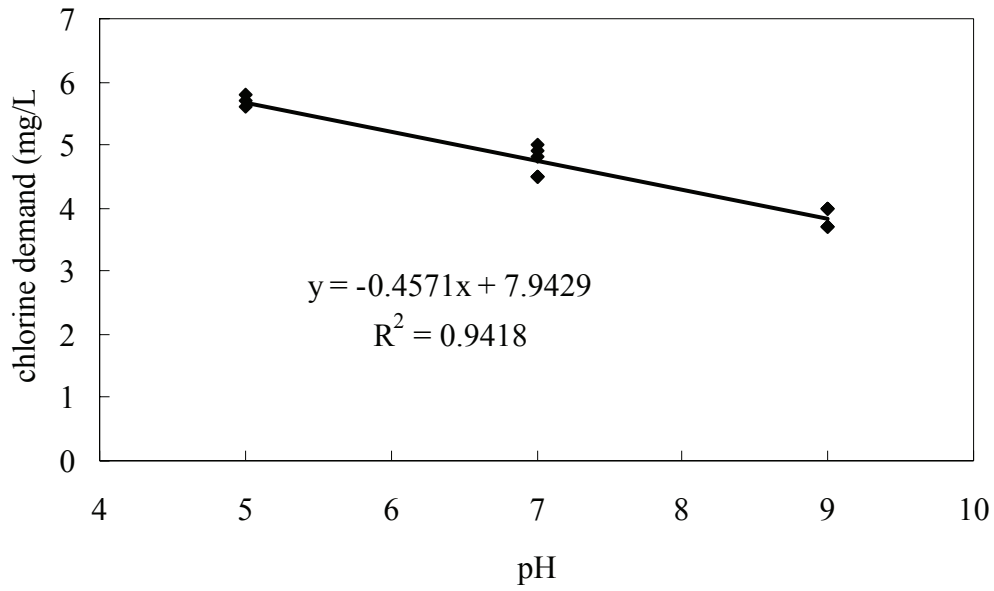

Figure 5.3.2 Correlation between pH and chlorine demand

Comparisons of chlorine demand among three organic precursors, for resorcinol and phloroglucinol with 2-OH and 3-OH phenolic groups under the attacks of ozone and hydroxyl radical would lead to ring cleavage and the formation of similar formic acid, C_2-C_6 dicarboxylic acid, and aldehyde (Gilbert, 1978; Yamamoto et al., 1979). Since similar products were generated by the ozonation process, one would expect to observe the difference of chlorine demand for resorcinol and phloroglucinol is insignificant. The difference in chlorine consumption between *p*-hydroxybenzoic acid and resorcinol (or phloroglucinol) is insignificant because of the similar benzene structure characterized by the three model compounds.

This hypothesis can be confirmed further by analyzing the data in Table 5.3.1 via the analysis of variance (ANOVA) — F test method. The assumption of H_0: difference of chlorine demand among the three model compounds is insignificant. In Table 5.3.1, F-test is $0.0035 < F(2, 12) = 2.8068$. Therefore, the assumption is accepted and difference of chlorine demand among the three model compounds is insignificant.

Table 5.3.1 Analysis of variance (ANOVA) — F test for chlorine demand

Source of variance	Sum of Square	Degree of freedom	Mean of square	F-ratio	F(2,12)
Between	0.0044	2	0.0022		
Within	7.502	12	0.6251	0.0035	2.8068
Sum	7.5064	14	-		

5-3-2 Chlorine Decay Model

The chlorine decay model is determined as the second order in the rapid reaction and the first order in the slow reaction, which is modified as:

$$C(t) = C_0\{[\frac{f}{f \cdot C_0 \cdot K_R \cdot t + 1}] + (1-f) \cdot e^{-K_s \cdot t}\}$$

The chlorine decay constants for three model compounds for parallel first and second order reaction in the ozonation (O_3/UV)/chlorination process are listed in Table 5.3.2. In the ozonation/chlorination processes, the rate constants for rapid reaction (K_R) are higher than those of the slow reaction (K_S) for these compounds, which suggests that the reaction proceeds rapidly in the beginning as K_R, and is followed by a slow reaction afterwards as K_S. Comparison of K_R value between the different pH levels, the K_R value increases with increasing pH, which indicates that the ozonated sample by hydroxyl radical result in a faster chlorine decay rate than that by the ozone molecule. In the presence of alkalinity, the inhibition resulted in the decreases of the K_R values. However, the predicted value of K_R and K_S in the O_3/UV process is different from that of the ozonation process. The value of K_R (0.001) is smaller than K_S (3.878 ~ 3.931) for three model compounds. In summary, the order of K_R in the ozonation and O_3/UV processes is O_3 (pH 9; Alk=0) > O_3 (pH 9; Alk=60) > O_3 (pH 7; Alk=0) > O_3 (pH 7; Alk=60) > O_3 (pH 5)>> O_3/UV.

The lower chlorine demand at high pH resulted in lowering f in the ozonation (O_3/UV) / chlorination process as shown in Table 5.3.2. In the presence of alkalinity, the inhibition would increase the value of f. Therefore, the order of f is O_3 (pH 5) > O_3 (pH 7; Alk=60) > O_3 (pH 7; Alk=0) > O_3 (pH 9; Alk=60) > O_3 (pH 9; Alk=0) >> O_3/UV. The deviation between the experimental data and predictive model, and the chlorine decay constants from a combination of three model compounds are listed in Table 5.3.3. It is noted that the low derivation (Table 5.3.3) and high correlation coefficient (Table 5.3.2) indicates the parallel first and second order chlorine decay model can accurately simulate the low-MW organic precursors in the ozonation (O_3/UV) / chlorination processes. Figure 5.3.3 shows the residual chlorine concentration for resorcinol, phloroglucinol and *p*-hydroxybenzoic acid at various reaction times and the predictive curve of the model, in which the plots are observed data, and the solid lines are predictive data for the predictive model.

5-4 DBP Formation and Predictive Model

5-4-1 THM formation

Chlorination of natural organic matter results in the formation of various chlorinated by-products. Trihalomethanes (THMs) are considered the major chlorinated by-products including chloroform ($CHCl_3$), dichlorobromomethane ($CHCl_2Br$), chlorodibromomethane ($CHClBr_2$), and Bromoform ($CHBr_3$). In this investigation, the THM formation for resorcinol, phloroglucinol and *p*-hydroxybenzoic acid, which was pretreated by the ozonation and O_3/UV

processes, is shown in Figure 5.4.1. The THM formation concentration raises with increasing chlorine consumption and contact time. At different pH levels, the order of THM concentration is as follows as O_3 (pH 9) > O_3 (pH 7) > O_3 (pH 5), which suggests that the hydroxyl radical destroys aromatic structure completely and form shorter chain hydrocarbon compounds that enhances the THM formation. The THM formation increases with increasing pH, which is consistent with the findings of a Reckhow and Singer study (1985).

In the presence of alkalinity, the inhibition reaction results in less THM formations at pH 7 and 9. The effect of alkalinity inhibition is more significant at pH 9 than that of pH 7 because the hydroxyl radical is the predominant oxidant at pH 9. Therefore, the difference of alkalinity inhibition in THM formations is more significant at pH 9.

Table 5.3.2 Chlorine decay constants for parallel first and second order reaction

organics	parameter	ozonation					O_3/UV
		Alkalinity = 0			Alkalinity = 60		
		pH 5	pH 7	pH 9	pH 7	pH 9	
R	K_R	0.235	0.359	0.841	0.254	0.660	0.001
	K_S	0.001	0.001	0.001	0.001	0.001	3.878
	f	0.515	0.415	0.250	0.482	0.283	0.166
	R^2	0.992	0.996	0.977	0.995	0.982	0.999
P	K_R	0.216	0.392	0.660	0.323	0.532	0.001
	K_S	0.001	0.001	0.001	0.001	0.001	3.931
	f	0.540	0.405	0.242	0.448	0.338	0.176
	R^2	0.997	0.997	0.978	0.999	0.995	0.999
PHBA	K_R	0.223	0.380	0.740	0.283	0.660	0.001
	K_S	0.001	0.001	0.001	0.001	0.001	3.957
	f	0.529	0.408	0.248	0.434	0.283	0.170
	R^2	0.996	0.997	0.998	0.978	0.982	0.999
combination of R, P, and PHBA	K_R	0.224	0.377	0.744	0.285	0.609	0.001
	K_S	0.001	0.001	0.001	0.001	0.001	3.922
	f	0.528	0.409	0.246	0.455	0.301	0.171
	R^2	0.993	0.996	0.975	0.989	0.969	0.999

Model: $C(t) = C_0\{[\frac{f}{f \cdot C_0 \cdot K_R \cdot t + 1}] + (1-f) \cdot e^{-K_s \cdot t}\}$

Table 5.3.3 Deviation between the experimental data and predictive model

Organics	Ozonation		Chlorination	Predictive Model	Statistics
(TOC)	pH	Alkalinity	Residual Cl_2 (mg/L)	Predictive Cl_2 (mg/L)	Deviation (%)
	5	**0**	4.44	4.13	6.98
R	**7**	**0**	5.49	4.96	9.65
(3 mg/L)	**9**	**0**	6.27	6.34	1.12
	7	**60**	4.97	4.40	11.47
	9	**60**	5.96	6.07	1.85
	O_3/UV	**0**	1.25	1.30	4.00
	5	**0**	4.18	3.92	6.22
P	**7**	**0**	5.49	5.04	8.20
(3 mg/L)	**9**	**0**	6.41	6.42	0.16
	7	**60**	5.12	4.68	8.59
	9	**60**	6.07	5.61	7.58
	O_3/UV	**0**	1.46	1.36	6.85
	5	**0**	4.34	4.00	7.83
PHBA	**7**	**0**	5.49	5.02	8.56
(3 mg/L)	**9**	**0**	6.33	6.37	0.63
	7	**60**	5.23	4.81	8.03
	9	**60**	5.96	6.07	1.85
	O_3/UV	**0**	1.31	1.32	0.76

The high TOC removal, high chlorine consumption, and less THM formation are found in the O_3/UV process. This suggests that TOC is a major parameter in evaluating THM formations, i.e., a high TOC removal results in less THM formations. However, the relationship between chlorine consumption and THM formations found by Boyce (1983) is not consistent with the experimental data in the O_3/UV process of this study, i.e., the higher chlorine consumption correspond to lower THM formation in the comparison between ozonation and O_3/UV processes. The order of THM formation potentials (THMFP) is O_3 (pH 9; Alk=0) > O_3 (pH 9; Alk=60) > O_3 (pH 7; Alk=0) ¡ O_3 (pH 7; Alk=60) >> O_3 (pH 5) > O_3/UV process.

The comparisons of THM formation potentials with these three organic precursors are listed in Table 5.4.1. The similar benzene structure of three model compounds destroyed by ozone and hydroxyl radical generates the insignificant difference of THM formation (Gilbert et al., 1976). This evidence was validated further by analyzing the data presented in Table 5.4.2 via the analysis of variance (ANOVA) — F test method. The assumption of H_0: difference of THM formations among the three model compounds is insignificant. In Table 5.4.2, F-test is $0.0012 < F(2, 12) = 2.8068$. Therefore, the assumption is accepted and the difference of THM formation among the three model compounds is insignificant.

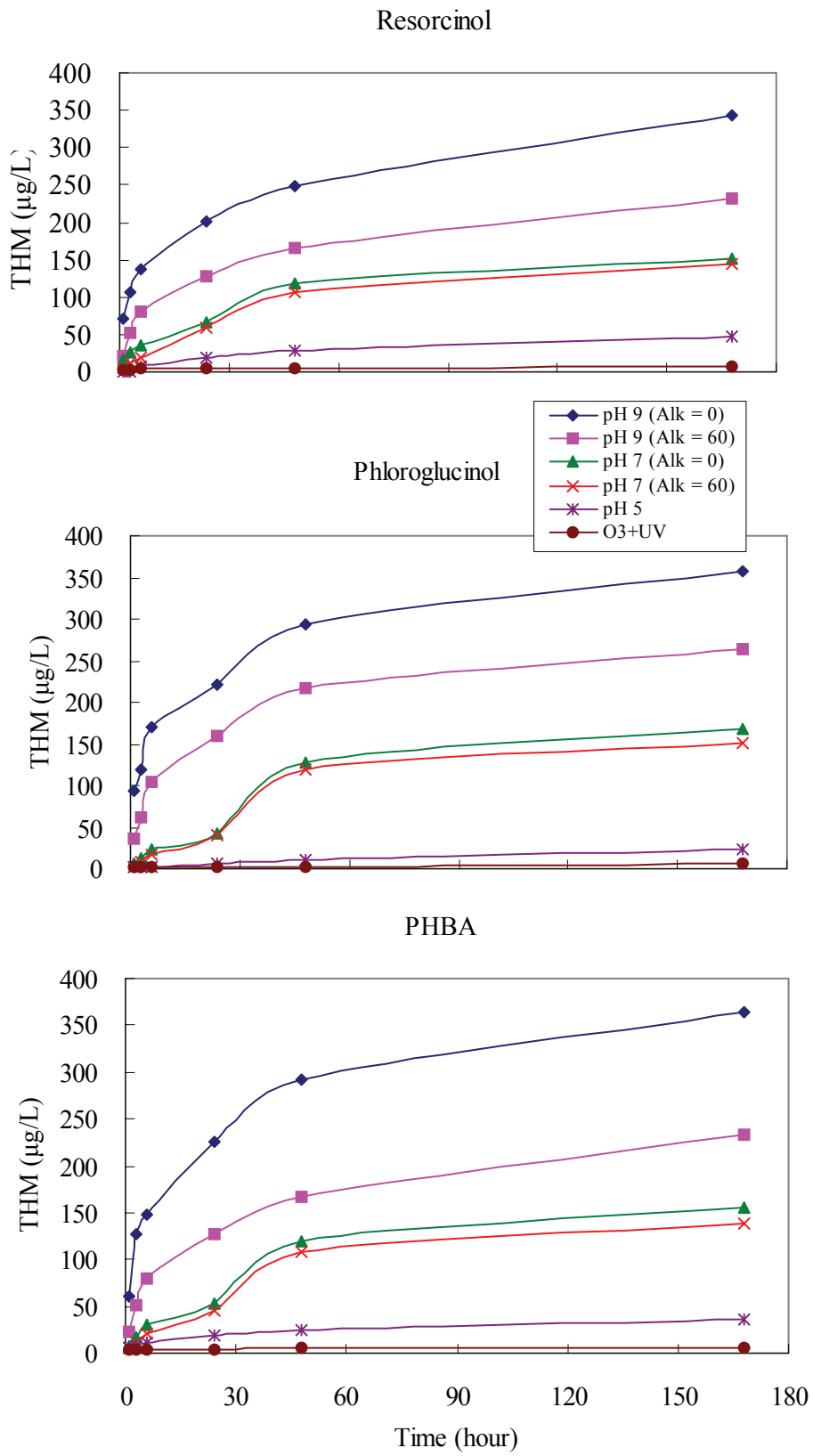

Figure 5.4.1 THM formation for resorcinol, phloroglucinol and p-hydroxybenzoic acid pretreated by ozonation at different level of pH and alkalinity, and O_3/UV processes

Other important indexes for predicting THM formation are specific THMFP (μg THM / mg TOC) and α (μg THM / mg Cl_2 consumed) as also listed in Table 5.4.1. Specific THMFP is used to evaluate the effect of TOC on THMFP. Because of the low TOC removal in the ozonation process, the value of specific THMFP is correlated to THMFP, and the order of the specific THMFP is O_3 (pH 9; Alk=0) > O_3 (pH 9; Alk=60) > O_3 (pH 7; Alk=0) > O_3 (pH 7; Alk=60) >> O_3 (pH 5). The value of α indicates THM formations is derived from per unit of Cl_2 consumed, called THM yield coefficient. The THM yield coefficient is an common index to determine the THM formation potential (Gang, 2002). The order of α is O_3 (pH 9; Alk=0) > O_3 (pH 9; Alk=60) > O_3 (pH 7; Alk=0) >O_3 (pH 7; Alk=60) >> O_3 (pH 5). Because of the low level of THM formations in the O_3/UV process, the specific THMFP and α are the smallest value among all the processes. It also indicates that the O_3/UV process has the least THMFP and the O_3 (pH 9; Alk=0) process has the highest THMFP.

Table 5.4.1 Summary of THM formation of three model compounds pretreated by ozone

Organics	**Ozonation**		**Chlorination**		
(TOC)	**pH**	**Alkalinity**	**THMFP * (μg/L)**	**Specific THMFP ****	**α*****
R (3 mg/L)	**5**	**0**	47.9	16.8	8.6
	7	**0**	152.2	51.9	33.7
	9	**0**	342.8	112.8	91.9
	7	**60**	145.4	49.3	29.7
	9	**60**	232.6	76.8	57.6
	O_3/UV	**0**	6.2	3.7	0.7
P (3 mg/L)	**5**	**0**	33.7	11.8	5.8
	7	**0**	169.0	58.0	37.5
	9	**0**	356.9	119.1	95.7
	7	**60**	150.9	51.4	30.9
	9	**60**	263.1	87.8	65.9
	O_3/UV	**0**	6.2	3.7	0.7
PHBA (3 mg/L)	**5**	**0**	36.9	12.9	6.5
	7	**0**	155.3	53.0	34.5
	9	**0**	364.1	121.0	98.4
	7	**60**	138.9	47.2	28.9
	9	**60**	232.6	77.3	58.2
	O_3/UV	**0**	6.4	3.8	0.7

* THMFP: THM formation in 168 hours

** Specific THMFP: THMFP (μg/L) / Residual TOC (mg/L) after ozonation

*** α: THMFP (μg/L) / Cl_2 demand (mg/L) after 168 hours

Table 5.4.2 Analysis of variance (ANOVA) — F test for THM formation

Source of variance	Sum of Square	Degree of freedom	Mean of square	F-ratio	F(2,12)
Between	335.536	2	167.768		
Within	167798.522	12	13955.248	0.0012	2.8068
Sum	168134.058	14	-		

5-4-2 HAA formation

The HAA is another important chlorinated by-product in the chlorination process. There are nine kinds of HAA compounds defined in Method 552.2, USEPA. Because no bromide ions were introduced in the samples of this study, only three HAA compounds were investigated in this study. These three HAA compounds are monochloroacetic acid (MCAA), dichloroacetic acid (DCAA) and trichloroacetic acid (TCAA).

The HAA formation for resorcinol, phloroglucinol and *p*-hydroxybenzoic acid is shown in Figure 5.4.2. In these figures, the amount of HAA increases with increasing contact time by chlorine, which correlates to THM formation. At different pH levels, the order of HAA formation is O_3 (pH 9) > O_3 (pH 7) > O_3 (pH 5). However, according to a Reckhow and Singer (1985) study, the low pH results in a large amount of HAA formation, which suggests that it might have other major factors beside pH influencing the HAA formation. At high pH levels, the destruction of organic compounds by hydroxyl radical forms more shorter hydrocarbon compounds than that effect of ozone molecules. These hydrocarbon compounds promote more HAA formations. Therefore, the HAA formation increases with increasing pH. A similar effect was observed for THM formations.

In the presence of alkalinity, the inhibition reaction leads to less HAA formations at pH 7 and 9. The hydroxyl radical oxidation process is the main reaction at pH 9, which results in a significant effect of alkalinity inhibition than at pH 7. Therefore, the difference of alkalinity inhibition in HAA formations is significant at pH 9. The high TOC removal reduces the HAA formation concentration in the O_3/UV process. In this study, the highest chlorine consumption and the least HAA formation in the comparison between ozonation and O_3/UV process indicates that the chlorine consumption is not a surrogate parameter to evaluate HAA formations. The order of HAA formation potential (HAAFP) is O_3 (pH 9; Alk=0) > O_3 (pH 9; Alk=60) > O_3 (pH 7; Alk=0) > O_3 (pH 7; Alk=60) >> O_3 (pH 5) > O_3/UV process.

The comparisons of HAA formation potential with these three organic precursors are shown in listed in Table 5.4.3. In this study, the 2-OH and 3-OH phenolic groups for resorcinol and phloroglucinol exhibit similar HAA formations. However, HAA formation for *p*-hydroxybenzoic

acid is higher than those observed for resorcinol and phloroglucinol. This suggests that the specific –COOH groups promote the HAA formation. This hypothesis might be verified by analyzing the data presented in Table 5.4.4 via the analysis of variance (ANOVA) — F test method. The assumption of H_0: difference of HAA formation among the three model compounds is insignificant. In Table 5.4.3, F-test is $0.0094 < F(2, 12) = 2.8068$. Therefore, the assumption is accepted and difference of HAA formation among the three model compounds is insignificant.

The order of the two important indexes for HAA formation, specific HAAFP, and β, is consistent with the order of the THM formation also listed in Table 5.4.3. Therefore, the O_3 (pH 9; Alk=0) process has the highest HAAFP and the O_3/UV process has the lowest.

5-4-3 DBP formation

The chlorinated THMs and HAAs are considered as the principal DBPs formation in chlorination process (Xie, 2004). The DBPs formation curve for resorcinol, phloroglucinol, and *p*-hydroxybenzoic acid is shown in Figure 5.4.3. The formation curve is similar to THM and HAA formation (Figures 5.4.1 and 5.4.2).

The relationship between DBPs formation and chlorine consumption at 168 hours reaction time is shown in Figure 5.4.4. The negative correlation exists between chlorine consumption and DBPs formation, which indicates that under the similar TOC concentration, the organic structure is a major parameter on the DBPs formation, and the chlorine consumption is not corresponded to DBPs formation at any situation (Boyce and Horning, 1983). The comparison between DBPs formation and pH at 168 hours experiment is also shown in Figure 5.4.4. The positive correlation between pH and DBPs formation concludes that the hydroxyl radical promotes the DBPs formation and ozone molecule inhibits the DBPs formation.

Comparison of DBPs formation in chlorination process between with and without ozonation, the ozone and hydroxyl radical could change the properties in the three model compounds via destroying the aromatic structure, which leads to more reductions of chlorine demand and CBPFP than those in the only chlorination process. The DBPs formation concentration in the only chlorination process is followed by P>>PHBA>R. The more electrophilic –OH group of phloroglucinol have lower pKa and increase the addition and substitution reactions by chlorine, which yields approximately 2-fold CBPs formation potential than resorcinol and *p*-hydroxybenzoic acid. Therefore, the distribution of various species of CBPs also depended on the acidity (pKa) and the characteristic of the substrate in solution (Gallard and Gunten, 2002).

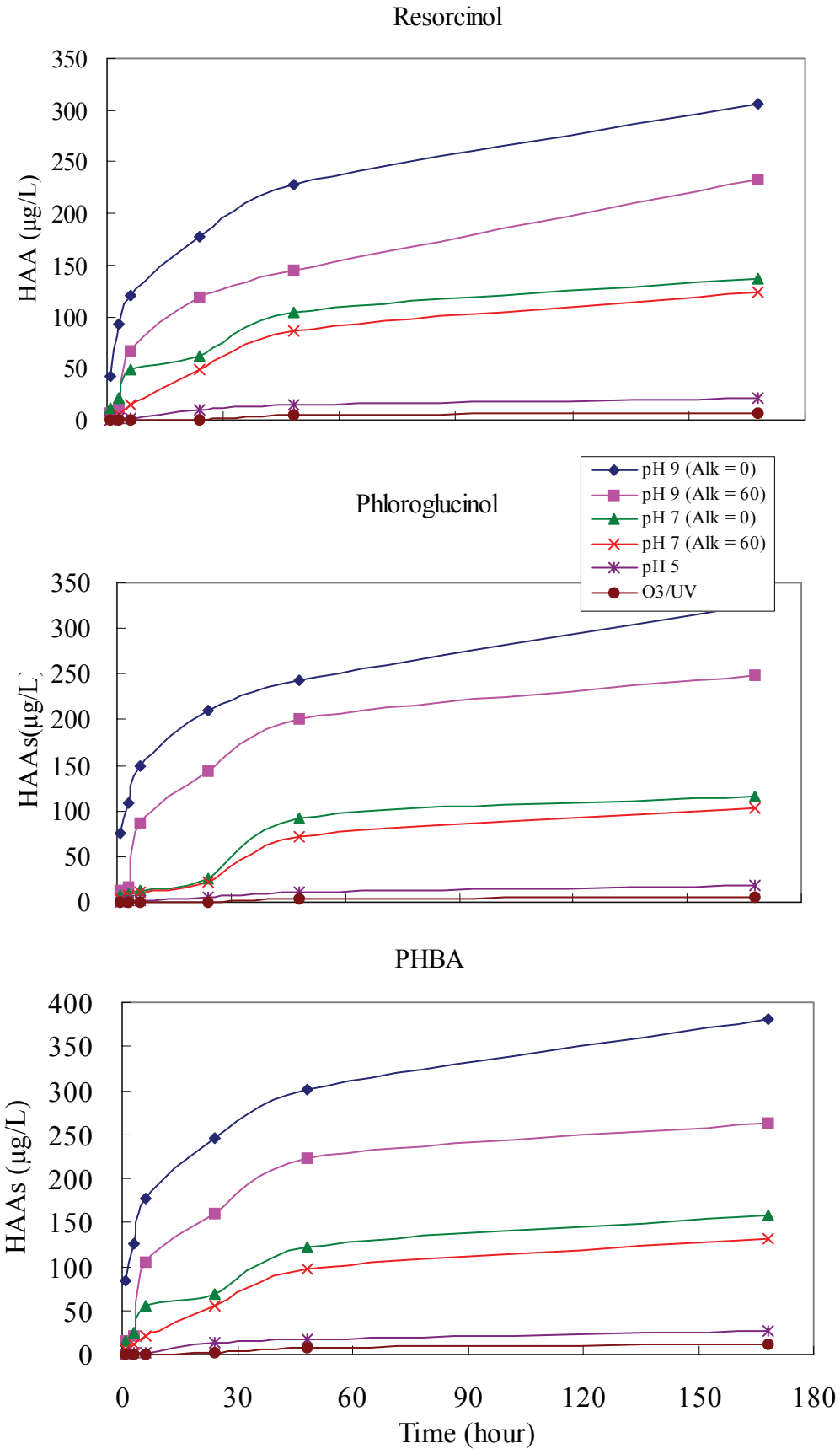

Figure 5.4.2 HAA formation for resorcinol, phloroglucinol and p-hydroxybenzoic acid pretreated by ozonation at different levels of pH and alkalinity, and O_3/UV processes

Table 5.4.3 Summary of HAA formation of model compounds pretreated by ozone

Organics (TOC)	Ozonation		Chlorination		
	pH	Alkalinity	HAAFP * (μg/L)	Specific HAAFP **	β***
R (3 mg/L)	**5**	**0**	21.2	7.4	3.8
	7	**0**	136.8	46.7	30.3
	9	**0**	305.9	100.7	82.0
	7	**60**	123.2	41.8	24.5
	9	**60**	232.0	76.6	57.4
	O_3/UV	**0**	6.2	3.6	0.7
P (3 mg/L)	**5**	**0**	17.9	6.3	3.1
	7	**0**	116.4	39.9	25.8
	9	**0**	325.2	108.7	87.2
	7	**60**	103.7	35.3	21.3
	9	**60**	247.8	82.7	62.1
	O_3/UV	**0**	5.7	3.4	0.7
PHBA (3 mg/L)	**5**	**0**	26.7	9.4	4.7
	7	**0**	158.5	54.1	35.2
	9	**0**	380.4	126.4	102.8
	7	**60**	131.4	44.7	27.3
	9	**60**	263.4	87.5	65.9
	O_3/UV	**0**	11.5	6.8	1.3

* HAAFP: HAA formation in 168 hours

** Specific HAAFP: HAAFP (μg/L) / Residual TOC (mg/L) after ozonation

***β: HAAFP (μg/L) / Cl_2 demand (mg/L) after 168 hours

Table 5.4.4 Analysis of variance (ANOVA) — F test for HAA formation

Source of variance	Sum of Square	Degree of freedom	Mean of square	F-ratio	F(2,12)
Between	2822.107	2	1411.054		
Within	183298.541	12	15039.703	0.094	2.8068
Sum	186120.648	14	-		

The comparisons of DBPs formation potential with these three organic precursors are listed in Table 5.4.5. The phenomenon is corresponded to the chlorine consumption for three model compounds. The similar benzene structure for three model compounds resulted in the insignificant difference of DBPs formation in the ozonation (O_3/UV)/ chlorination process. The above evidence can be validated further by analyzing the data presented in Table 5.4.6 via the

analysis of variance (ANOVA) — F test method. The results reveal the difference of DBPs formation among the three model compounds is insignificant. The order of the two important indexes for DBPs formation, specific CBPFP and *D*, are listed in Table 5.4.5. And, the order of specific DBPFP and *D* is without ozonation > O_3 (pH 9; Alk=0) > O_3 (pH 9; Alk=60) > O_3 (pH 7; Alk=0) > O_3 (pH 7; Alk=60) > O_3 (pH 5) > O_3/UV process. Therefore, the three model compounds with different functional groups would lead to the greater difference on DBPs formation. However, the model compounds under the attack of ozone and hydroxyl radical would destroy the aromatic structure and show the consistency on DBPs formation between three compounds. The order of the two important indexes for DBP formation, specific DBPFP and *D*, is consistent with the order of the THM and HAA formations shown in Table 5.4.5. Therefore, the order of specific DBPFP and *D* is O_3 (pH 9; Alk=0) > O_3 (pH 9; Alk=60) > O_3 (pH 7; Alk=0) > O_3 (pH 7; Alk=60) >> O_3 (pH 5) > O_3/UV process.

Table 5.4.5 Summary of DBP formation of three model compounds pretreated by ozone

Organics	**Ozonation**		**Chlorination**		
(TOC)	**pH**	**Alkalinity**	**DBPFP * (μg/L)**	**Specific DBPFP ****	**D*****
R (3 mg/L)	**5**	**0**	69.1	23.6	12.4
	7	**0**	289.0	98.6	64.1
	9	**0**	648.7	219.9	173.9
	7	**60**	268.5	88.5	53.4
	9	**60**	464.6	153.5	115.0
	O_3/UV	**0**	12.4	7.3	1.4
P (3 mg/L)	**5**	**0**	51.7	18.2	8.8
	7	**0**	285.4	97.9	63.3
	9	**0**	682.1	232.5	190.0
	7	**60**	254.6	85.1	52.2
	9	**60**	511.5	170.7	130.2
	O_3/UV	**0**	12.0	7.2	1.4
PHBA (3 mg/L)	**5**	**0**	63.6	22.3	11.2
	7	**0**	313.7	107.1	69.7
	9	**0**	744.5	247.3	201.2
	7	**60**	270.3	91.9	56.3
	9	**60**	496.0	164.8	124
	O_3/UV	**0**	17.9	10.7	2.1

* DBPFP: DBP formation in 168 hours

** Specific DBPFP: DBPFP (μg/L) / Residual TOC (mg/L) after ozonation

***D: DBPFP (μg/L) / Cl_2 demand (mg/L) after 168 hours

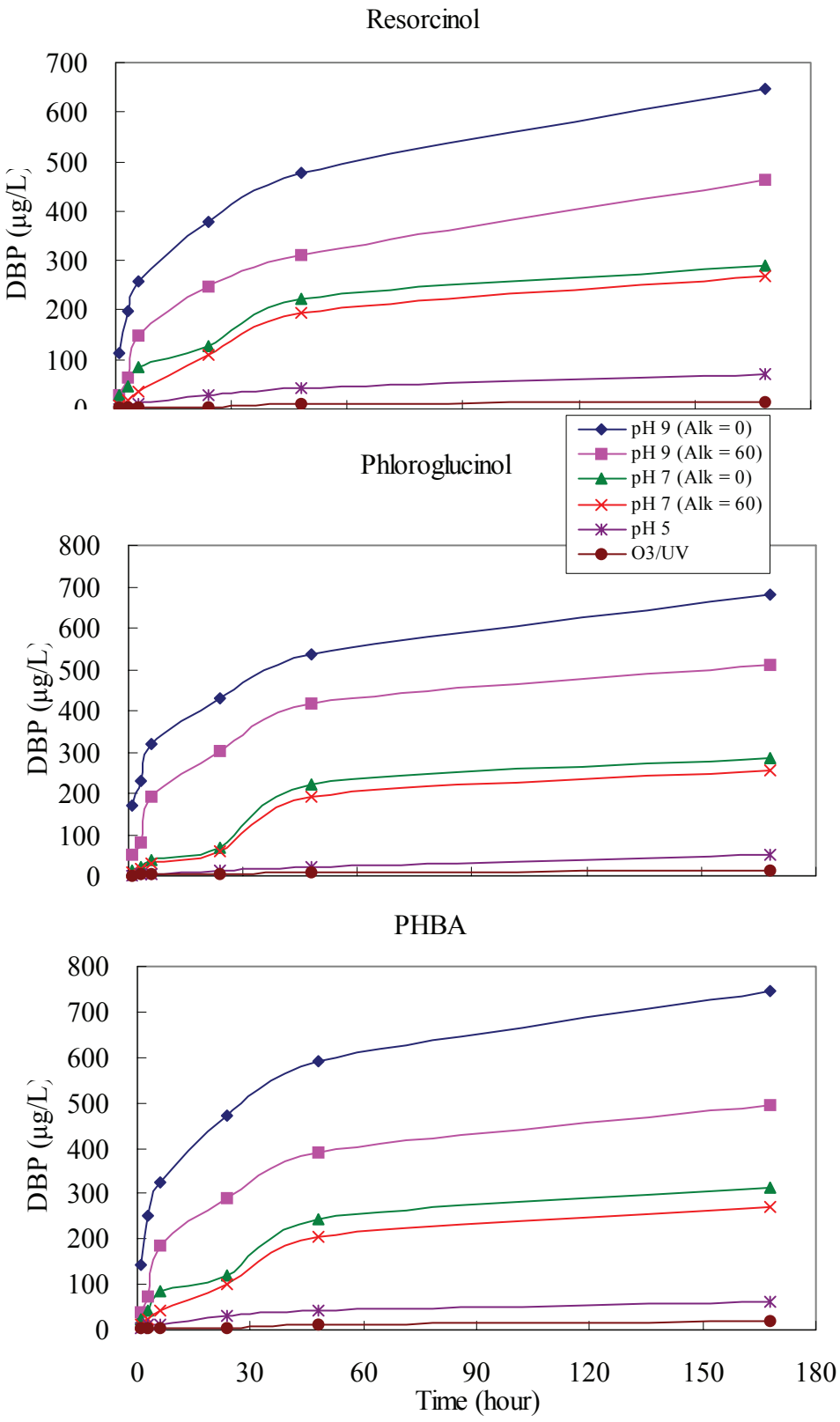

Figure 5.4.3 DBP formation for resorcinol, phloroglucinol, and p-hydroxybenzoic acid pretreated by ozonation at different levels of pH and alkalinity, and O_3/UV process

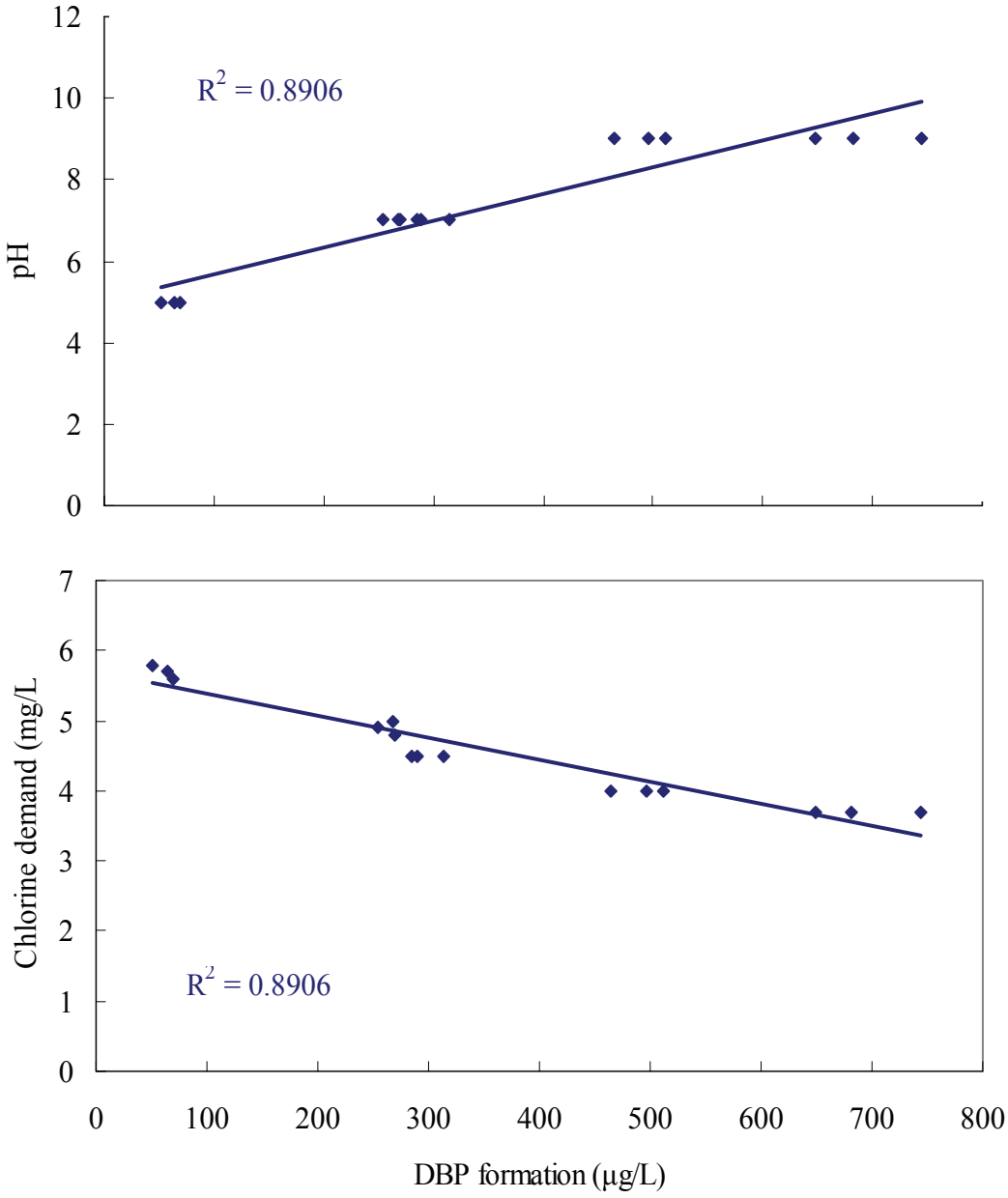

Figure 5.4.4 Correlation between DBP formation and pH (chlorine consumption)

Table 5.4.6 Analysis of variance (ANOVA) — F test for DBP formation

Source of variance	Sum of Square	Degree of freedom	Mean of square	F-ratio	F(2,12)
Between	2308.624	2	1154.312		
Within	695105.251	12	57733.052	0.020	2.8068
Sum	697413.875	14	-		

5-4-4 Predictive DBP Formation Model

Model development

According to the predictive model (Gang et al., 2003), the DBP formation is proportional to chlorine demand which is expressed as follows:

$$DBP = D(C_0 - C),\ [D = \frac{DBPFP\ (\mu g/L)}{Chlorine\ Demand\ (mg/L)}] \qquad (5.4.1)$$

Based on the assumption of Equation 5.3.1, the DBP predictive model is derived as:

$$DBP = D \cdot C_0 \cdot \{1 - f \cdot e^{-K_R \cdot t} - (1-f) \cdot e^{-K_S \cdot t}\} \qquad (5.4.2)$$

Recently, the modified the chlorine decay model, which also uses the chlorine decay model to predict the THM, HAA and DBP formation. The Equations 5.4.3 to 5.4.5 assume that the THM, HAA and DBP formation are a function of chlorine consumption with respect to the rapid and slow reaction (Chang et al., 2006):

$$THM = A\{f \cdot C_0 \cdot \left[1 - \frac{1}{f \cdot C_0 \cdot K_R \cdot t + 1}\right]\}^n + B\{(1-f) \cdot C_0 \cdot \left[1 - e^{-k_s t}\right]\}^m \qquad (5.4.3)$$

$$HAA = C\{f \cdot C_0 \cdot \left[1 - \frac{1}{f \cdot C_0 \cdot K_R \cdot t + 1}\right]\}^n + D\{(1-f) \cdot C_0 \cdot \left[1 - e^{-k_s t}\right]\}^m \qquad (5.4.4)$$

$$DBP = E\{f \cdot C_0 \cdot \left[1 - \frac{1}{f \cdot C_0 \cdot K_R \cdot t + 1}\right]\}^n + F\{(1-f) \cdot C_0 \cdot \left[1 - e^{-k_s t}\right]\}^m \qquad (5.4.5)$$

In the model, the n and m are different from the selected model compounds. However, the investigation assumes that the THM, HAA and DBP formation is the second order to chlorine consumption in the rapid reaction and the first order to chlorine consumption in the slow reaction is consistent to the assumption of chlorine consumption in the chlorination process. Therefore, the predictive model for THM, HAA and DBP formation in the investigation is followed as (n=2; m=1):

$$THM = A\{f \cdot C_0 \cdot \left[1 - \frac{1}{f \cdot C_0 \cdot K_R \cdot t + 1}\right]\}^2 + B(1-f) \cdot C_0 \cdot \left[1 - e^{-k_s t}\right] \qquad (5.4.6)$$

$$HAA = C\{f \cdot C_0 \cdot \left[1 - \frac{1}{f \cdot C_0 \cdot K_R \cdot t + 1}\right]\}^2 + D(1-f) \cdot C_0 \cdot \left[1 - e^{-k_s t}\right] \qquad (5.4.7)$$

$$DBP = E\{f \cdot C_0 \cdot \left[1 - \frac{1}{f \cdot C_0 \cdot K_R \cdot t + 1}\right]\}^2 + F(1-f) \cdot C_0 \cdot \left[1 - e^{-k_s t}\right] \qquad (5.4.8)$$

Table 5.4.7 lists the parameters of the THM predictive model for the model. The high correlation coefficient (R^2) between the measured and predicted data from the model indicates that this model is more suitable for predicting THM formations than the predictive model (Gang et al., 2002). In Table 5.4.7, the A and B represent the THM yield coefficients in the rapid and slow reactions, respectively. As with the THM formation, A and B increase with increasing pH, which confirms that high THM formation resulted in high THM yield coefficients. In addition, B is significantly higher than A in ozonation process, which indicates that the amount of THM formation per unit chlorine consumed in a slow reaction is higher than that in a rapid reaction. In the presence of alkalinity, the inhibition reduces THM formation and lowers the yield coefficient. In the O_3/UV process, the predicted values of A and B are different from those in the ozonation process. The A is higher than B, which indicates that most THM forms in the rapid reaction and little THM formation in the slow reaction.

The THM yield coefficients from combination of three model compounds also are listed in Table 5.4.7. The higher correlation coefficients (R^2) associated with the experimental data for three model compounds indicates that the parallel first and second order THM formation models can accurately predict the behavior of low-MW organic precursor in the ozonation (O_3/UV) / chlorination process. The high R^2 shown in HAA and DBP predictive models represents that the model can accurately predict the HAA and DBP formations as shown in Table 5.4.8 and 5.4.9, respectively.

Figure 5.4.5 presents the observed THM formation concentrations and the predictive curve from the predictive model for resorcinol, phloroglucinol and *p*-hydroxybenzoic acid. The figures for comparing of the measured and predicted HAA and DBP formations for resorcinol, phloroglucinol and *p*-hydroxybenzoic acid are shown in Figure 5.4.6 and 5.4.7, respectively.

Table 5.4.7 Parameters of the THM predictive model for the model

organics	parameter	Ozonation					O_3/UV
		Alkalinity = 0			Alkalinity = 60		
		pH 5	pH 7	pH 9	pH 7	pH 9	
R	*A*	0.37	3.22	26.54	1.77	12.11	17.66
	B	53.50	116.91	161.58	142.50	131.34	0.49
	R^2	0.97	0.97	0.99	0.95	0.98	0.98
P	*A*	0.06	2.24	36.21	1.60	11.50	22.59
	B	44.29	157.15	133.61	153.57	143.74	0.31
	R^2	0.99	0.93	0.99	0.92	0.98	0.99
PHBA	*A*	0.55	2.64	31.65	2.00	12.11	19.56
	B	30.80	133.13	158.81	127.17	131.34	0.46
	R^2	0.99	0.95	0.99	0.94	0.98	0.98
combination of R, P, and PHBA	*A*	0.32	2.71	31.48	1.78	11.98	20.03
	B	42.92	135.8	151.49	141.11	135.09	0.42
	R^2	0.93	0.95	0.99	0.94	0.97	0.97

A: THM yield coefficients in the rapid reaction

B: THM yield coefficients in the slow reaction

Table 5.4.8 Parameters of the HAA predictive model for the model

organics	parameter	ozonation					O_3/UV
		Alkalinity = 0			Alkalinity = 60		
		pH 5	pH 7	pH 9	pH 7	pH 9	
R	*C*	0.18	3.16	23.11	1.32	8.58	44.51
	D	23.73	98.67	149.49	125.64	157.14	0.09
	R^2	0.94	0.97	0.99	0.95	0.96	0.97
P	*C*	0.13	1.50	31.74	0.93	8.70	33.64
	D	21.07	109.69	125.07	106.96	163.27	0.08
	R^2	0.97	0.92	0.99	0.94	0.94	0.98
PHBA	*C*	0.27	3.69	35.14	2.10	14.38	75.02
	D	28.67	114.93	152.67	114.98	152.43	0.17
	R^2	0.95	0.97	0.99	0.96	0.94	0.95
combination of R, P, and PHBA	*C*	0.19	2.79	30.06	1.42	10.44	50.27
	D	24.50	107.83	142.44	116.04	157.23	0.11
	R^2	0.92	0.93	0.98	0.93	0.93	0.94

C: HAA yield coefficients in the rapid reaction

D: HAA yield coefficients in the slow reaction

Table 5.4.9 Parameters of the DBP predictive model for the model

organics	parameter	ozonation					O_3/UV
		Alkalinity = 0			Alkalinity = 60		
		pH 5	pH 7	pH 9	pH 7	pH 9	
R	*E*	0.55	6.38	49.65	3.10	20.69	62.15
	F	77.24	215.58	311.07	268.13	288.48	0.57
	R^2	0.97	0.97	0.99	0.95	0.97	0.91
P	*E*	0.19	3.73	67.95	2.54	20.20	56.23
	F	65.38	266.84	258.69	260.54	307.01	0.39
	R^2	0.99	0.93	0.99	0.93	0.96	0.95
PHBA	*E*	0.82	6.33	66.79	4.09	26.49	94.58
	F	59.48	248.07	311.47	242.15	283.78	0.62
	R^2	0.98	0.96	0.99	0.95	0.96	0.91
combination of R, P, and PHBA	*E*	0.52	5.50	61.54	3.20	22.41	20.03
	F	67.43	243.63	293.93	257.16	292.33	0.42
	R^2	0.94	0.95	0.99	0.94	0.96	0.97

E: DBP yield coefficients in the rapid reaction

F: DBP yield coefficients in the slow reaction

5-5 Comparison of DBPs Formations between with and without ozonation and O_3/UV processes

5-5-1 Chlorine Consumption

In the pervious ozonation (O_3/UV) / chlorination experiment, an initial chlorine dosage of 10 mg/L was used. However, a high chlorine demand in the only chlorination process results in increasing initial chlorine dosage to 28 mg/L in this study. In the Gang study (2002), the different initial chlorine concentration influenced the chlorine consumption in chlorination. However, in order to simplify and facilitate the comparison between with and without ozonation (O_3/UV) processes, the effect of initial chlorine dosage on chlorine consumption found in Gang's study (2002) was disregarded in this study.

The comparison of chlorine consumption in a 168 hours experiment period between with and without ozonation (O_3/UV) processes is listed in Table 5.5.1. According to Table 5.5.1, the higher chlorine consumption was observed in the only chlorination process. The electrophile of aromatic structure of these residual organic precursors leads to the powerful electrophilic addition and substitution reactions by chlorine. However, in the ozonation process, the ozone and hydroxyl radical destroy organic precursors resulting in the cleavage of aromatic structure and reduce the chlorine consumption. As a result, the chlorine consumption in the only chlorination process is higher than that in the ozonation and O_3/UV processes.

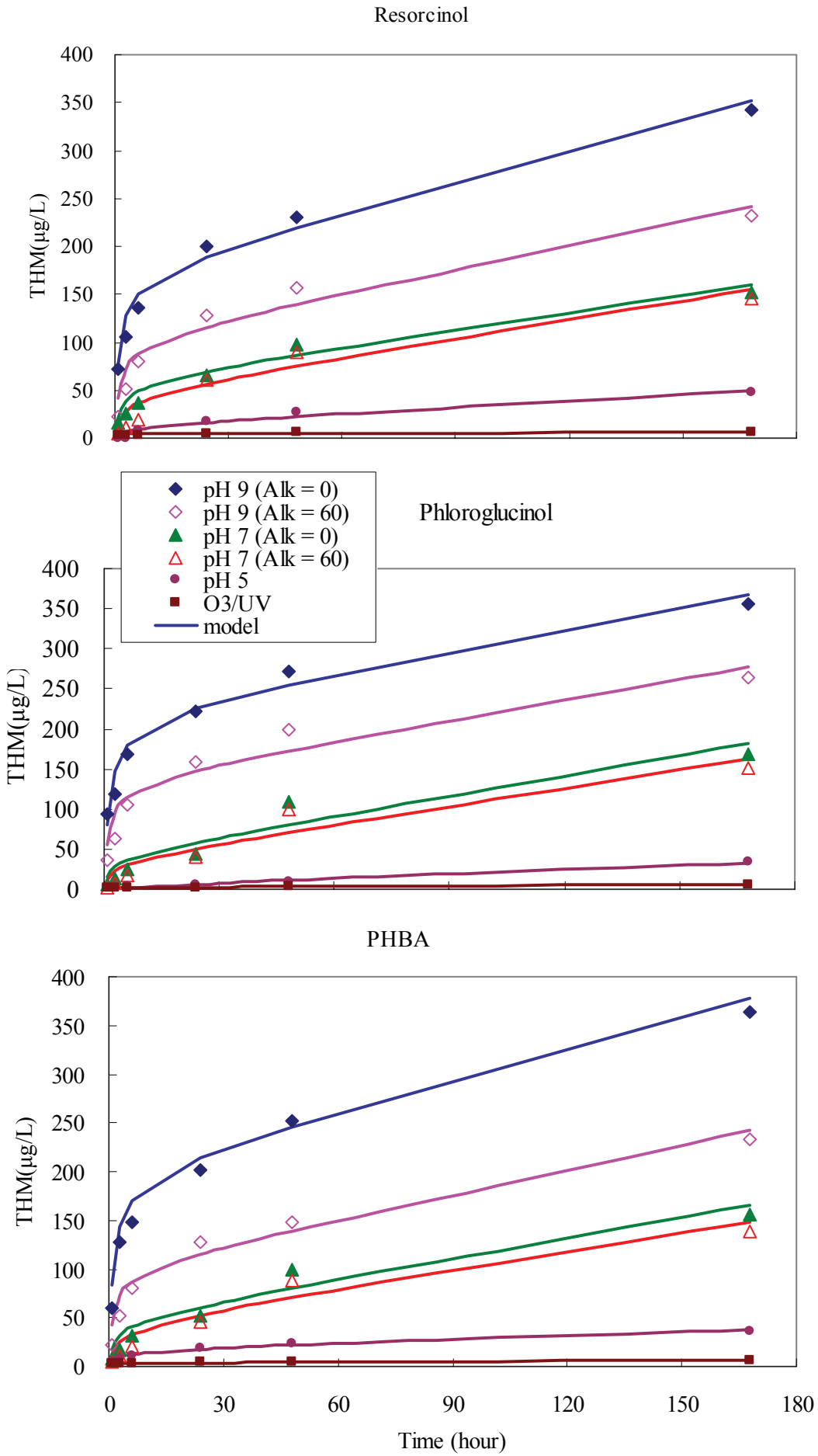

Figure 5.4.5 Comparison of the measured and predictive THM formation concentration for resorcinol, phloroglucinol and p-hydroxybenzoic acid in the predictive model.

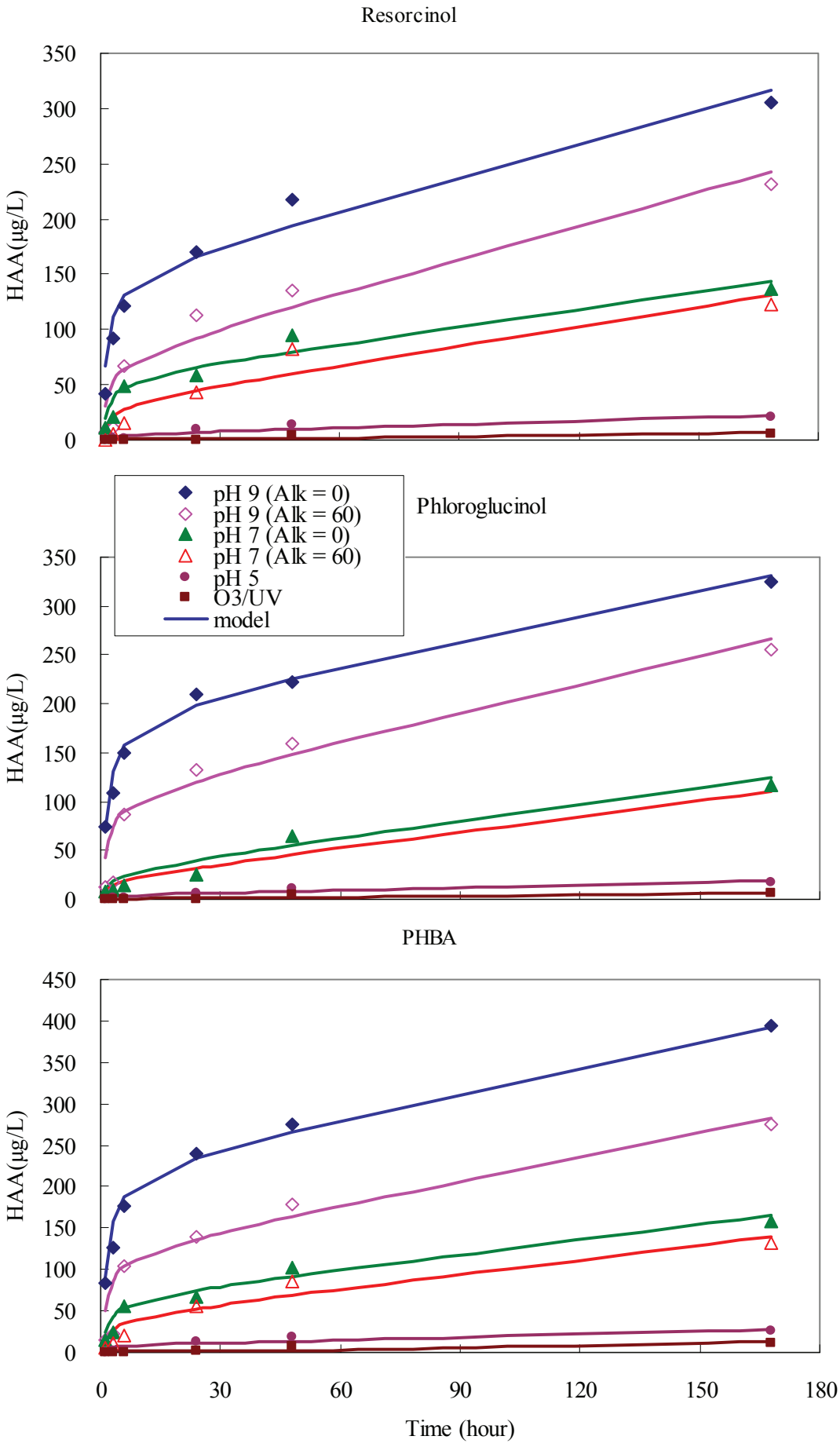

Figure 5.4.6 Comparison of the measured and predictive HAA formation concentration for resorcinol, phloroglucinol and p-hydroxybenzoic acid in the predictive model ..

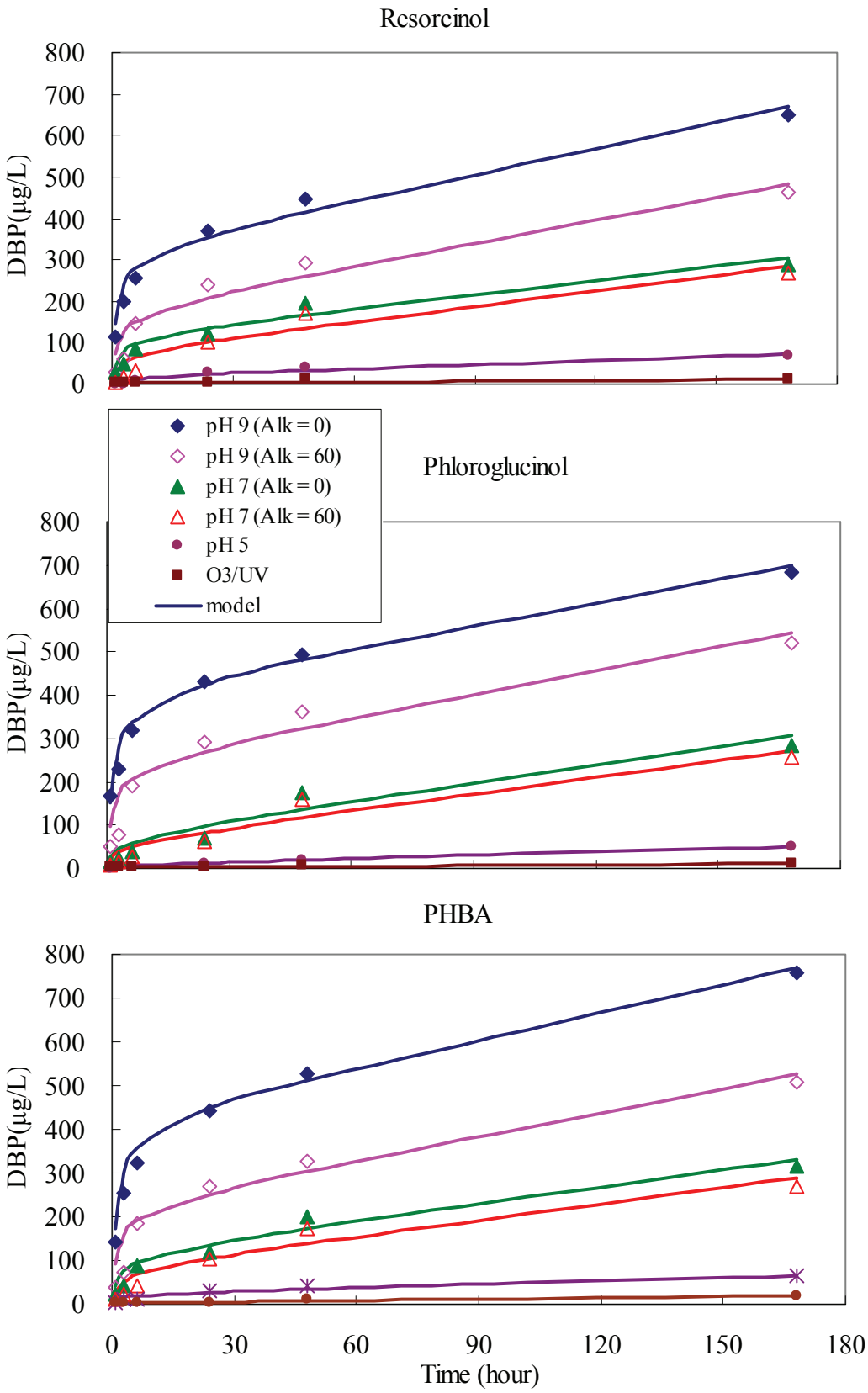

Figure 5.4.7 Comparison of the measured and predictive DBP formation concentration for resorcinol, phloroglucinol and *p*-hydroxybenzoic acid in the predictive model

Among the chlorine demands for these three model compounds, the order is P>>R¡ PHBA. Larson et al. (1979) and Gallard et al. (2002) revealed that the resorcinol with two activating –OH group could release the electrons rapidly, which leads to the intensely electrophilic addition and substitute reactions by chlorine. However, the symmetric structure for phloroglucinol flanked with three –OH groups may form a resonance-stabilized intermediate, which could confine the hydrolysis and decarboxylation with C–C bond cleavage on the aromatic structure and result in more chlorine demand (Chang et al., 2006). Therefore, the chlorine demand of phloroglucinol is higher than resorcinol.

For *p*-hydroxybenzoic acid, the moderately deactivating group (–COOH) would lower the electron density on aromatic structure and decrease the chlorine demand, but the p-position of –OH and –COOH would increase the activation. Therefore, the order of chlorine demand is P>>R¡ PHBA.

Table 5.5.1 Comparison of chlorine consumption for three model compounds

Organics	Chlorine consumption (mg Cl_2/mg C)						
	Ozonation					O_3/UV	Only Chlorination
	Alkalinity = 0			Alkalinity =60			
	pH 5	pH 7	pH 9	pH 7	pH 9		
R	2.0	1.5	1.3	1.6	1.3	5.2	8.6
P	2.0	1.5	1.3	1.6	1.3	5.1	9.2
PHBA	2.0	1.5	1.2	1.6	1.3	5.2	8.6

5-5-2 Chlorination Disinfection By-Products Formation

The comparisons of DBP formation potentials (DBPFP) and DBP yield coefficient (*D*) between with and without ozonation (O_3/UV) processes during the chlorination process are shown in Table 5.5.2. According to Table 5.5.2, the ozonation and O_3/UV processes could inhibit the DBPFP during the chlorination process.

The ozone and hydroxyl radical could change the properties in the three model compounds by destroying the aromatic structure, which leads to more reductions of chlorine demand and DBPFP than those in the only chlorination process. In the O_3/UV process, the 40% TOC removal efficiency by the hydroxyl radical would enhance the reduction of DBPFP. Therefore, the order of DBPFP in different treatment processes is O_3/UV system<<ozonation<only chlorination. The DBP formation concentration in the only chlorination process is followed by P>>PHBA>R. The more electrophilic –OH group of phloroglucinol have lower pKa and increase the addition and substitution reactions by chlorine, which yields approximately 2-fold DBP formation potential than resorcinol and *p*-hydroxybenzoic acid. Therefore, the distribution of various species of chlorinated products also depended on the acidity (pKa) and the characteristic of the substrate in solution (Chang et al., 2006; Gallard and Gunten, 2002). The DBP formation is corresponded to chlorine consumption, which was consistent with other findings (Boyce and Horing, 1983;

Larson and Rockwell, 1979).

The relationship between DBP formation and chlorine demand could be evaluated by the DBP yield coefficient (*D*). Table 5.5.3 shows the values of *D* in different processes. In the only chlorination process experiment, the high DBP formation is corresponded to high chlorine consumption. Therefore, the *D* value in the only chlorination process is not obviously higher than that in the ozonation (O_3/UV) / chlorination process.

Table 5.5.2 Comparison of DBPFP for three model compounds

Organics	Specific DBP (μg DBP /mg C)						
	Ozonation					O_3/UV	Only Chlorination
	Alkalinity = 0			Alkalinity = 60			
	pH 5	pH 7	pH 9	pH 7	pH 9		
R	23	98	220	89	154	7	509
P	18	98	232	85	170	7	1068
PHBA	22	107	247	92	165	11	687

Table 5.5.3 The comparison in D during chlorination

Organics	*D* (μg DBP /mg Cl_2)						
	Ozonation					O_3/UV	Only Chlorination
	Alkalinity = 0			Alkalinity = 60			
	pH 5	pH 7	pH 9	pH 7	pH 9		
R	12	64	173	53	115	1	59
P	9	63	190	52	130	1	116
PHBA	11	70	201	56	124	2	79

5-5-3 Risk Assessment

During this study, it was found that ozonation of organic precursors is successful in reducing the DBP formation in chlorination, especially at pH 5 for the ozonation and the O_3/UV processes. However, it is noted that there are other by-products harmful to human health, such as aldehyde would be occurred in the course of ozonation. Therefore, it is required to a risk assessment to determine if the ozonation (O_3/UV) process is an appropriate treatment process based on the carcinogenic DBPs concerns.

Figures 5.5.1 to 5.5.3 illustrate the DBP and aldehyde formations in the only chlorination and ozonation (O_3/UV) / chlorination processes. The DBP (THM and HAA) and aldehyde are considered carcinogenic substances by USEPA, and its carcinogenic risk can be determined by

the following equation (Equation 5.5.1).

$$Carcinogenic\ \ risk = CDI \times SF \qquad (5.5.1)$$

Where chronic daily intake (CDI) is the quantity of ingestion (mg/kg-day), and slope factor (SF) is the carcinogenic slope factor (mg/kg-day)$^{-1}$ The value of CDI is calculated based on the assumption that one person drinks 2 liters of water per day, with an average weight of 70 kilogram. The value of SF is varied with different carcinogenic substances, which represents the slope of diagram of dose-response relationship. According to toxicity data of DBP and aldehyde proposed by USEPA, the value of SF is 4.4×10^{-3} for chlroform, 4×10^{-3} for HAA, and 0.08 for formaldehyde. The final carcinogenic risk is assumed to be the sum of these three carcinogenic substances and listed in Table 5.5.4.

According to Table 5.5.4, the lowest carcinogenic risk is in the O_3/UV / chlorination processes and the highest carcinogenic risk is in the only chlorination process. The order of carcinogenic risk is O_3/UV << O_3 (pH 5) < O_3 (pH 7; Alk=60) < O_3 (pH 7; Alk=0) < O_3 (pH 9; Alk=60) < O_3 (pH 9; Alk=0) << only chlorination. Therefore, both the ozonation with proper operation and O_3/UV processes can reduce the organic precursors by providing the safe drinking water. Further, the O_3/UV process is considered as the appropriate treatment technology for reducing DBPs and aldehyde formation.

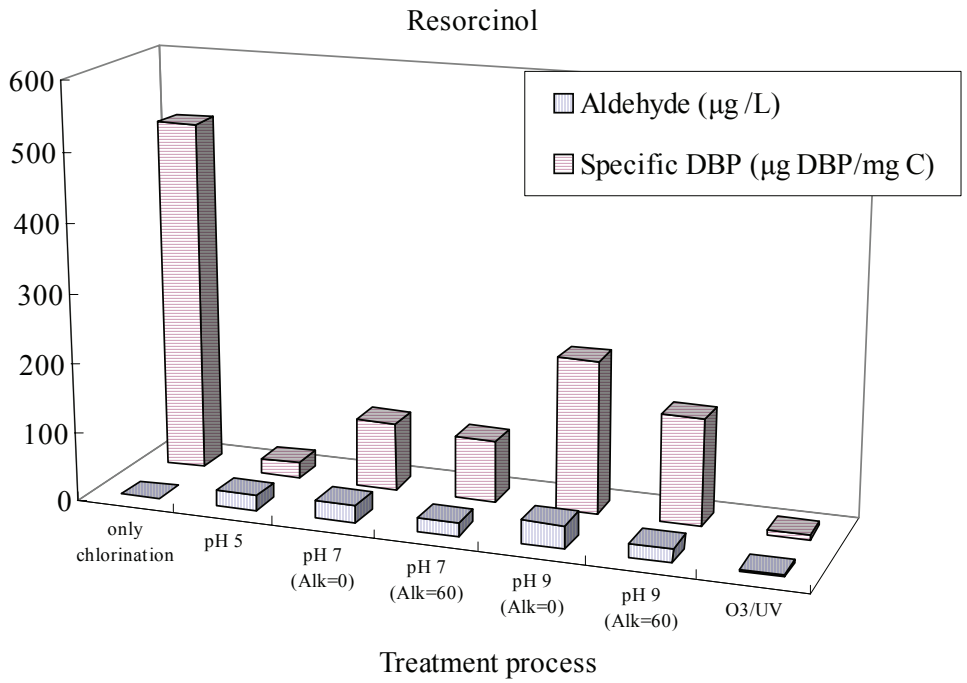

Figure 5.5.1 Comparison of aldehyde and DBP formation for resorcinol

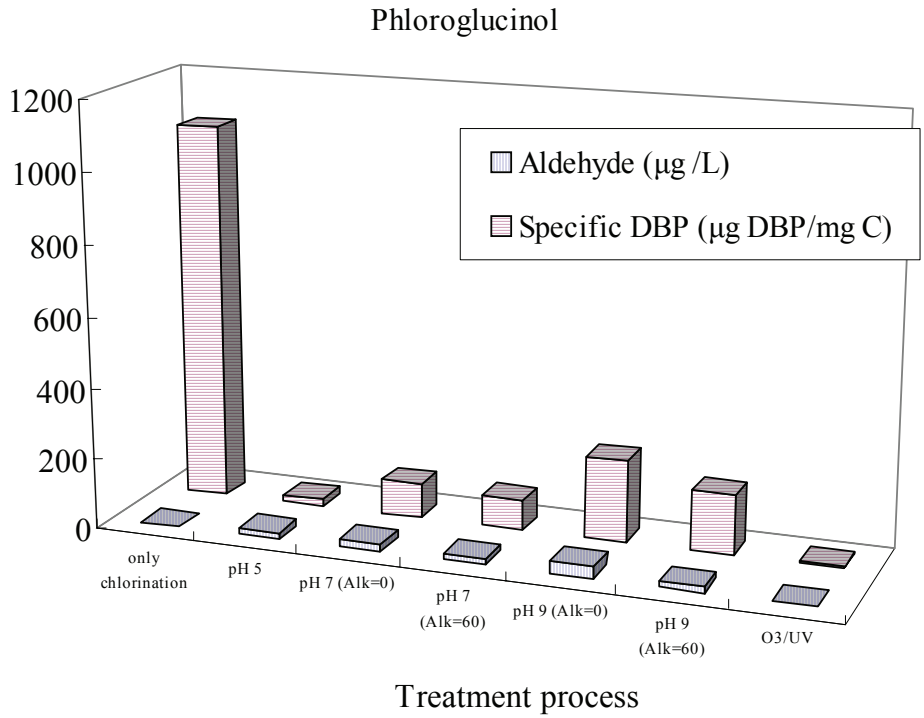

Figure 5.5.2 Comparison of aldehyde and DBP formation for phloroglucinol

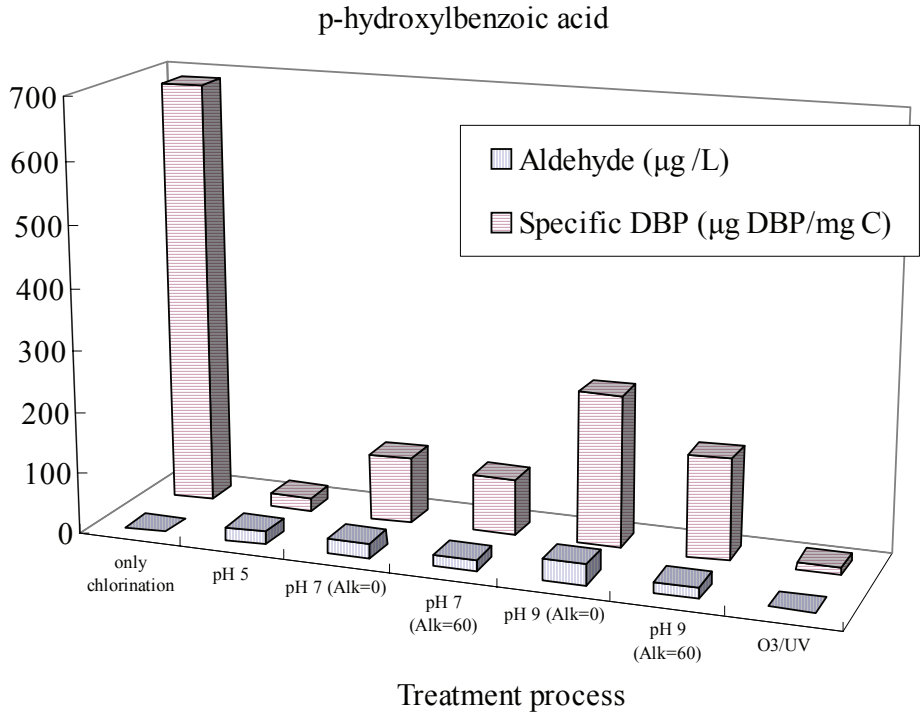

Figure 5.5.3 Comparison of aldehyde and DBP formation for p-hydroxybenzoic acid

Table 5.5.4 The carcinogenic risk in different treatment processes

Organics		Carcinogenic risk						
		Ozonation					O_3/UV	Only Chlorination
		Alkalinity=0			Alkalinity=60			
		pH 5	pH 7	pH 9	pH 7	pH 9		
R	THM	7×10^{-7}	4×10^{-6}	1×10^{-5}	3×10^{-6}	8×10^{-6}	6×10^{-7}	4×10^{-5}
	HAA	2×10^{-7}	1×10^{-6}	1×10^{-5}	9×10^{-7}	5×10^{-6}	6×10^{-9}	3×10^{-5}
	aldehyde	3×10^{-6}	7×10^{-6}	1×10^{-5}	5×10^{-6}	6×10^{-6}	7×10^{-7}	0
	Risk	$\mathbf{4\times10^{-6}}$	$\mathbf{1\times10^{-5}}$	$\mathbf{3\times10^{-5}}$	$\mathbf{9\times10^{-6}}$	$\mathbf{2\times10^{-5}}$	$\mathbf{1\times10^{-6}}$	$\mathbf{7\times10^{-5}}$
P	THM	1×10^{-7}	3×10^{-6}	2×10^{-5}	2×10^{-6}	1×10^{-5}	4×10^{-7}	1×10^{-4}
	HAA	2×10^{-7}	1×10^{-6}	1×10^{-5}	9×10^{-7}	5×10^{-6}	6×10^{-9}	5×10^{-5}
	aldehyde	6×10^{-6}	7×10^{-6}	9×10^{-6}	5×10^{-6}	5×10^{-6}	5×10^{-7}	0
	Risk	$\mathbf{6\times10^{-6}}$	$\mathbf{1\times10^{-5}}$	$\mathbf{4\times10^{-5}}$	$\mathbf{8\times10^{-6}}$	$\mathbf{2\times10^{-5}}$	$\mathbf{1\times10^{-6}}$	$\mathbf{2\times10^{-4}}$
PHBA	THM	1×10^{-6}	3×10^{-6}	2×10^{-5}	2×10^{-6}	8×10^{-6}	6×10^{-7}	5×10^{-5}
	HAA	3×10^{-7}	3×10^{-6}	1×10^{-5}	2×10^{-6}	6×10^{-6}	3×10^{-8}	4×10^{-5}
	aldehyde	6×10^{-6}	7×10^{-6}	1×10^{-5}	5×10^{-6}	5×10^{-6}	5×10^{-7}	0
	Risk	$\mathbf{7\times10^{-6}}$	$\mathbf{1\times10^{-5}}$	$\mathbf{4\times10^{-5}}$	$\mathbf{9\times10^{-5}}$	$\mathbf{2\times10^{-5}}$	$\mathbf{1\times10^{-6}}$	$\mathbf{1\times10^{-4}}$

Reference : www.epa.gov/iris/index.html.

VI Conclusions

The ozone decomposition mechanism changes at different pH levels. There are more hydroxyl ions (OH^-) at high pH, which promotes ozone decomposition reaction to form hydroxyl radical. A modified ozonation decomposition model, $[O_3]=[O_3]_0\cdot\{F\cdot e^{-K_1\cdot t}+(1-F)\cdot e^{-K_2\cdot t}\}$, is developed in this investigation.

Hydroxyl radical is the predominant oxidant in the indirect ozonation process. In the investigation, the effect of alkalinity as an inhibitor on hydroxyl radical formation is significant. A linear relationship between hydroxyl radical exposure and alkalinity reduction is proposed. Based on the hydroxyl radical formation mechanism and the parameters of ozone, pH, and alkalinity the hydroxyl radical predictive model is proposed in this study. In the ozonation and chlorination by-products formation, the hydroxyl radical formed in the indirect ozonation would promote the aldehyde, THMs, and HAAs formation. However, the alkalinity inhibition would decrease these by-products formation.

In the O_3/UV system, the large amount of hydroxyl radical (5-fold than pH 9) has a different effect on ozonation and chlorination by-products. The more chlorine consumption and less by-products formation including aldehyde, THMs, and HAAs are observed in the O_3/UV system. Therefore, the enough hydroxyl radical formation (O_3/UV system) resulted in a good reduction

on by-products formation but the less hydroxyl radical (indirect ozonation) would promote the by-products formation.

In the only chlorination process, the selected model compounds with different functional group and electrophile character resulted in unlike chlorine demand, THMs, and HAAs formation. The order of these is P>>R¡ PHBA. However, in the ozonation (O_3/UV)/chlorination processes, the similar structure formed under the ozone and hydroxyl radical attack would have the similar chlorine demand, THM, and HAAs formation. Therefore, the difference of chlorine demand, THM, and HAAs formation for the selected model compounds is insignificant in the ozonation (O_3/UV)/chlorination processes.

In the ozonation process, the carcinogenic bromate formation is the other important study in this investigation. Because the ozone dose is not sufficient to react with bromide to form hypobromous acid resulting in reducing the bromate formation, the effect of ammonia concentration on reducing bromate formation is insignificant in this investigation. Since the ammonia could be oxidized to nitrate by ozonation, the fraction of the ammonia attributed to reducing the bromate formation in ozonation should be identified.

According to the risk assessment between the ozonation (O_3/UV)/chlorination processes, and only chlorination process, the highest and lowest risks were found in the only chlorination and O_3/UV processes, respectively. The results of this investigation could be utilized to the water treatment plants by introduction of the ozonation and O_3/UV processes prior to the chlorination process

The predictive model proposed by Gang (2002) can not fit the experimental data of THM, and HAAs formation in the ozonation / chlorination processes in this investigation. However, the modified predictive model (Chang et al., 2006) based on the parallel first-order (slow reaction) and second-order (rapid reaction) reactions in chlorine consumption can fit the chlorine decay quite well. In the DBP predictive model, the assumption of the DBP formation corresponded to the second order to chlorine consumption in the rapid reaction and the first order to that in the slow reaction (n=2, m=1) exhibits the high correlation coefficient (good fit) in the study. Therefore, the modified model could predict the THMs and HAAs formation accurately and achieve the minimization formation purpose for the water treatment plant in the investigation.

Reference

Amirsaedari, Y., Yu, Q., Williams, P., 2000. Effect of ozonation and UV irradiation with direct filtration and disinfection by-product precursors in drinking water treatment. Environmental Science and Technology. 22, 1015-1023.

APHA, 1998. Standard Methods for the examination of Water and Wastewater, nineteenth ed.. American Public Health Association, Washington, DC.

Bader, H., Sturzenegger, V., and Hoigne, J., 1988. Photometric method for the determination of low

concentration of hydrogen peroxide by the peroxidase catalyzed oxidative of N,N-Diethyl-p-phenylenediamine (DPD). Wat. Res. Vol. 22, No. 9, 1109-1115.

Boyce, S.D., Horning, J. F., 1983. Reaction pathways of trihalomethane formation from the halogenation of dihydroxyaromatic model compounds for hunic acid. Environ. Eng. 124(1), 16-24.

Buhler, R.E., Staehelin, J., and Hoigne, J., 1984. Ozone decomposition in water studied by pulse radiolysis. 1. HO_2/O_2^- and HO_3/O_3^- as intermediates. J. Phys. Chem. 88, 2560-2564.

Chang, E.E., Chiang, P.C., Chao, S.H., and Lin, Y. L., 2006. Relationship between chlorine consumption and chlorination by-products formation for model compounds. *Chemosphere* 64, 1196-1203.

Chin, A. and Bérubé, P.R., 2005. Removal of disinfection by-product precursors with ozone-UV advanced oxidation process. Water Research 39, 2136-3144.

Clark, R.M., 1998. Chlorine demand and TTHM formation kinetics: A second-order model. Journal of Environment Engineering, 124(1), 16-24.

Cotton, F. A.; Wilkinson, G., 1972. "Advanced Inorganic Chemistry"; Interscience: New York, 476.

Daniel, U., Peter, M. H., Graham, A.G., and Dennis, M., 1999. Modeling enhanced coagulation to improve ozone disinfection. AWWA, 91(3), 59-73.

Edzwald, J.K. and Tobiason, J.E., 1999. Enhanced coagulation: US requirements and a broader view. Water Science and Technology. Vol. 40, No. 9, 55-62.

Fernando J. Beltrán, 2004. "Ozone Reaction Kinetics for Water and Wastewater Systems" Lewis Publishers. New York Washington, D.C.

Gallard, Herve and von Gunten, Urs, 2002. Chlorination of natural organic matters: Kinetics of chlorination and of THM formation. Water Research 36, 65-74.

Gang, Dianchen, Singer J.R. Clevenger, T.E., Banerji, S.K., 2002. Using chlorine demand to predict TTHM and HAA9 formation. Journal of American Water Work Association, 94 (10), 76-86.

Gang Dianchen, Thomas E. Clevenger, Shankha K. Banerji, 2003. Relationship of chlorine decay and THMs formation to NOM size. Journal of Hazardous Materials A96, 1-12.

Gilbert, E., 1978. Reaction of ozone with organic compounds in dilute aqueous solution: identification of their oxidation product. In R.G. Rice and I.A. Cotruvo, Eds. Ozone-Chlorine Dioxide Products of Organic Material, 227-242.

Glaze, W. H., 1986. "Chemistry of Ozone, By-products, and Their Health Effects", In Ozonation: Recent Advances and Research Needs, AWWARF, Denver, Colo., Jun.

Gordon, G., Gauw, R. D., Emmert, G. L., Walters, B. D., and Bubnis, B., 2002. CHEMICAL REDUCTION METHODS for Bromate Ion Removal. American Water Works Association, 94, 91-98.

Gracia, R., J. L. Aragues and J. L. Ovelleiro., 1996. Study of catalytic ozonation of Humic Substances in water and their ozonation byproducts, Ozone Sci. and Eng., Vol. 18, No. 3, 195-208.

Guittonneau, S., Thibaudeau, D. and Meallier, P., 1996. Free radicals formation induced by the ozonation of humic substances in aqueous medium. Catalysis Today 29, 323-327.

Haag, W. R., and Hoigne, J., 1983. Ozonation of Bromide-Containing Waters: Kinetics of Formation of Hypobromous Acid and Bromate. Environ. Sci Technol., 17, 261-267.

Hass, C.N., and Karra S.B., 1984. Kinetics of wastewater chlorine demand exertion. J. Water Pollut. Control Fed. 56(2)170.

Hass, C.N., and Karra S.B., 1985. Kinetics of wastewater chlorine demand exertion. J. Water Pollut. Control Fed. 56(2)170

Hoigné, J., 1998. "Chemistry of aqueous ozone and transform of polluants by ozonation and advanced oxidation process", in the Handbook of Environmental Chemistry (ed. By J. Hrubec), Vol.5, Part C: Quality and Treatment of Drinking Water II, Spring-Verlag, Berlin.

Huang, C.H., Marinas, B.J., and Blake, D.M., 1993. The reaction mechanism between hydroxyl radical and organic matters. Ozone Sci. Eng. Vol. 12, No. 3, 156-167.

Jans, U. and Hoigne, J., 1998. Activated carbon black catalyzed transformation of aqueous ozone into OH-radicals, Ozone Sci. Eng., 20, 67-89.

Karin Tornberg and Stefan Olsson, 2002. Detection of hydroxyl radicals produced by wood-decomposing fungi. FEMS Microbiology Ecology 40, 13-20.

Karanfil, T. Schlautman, MA, Erdogan, I., 2002. Survey of DOC and UV measurement particles with implications for SUVA determination. AWWA, Dec., 68-80.

Keiichi Tanaka, Keiji Abe, and Teruaki Hisanaga, 1996. Photocatalytic water treatment on immobilized TiO_2 combined with ozonation. Journal of Photochemistry and Photobiology A¡G Chemistry 101, 85-87.

Kitis, M., 2001. The Reactivity of Natural Organic Matter to Disinfection By-products Formation and its Relation to Specific Ultraviolet Absorbance. Water Science and Technology. 43:2:9.

Krasner, S.W., Sclimenti, M.J., and Means, E.G., 1994. Quality degradation: implications for DBP formation, J. Am. Water Works Assoc., 86 (4), 34.

Langlais, B., D.A. Reckhow, and D.B. Brink, 1991. "Ozone in Water Treatment-Application and Engineering", Lewis Publisher.

Larson, R.A., Rockwell, A.L., 1979. Chloroform and chlorophenol production by decarboxylation of natural acids during aqueous chlorination. Environment Science and Technology 13(3), 315-319.

Legube, B., Parinet, B., Gelient, K., Berne, F., and Croue, J. P., 2004. Modeling of bromate formation by ozontion of surface waters in drinking water treatment. Water Research, 38, 2185-2195.

Marhaba T. F. and Van D., 2000. The variation of mass and disinfection by product formation potential of dissolved organic matter fractions along a conventional surface water treatment plant. J. Hazardous Materials 74, 133.

Miltner R. J., Shukairy H. M. and Summers R. S., 1992. Disinfection by-products formation and

control by ozonation and biotreatment. J. Am. Water Works Assoc. 11, 83.

Mirat D. G. and Vatistas R., 1987. Oxidation of phenolic compounds by ozone and ozone/UV¡GA comparative study. Water Research 21, 895-900.

Mohamed S. Siddiqui, Gary L. Amy, and Brian D. Murphy, 1997. Ozone enhanced removal of natural organic matter from drinking water sources. Water Research 31, 3098-3106.

N. H. Ince, G. Tezcanli, 1999. Treatability of textile dyebath effluents by advanced oxidation: preparation for reuse, Water Sci. Tenchnol (40), 183-190.

Patrik Kopf, Ernst Gilbert, and Siegfried H. Eberle, 2000. TiO_2 photocatalytic oxidation of monochloroacetic acid and pyridine :influence of ozone. Journal of Photochemistry and Photobiology A¡GChemistry 136, 163-168.

Paul Westerhoff, George Alken, Gary Amy, and Jean Debroux, 1998. Relactionships between the structure of natural organic matter and its reactivity towards molecular ozone and hydroxyl radicals. Water Research 33, 2265-2276.

Pinkernell, U., and Von Gunten, U., 2001. Bromate Minimization during Ozonation: Mechanistic Considerations. Environ. Sci. Technol., 35, 2525-2531.

Radzik, D.M., Roston, D.A., Kissinger, P.T., 1983. Determination of hydroxylated aromatic compounds produced via superoxide- dependent formation of hydroxyl radical by liquid chromatography/ electrochemistry. Anal. Biochem. 131, 458-464.

Reckhow, D.A., Singer, P. C., and Malcolm, R. L., 1990. Chlorination of humic materials: byproduct formation and chemical interpretation. Environ. Sci. Technol. 24, 1665.

Richardson SD, Thruston Jr AD, Caughran TV, Chen PH, Collette TW, and Floyd TL, 1999. Identification of new ozone disinfection by-products in drink water. Environ Sci Technol 33, 3368-3377.

Richmond, R., Halliwell, B., Chauhan, J., Darbre, A., 1981. Anal. Biochem. 149, 189-189.

Rook J. J., 1976. Haloforms in drinking water. J. Am. Water Works Assoc. 68 (3).

Schechter D. S. and Singer P., 1995. Formation of aldehydes during ozonation. Ozone Sci. Emgng 17.

Siddiqui M. Amy G., 1993. Fectors affecting DBP formation during ozone-bromide reactions. J. Amer. Water Works Assoc., 85(1): 63-72.

Siddiqui M. Amy G, Rice RG., 1995. Bromate ion formation: a critical review. J. Amer. Water Works Assoc., 87(10): 58-70.

Slawomir W. H., William D. B., and Leo C. F., 1999. Variability of ozone reaction kinetics in batch and continuous flow reactors. Water Research 33, 2130-2318.

Song, R., Westerhoff, P., Minear, R., and Amy, G., 1997. Bromate minimization during ozonation. American Water Works Association, Vol, 89, 69-78.

Staehelin, S. and Hoigné, J., 1982. Decomposition of ozone in water: rate of initiation by hydroxide ions and hydrogen peroxide, Environ. Sci. Technol., 16, 666-681.

Staehelin, J., Buhler, R.E., and Hoigné, J., 1984. Ozone decomposition in water studied by pulse

radiolysis. 2. OH and HO_4 as chain intermediates. J. Phys. Chem. 88, 5999-6004.

Tezcanli-Guyer G. and Ince N. H., 2004. Individual and combined effects of ultrasound, ozone and UV irradiation: a case study with textile dyes. Ultrasonics 42, 603-609.

Tomasi, A. and Lannone, A., 1993. ESR Spin-Trapping Artifact in Biological System. Biol. Magn. Reson. Vol 13, 353-384.

von Gunten, U., and Hoigne, J., 1994. Bromate Formation during Ozonation of Bromide-Containing Waters: Interaction of Ozone and Hydroxyl Radical Reactions. Environ. Sci. Technol., 28, 1234-1242.

von Gunten U, Oliveras V., 1998. Advanced oxidation of bromide-containing waters: bromate formation mechanisms. Environ Sci Technol; 32, 63-70.

von Gunten, U. V., 2003 (a). Ozonation of drinking water: Part I. Oxidation Kinetics and product formation. Water Research, Vol.37, 1443-1467.

von Gunten, G., 2003 (b). Review, Ozonation of drinking water: Part II. Disinfection and by-production formation in presence of bromide, iodide, or chlorine. Water Research, 37, 1469-1487.

Wei Chu, and Chi-Wai Ma, 2000. Quantitative prediction of direct and indirect dye ozonation kinetics. Water Research 34, 3153-3160.

Weinberg H. S., W. H. Glaze, S. W. Krasner and M.J. Sclimenti., 1993. Formation and Removal of aldehyde in plants that use ozonation. J. Am. Water Works Assoc.

Weinberg H. S., W. H. Glaze, 1996. “An overview of ozonation disinfection by-product”, Chapter 7 of Disinfection By-Product in Water Treatment, edited by R. A. Minear and G. L. Amy, CRC Press.

WHO, 1990. IARC Monographs on the evaluation of carcinogenic risks to humans, Vol 52, WHO: Geneva.

Wu, Z. C., 2002. The study on Hydroxyl Radicals Generation in UV/TiO_2 Photocatalysis Process. NCHU Thesis.

Xie, Yuefeng F.., 2004. DISINFECTION BYPRODUCTS in DRINKING WATER (Formation, Analysis, and Control). Lewis Publishers. New York Washington, D.C.

Yamamoto, Y., E. Niki, H. Shiokaua and Y. Kamiya, 1979. ozonation of organic compounds.2. Ozonation phenol in water. J. Org. Chem 44, 2137-2142.

Yurter C. and Gurol M. D., 1988. Ozone consumption in natural water: effects of background organic matter, pH and carbonate species. Ozone Sci. Eng. 10, 3.

Zhiru M., 1999. Application of Electrochrochemical and Spin Trapping Technuques in the Investigation of Hydroxyl Radicals. Analytica chemical Acta 389, 213-218.

ELSEVIER

Chemosphere 58 (2005) 1141–1150

CHEMOSPHERE

www.elsevier.com/locate/chemosphere

Effects of polyelectrolytes on reduction of model compounds via coagulation

E.-E. Chang [a], Pen-Chi Chiang [b,*], Wei-Yan Tang [b], Su-Hei Chao [a], Hao-Jan Hsing [b]

[a] *Department of Biochemistry, Taipei Medical University, Taipei, Taiwan, ROC*
[b] *Graduate Institute of Environmental Engineering, National Taiwan University, 71, Chou-Shan Road, Taipei, Taiwan 106, Taiwan, ROC*

Received 17 March 2004

Abstract

The objective of this research work was to evaluate the performance of enhanced coagulation by alum and polymer. Synthetic source waters containing high molecular weight humic acids, medium molecular weight tannic acids and low molecular weight *p*-hydroxybenzoic acid were formulated by adjusting the concentration of turbidity and pH; and jar tests were used to study the effect of various types and dosages of polymer on reducing the above model compounds.

At a specific pH condition, the applied alum dosage would efficiently decrease the turbidity to 2 NTU follows the order: humic > tannic > *p*-hydroxybenzoic acid. Adjustment of pH influenced the performance of alum obviously but not of *p*-DADMAC. High *p*-DADMAC dosage overwhelming the effects of alum is less affected by pH adjustment.

The results of this investigation reveal that enhanced coagulation with *p*-DADMAC was founded to be very effective for removing high-molecular-weight THM precursors, i.e., humic acid and tannic acid, and markedly reduced the alum dosages required for turbidity removal. The other two polymers, i.e., cationic PAM and non-ionic PAM, which had higher molecular weight but lower charge density than *p*-DADMAC, were not capable of removing organic precursors. It was thus concluded that enhanced coagulation with polymer, *p*-DADMAC, could be considered as a promising technique for removal of NOMs with hydrophobic and higher-molar-mass (>1 K) in water treatment plants.
© 2004 Elsevier Ltd. All rights reserved.

Keywords: Enhance coagulation; Polymer; Polyacryamide; *p*-diallyldimethyl ammonium chloride; *p*-hydroxybenzoic acid; Tannic acid; Humic acid; Trichloromethane (THM) formation

1. Introduction

The coagulation process is optimized primarily for the removal of turbidity. Although, nature organic matter (NOM) is also removed by coagulation, the removal efficiency varied with the physical and chemical characteristics of the water as well as the operating conditions of the coagulation process (Ratnaweera et al., 1999). Unless the raw water has a low total organic carbon (DOC) concentration, coagulant dosages are determined by the content of NOM in raw water rather than by turbidity (O'Melia et al., 1999). Generally, the higher-molar-mass fraction of organic matter (OM) is readily removed by

* Corresponding author. Tel.: +886 2 2362 2510; fax: +886 2 2366 1642.
E-mail address: pcchiang@ntu.edu.tw (P.-C. Chiang).

0045-6535/$ - see front matter © 2004 Elsevier Ltd. All rights reserved.
doi:10.1016/j.chemosphere.2004.08.008

coagulation. The type of OM in raw water is also a factor affecting its removal by coagulation. Functional groups of OM influence the solubility of organic compounds; hydrophobic OM is easier to be removed than hydrophilic OM (Collins et al., 1986; White et al., 1997). Owen et al. (1993) indicated that a large percentage of disinfection by products (DBPs) was formed from the non-humic fraction of NOM. This fraction is generally more hydrophilic than humic substances and thus more difficult to remove by coagulation.

Polymers have particular advantages over inorganic coagulants for NOM removal. The performance is less pH dependent and there is a lower level of dissolved ions in the product water. Mallevialle et al. (1984) found that chlorination of polyacryamide (PAM) and acryamide monomers shows low reactivity, and generated a small amount of total organic halides (TOX) and trihalomethane (THM). Chang et al. (1999) found that the polydiallyldimethyl ammonium chloride (*p*-DADMAC) not only effectively removed the turbidity but also reduced the formation of THM. In evaluating cationic polyelectrolytes for the removal of UV absorbers, addition of alum followed by cationic polymethacrylate, *p*-DADMAC or cationic PAM (CPAM) was found to be effective. A polymer with higher charge density (CD) is more effective in reducing UV absorbers than that with low CD. *p*-DADMAC is not considered to be toxic and accepted for use in treatment of municipal water supplies by USEPA. However, the USEPA acceptance is only by the specific name of the suppliers and not by generic type, the maximum dose for *p*-DADMAC is $10\,mg\,l^{-1}$ (AWWA, 1987). PAM is a high molecular weight organic polymer and solute in water easily, and can resist the attack from microbial (Seybold, 1994). Chronic environmental studies indicated that no adverse effects were discovered in workers exposed to PAM dust over a period of 5 years. It has also been known to be non-toxic to human animals, and fish (Anonymous, 1991).

A thorough understanding of the reaction mechanism is a necessary step in determining the proper type of polymer to be used for the coagulation process. The reaction of polymers with other chemicals such as disinfectants in the form of chlorine may adversely affect the success of the coagulation process. Therefore, the objectives of this paper were intended to investigate the effects of three organics acids i.e., humic acid (HA), tannic acid (TA) and *p*-hydroxybenzoic acid (PHBA) on coagulation performance and THM formation potential as well as to determine the most suitable polymer as a coagulant-aid in the coagulation process.

2. Materials and methods

Three model organic compounds with different molar masses and degrees of hydrophobicity were used to simulate some of the wide range of organics found in NOM (Exell and Vanloon, 2000). HA represents fairly hydrophobic, high-molar-mass (molecular weight (MW) = 10 to 100 thousands) natural compounds and is a negatively charged polyelectrolyte due to the dominance of carboxylic acid groups. A number of previous studies have utilized this material; it represents a good model humic substance (Chang et al., 2001; Mustafa and Walker, 2001). TA represents relatively hydrophilic compounds of medium molar mass (MW = 1700), and PHBA (MW = 138) represents small organic molecules found in nature. All of the model compounds containing carboxylic and phenolic groups. Jar tests with rapid mixing, followed by settling were conducted to evaluate the efficiencies of the coagulant and coagulant-aid in removing these compounds and reducing turbidity, as well as THM formation potential under various pH conditions.

2.1. Polymers

Two types of polyacryamide (SNF Co.) including non-ionic PAM of high MW ranging from 5 to 15 million, and CPAM of positively-charged, with CD < 15% containing very high molecular weight (3 to 15 million) were used in this study as coagulant aid. Another cationic polymer, *p*-DADMAC, which has a high CD (100%) and varying MW was also used in this study.

2.2. Synthetic water

Synthetic water was made up to resemble the alkalinity, turbidity, and OM (HA, TA, and PHBA) levels of natural water. In 11 of distilled water, sodium bicarbonate was added to produce on alkalinity of $100 \pm 10\,mg\,l^{-1}$ as $CaCO_3$, and 0.662 mg bentonite was added to obtain an approximate turbidity of 200 NTU. The DOC of the synthetic water prepared above was near $7\,mg\,l^{-1}$ as C. This solution was mixed on a stir plate for 1 h before being transferred to 21. The water was then left in a closed container overnight (>18 h) and the pH was adjusted before it was used in jar tests.

2.3. Jar tests and analyses

All three coagulant-aids and each type of organic compounds were used to compare the effectiveness of each coagulant-aid in removing various types of OM and turbidity under different pH condition. The alum used as a coagulant that chemical formula was $Al(SO_4)_3 \cdot 18\,H_2O$ (Kento Chemical). The solutions with coagulant were rapid-mixed at 100 rpm for 3 min, slow-mixed at 30 rpm for 15 min, and allowed to settle for 20 min. After completion of the settling process, supernatant samples were taken for measurement of turbidity via a turbidimeter (Hach).

Dissolved organic carbon (DOC), chlorine demand, THM, pH, and alkalinity analyses were performed for

the treated water samples. The QA/QC programs set forth in Standard Methods (APHA, 1995) were followed for all sample analyses. Water samples for DOC and UV_{254} analyses were filtered through 0.45 μm filters and determined by a TOC instrument (model 700, O.I. Corp.), and UV spectrophotometer (Hitachi U-2000) respectively. The chlorine concentration were adjusted to about 3 to 40 $mg l^{-1}$, which were depending on the chlorination period and would provide a free residual chlorine of at least 0.2 to 5 $mg l^{-1}$ at the end of the incubation period (APHA, 1995). The analysis of residual chlorine was performed by using the DPD (*N*,*N*-diethyl-*p*-phenylene-diamine) ferrous titration method.

3. Results and disscussion

3.1. Effects of polymers on coagulation enhancement at neutral (pH 7) condition

Fig. 1 presents the results of jar test for water samples containing HA, TA and PHBA with alum coagulant at pH 7. Under the neutralized condition, the concentration of flocs formed by $Al(OH)_3$ was low and, therefore, flocs could not sweep the particles in water. Under acidic conditions, corrosion rate was accelerated that was not feasible in water treatment. They contribute to the concentration of suspension and resulted in high turbidity in alum-treated water (Adin et al., 1998). The dissolved organic carbon (DOC) in raw water was converted to a non-settling particulate form at low alum dosage and contributed to turbidity resulting in so-called "negative effect" phenomenon (White et al., 1997; Singer and Bilyk, 2002). Manahan (1994) found that the humic substances could bind the metal ions such as aluminum and iron. This binding can occur as chelation between a carboxyl group and a phenolic hydroxyl group. It was evidently shown in Fig. 1a that it required over 140 $mg l^{-1}$ of alum to render the residual turbidity lower than 2 NTU. Compared with the HA water, it requires less dosage of alum for treating the TA and PHBA water. At a specific alum dosage (<140 $mg l^{-1}$), the lower residual is associated with decreasing organic MW. The more complex structure and functional groups, the higher

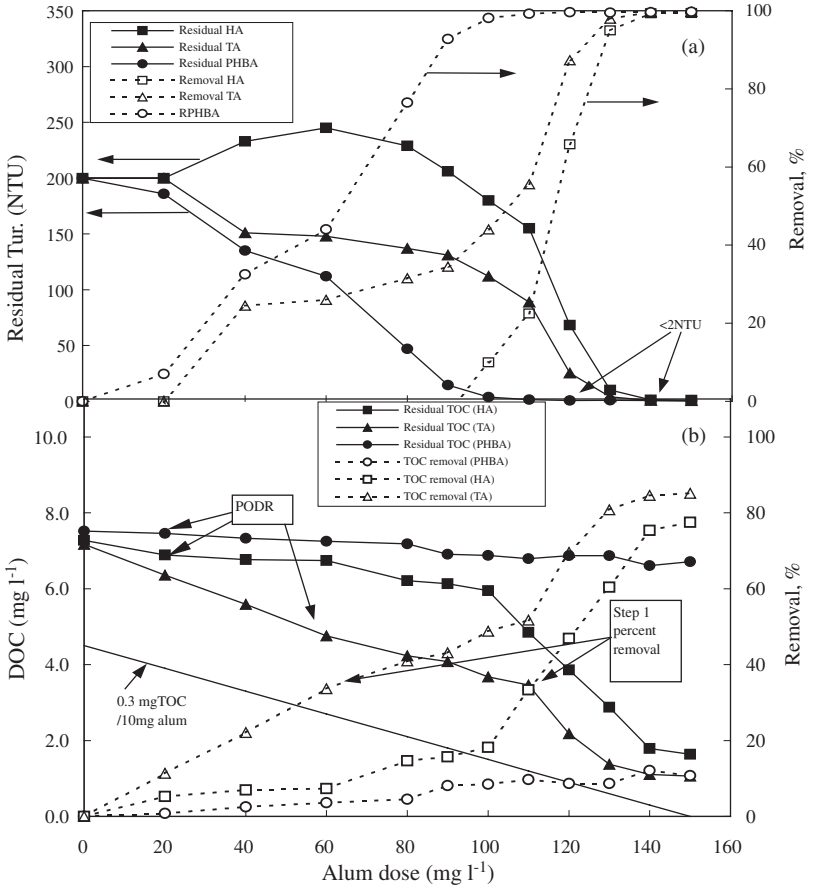

Fig. 1. Results of jar tests of (a) turbidity and (b) DOC for water samples by introducing alum dose at pH 7. (Raw water: DOC = 7.0 ± 0.7 $mg l^{-1}$, Turbidity = 200 ± 10 NTU, Alkalinity = 100 ± 10 $mg l^{-1}$ as $CaCO_3$.)

chemical dosage is needed to destabilize the system (Divakaran and Pillai, 2001).

The requirement of DOC removal for enhanced coagulation suggested in the USEPA D/DBP Rules, provides an operational procedure to establish a point of diminishing returns (PODR) which is defined as the alum dosage beyond which $<0.3\,mg\,l^{-1}$ DOC is removed per $10\,mg\,l^{-1}$ addition of alum in various jar tests. 35% of DOC removal efficiency was set as an evaluation criterion in this research. It could be seen from Fig. 1b that the slope of DOC/alum became steeper over $100\,mg\,l^{-1}$ of alum, therefore, $100\,mg\,l^{-1}$ was the threshold dosage for HA water. It was obvious that TA was relatively easy to be removed by coagulation than HA. Alum has very little effects on PHBA removal at lower alum dosage, although it could remove the turbidity quite successfully.

Since great amounts of coagulants were needed to achieve DOC and turbidity removal requirements, various polymers are chosen as coagulant aids to enhance coagulation and reduce alum consumption. While treating HA water, the addition of CPAM could only reduce turbidity slightly. Non-ionic PAM had better efficiency in removing turbidity than CPAM (Table 1). It is because CPAM could neither adsorb positively charged flocs nor neutralize the charge of particles due to its low CD. Contrarily, using *p*-DADMAC as coagulant-aid, the residual turbidity could be reduced to a lower level, even less than 1 NTU at higher dosages. For example, an alum dosage of $20\,mg\,l^{-1}$, 80% of turbidity was removed with $8\,mg\,l^{-1}$ of *p*-DADMAC for both TA and HA. As alum dose increased, *p*-DADMAC addition could reduce turbidity significantly.

While treating PHBA water, both PAMs had better effects on enhancing the turbidity removal than treating HA or TA water. Non-ionic PAM was still better than CPAM in turbidity removal, but even at the highest chemical dosage, $60\,mg\,l^{-1}$ of alum and $10\,mg\,l^{-1}$ of non-ionic PAM, the residual turbidity of treated water (41 NTU), was extremely higher than the Drinking Water Quality Standard in Taiwan. About $5\,mg\,l^{-1}$ of *p*-DADMAC does reduce the turbidity of treated water to lower than 2 NTU, regardless of the amount of alum dosage. It was evident that the addition of *p*-DADMAC had significant improvement on turbidity removal.

Among three types of polymers, *p*-DADMAC exhibits the most efficient performance for turbidity removal. Comparing the properties of polymers, both PAMs had higher molecular weight and lower CD than *p*-DADMAC. The difference in coagulation performances exhibited by the various type of polymer suggests that the CD of a polymer should be more influential than the molecular weight. In this investigation, it was found that the organic composition in water would affect the efficiency of turbidity removal. The organic compounds with complex structures and functional groups required higher chemical dosages to produce sufficient positive charged flocs for turbidity removal by charge neutralization and adsorption. It was thus concluded that the sequence of the amounts of chemical needed for turbidity removal be: HA > TA > PHBA.

Fig. 2 show DOC removal efficiencies for HA treated with polymers. While treating HA water, *p*-DADMAC is the only one to enhance the coagulation efficiency over the threshold of enhanced coagulation requirement over 35% of DOC removal. Both cationic and non-ionic PAM had little effects on DOC removal. Moreover, higher PAM dosage would remain in treated water and result in higher residual of DOC concentration.

Table 1
Residual turbidity in three types of NOMs water samples treated by alum plus polymer coagulation process[a]

Polymer		Residual turbidity—NTU								
Type	Dose level ($mg\,l^{-1}$)	Alum $20\,mg\,l^{-1}$			Alum $40\,mg\,l^{-1}$			Alum $60\,mg\,l^{-1}$		
		HA	TA	PHBA	HA	TA	PHBA	HA	TA	PHBA
		200	162	186	236	130	167	262	117	113
p-DADMAC	2	175	140	37.6	181	105	30.8	137	22.4	10.5
p-DADMAC	5	103	98.0	0.9	38.3	7.6	1.8	11.2	1.2	1.7
p-DADMAC	8	40.4	39.4	0.2	5.0	0.4	0.2	0.9	3.9	1.5
p-DADMAC	10	3.8	14.0	0.7	0.6	0.5	0.6	0.4	3.3	4.9
PAM (+)	2	185	159	197	213	130	177	220	114	98.3
PAM (+)	5	174	144	182	206	120	142	204	104	86.1
PAM (+)	8	166	147	165	197	118	134	183	104	81.2
PAM (+)	10	168	161	153	182	116	119	174	106	70.0
PAM (non)	2	171	131	171	205	127	140	218	113	74.5
AM (non)	5	149	120	145	165	103	121	182	102	54.6
PAM (non)	8	138	105	132	137	92.3	96.6	155	88.0	45.2
PAM (non)	10	122	97.9	126	129	98.1	89.9	135	81.8	41.4

[a] Raw water: DOC = 7.0 ± 0.7 $mg\,l^{-1}$, turbidity = 200 ± 3 NTU, alkalinity = 100 ± 10 $mg\,l^{-1}$ as $CaCO_3$, pH = 7.

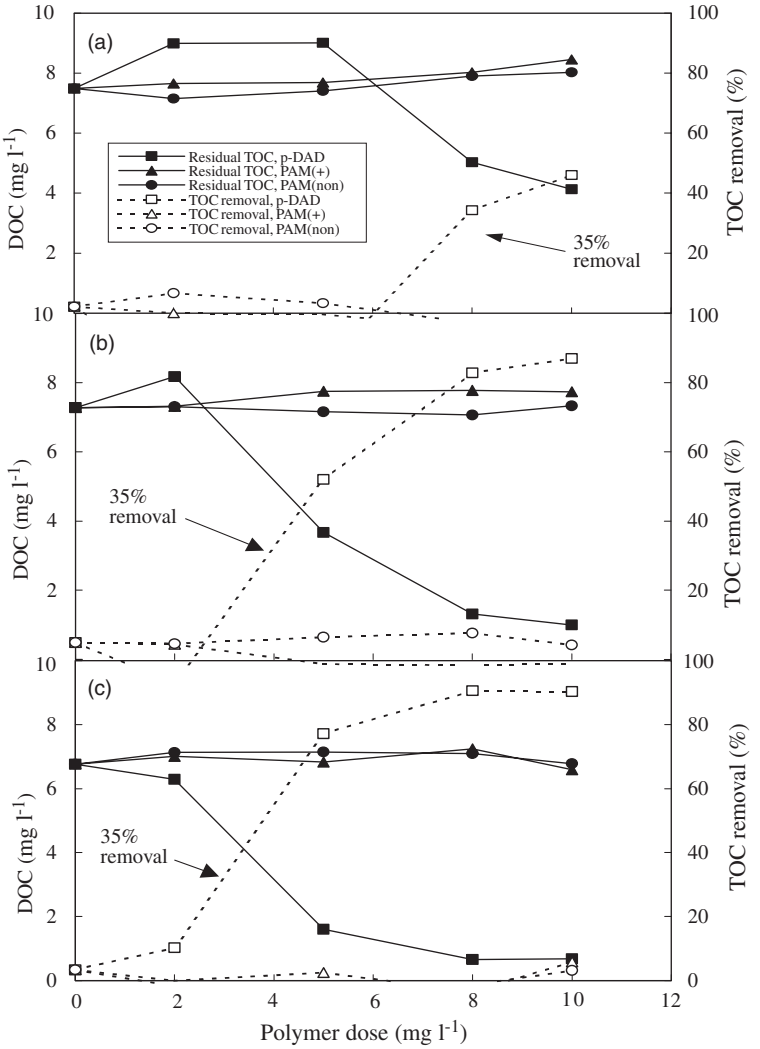

Fig. 2. Results of jar tests (DOC) for introducing alum as (a) Alum 20, (b) Alum 40, (c) Alum 60 plus polymers to humic acid water samples. (Raw water: DOC = 7.0 ± 0.7 mgl^{-1} as HA, Turbidity = 200 ± 10 NTU, Alkalinity = 100 ± 10 mgl^{-1} as $CaCO_3$.)

p-DADMAC could strengthen the linkage between particles and flocs, which enlarge the size of flocs and make them easier to settle. Furthermore, the organic matter might be adsorbed on to the flocs and be removed along with the precipitates. However, insufficient dosage of *p*-DADMAC would increase DOC concentration in treated water, and it was even much significant than the over-dosage of cationic and non-ionic PAM. While dosing 20 mgl^{-1} of alum, over 8 mgl^{-1} of *p*-DADMAC was needed to achieve the 35% DOC removal requirement. Similar patterns were observed that over 5 mgl^{-1} *p*-DADMAC was needed when 40 mgl^{-1} of alum was added and 2 mgl^{-1} of *p*-DADMAC with 60 mgl^{-1} of alum. Thus, it can be concluded that the higher the alum dosage, the lower dosing *p*-DADMAC is needed for DOC removal. Consequently, lower dose of *p*-DADMAC could easily link the particles and flocs together due to its high positive CD and results in the formation of polymer–floc complexes.

In general, results regarding DOC removals from the treatment of water containing TA were similar to those of HA water. Dosing 60 mgl^{-1} of alum could reduce TOC concentration effectively, polymers might not be necessary unless higher removal requirement is needed. Both PAMs not only had little effects on DOC removal, but also impeded the coagulation performances regardless of changes in alum dosage. When the dosage of alum was 20 mgl^{-1}, more than 6 mgl^{-1} of *p*-DADMAC was needed to achieve the enhanced coagulation requirement.

Since alum alone was not capable of removing PHBA, different polymers were dosed to improve the coagulation performance. However, none of the polymers used in this research could enhance coagulation performance. It is evident that the hydrophilic property and smaller molecular weight of PHBA could impede the co-precipitation and adsorption of organic carbon resulted in lowering reduction of DOC.

3.2. Effect of pH adjustment on turbidity and DOC removal for p-DADMAC

The pH adjustment with metal salt coagulants is an important operating parameter for the coagulation process. Adjusting the pH to the range between 4 and 5 are generally believed to enhance the coagulation performance with alum. The pH of synthetic water was adjusted to 5, 6, and 7 prior to coagulant addition. While treating the HA water, *p*-DADMAC could help to remove most of the turbidity in water. At low alum dosage, e.g., 20 mg l^{-1}, the coagulation effects mainly were contributed by *p*-DADMAC, however, pH effect is not significant shown in Fig. 3a. When the alum dosage was increased to 60 mg l^{-1}, pH effects became obvious. As shown in Fig. 3b, the percent turbidity removal at pH 5 is higher than that at pH 6 or 7. The addition of *p*-DADMAC became useless at pH 5 due to the sufficient alum and dosage. The role of *p*-DADMAC on treating TA water is similar to that on treating HA water. In general, the effects of pH became obvious with increasing alum dosage.

It was concluded that pH would affect the performance of alum in removing turbidity but not of *p*-DADMAC. Therefore, low *p*-DADMAC dosage in cooperation with high alum dosage would be affected by pH adjustment. Since a slight reverse of turbidity removal was observed at high polymer dosage and low pH for treating the above organic precursors, the dosage of polymer must be controlled well in low pH conditions.

In Fig. 3c and d, it was observed that DOC removal increased with decreasing pH value at 20 mg l^{-1} of alum dosage. It took about 5 mg l^{-1} of *p*-DADMAC to achieve the same percent DOC removal requirement at pH 5, while higher dosage was needed at higher pH.

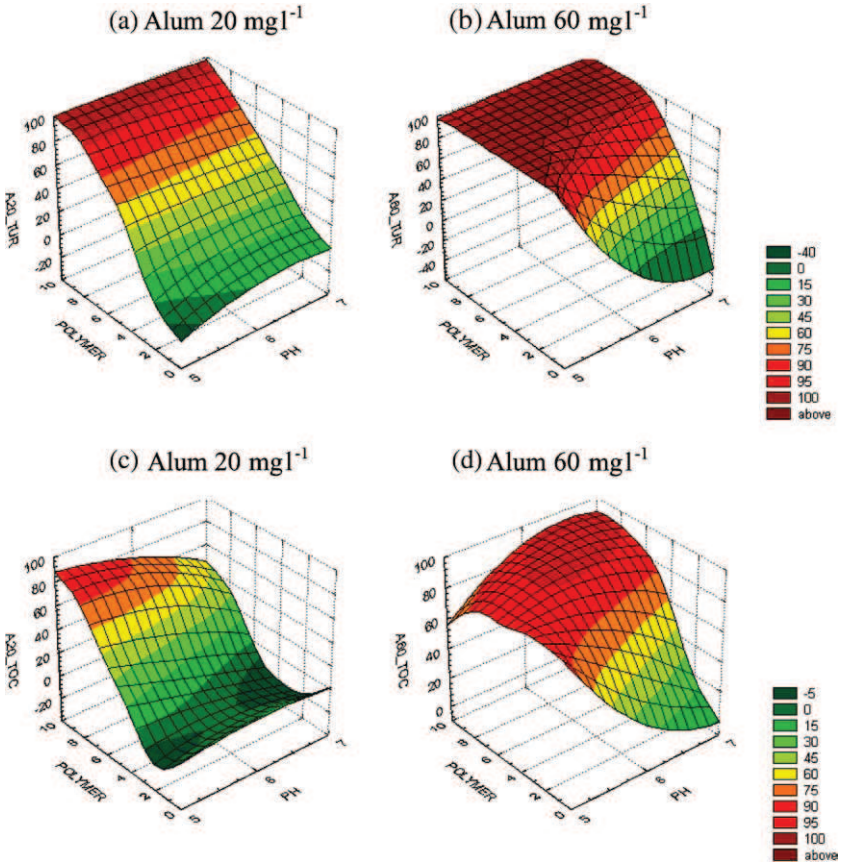

Fig. 3. Parameter removal (%) as a function of *p*-DADMAC polymer dosage and pH for humic acid water. turbidity: (a) and (b); DOC: (c) and (d).

However, when dosing 60 mg l^{-1} of alum at pH 5, higher dosage of *p*-DADMAC decreased DOC removal. High concentration of aluminum hydroxide species and hydrogen ions neutralized the negative charges on suspended particles during rapid mixing; part of the *p*-DADMAC added was utilized to bridge the particles. Therefore, excessive *p*-DADMAC dose would remain in water sample and contribute to DOC concentration. While treating the most irresponsive-to-coagulation organic matter, PHBA, pH adjustment combining polymer addition is ineffective, and there is no obvious relationship between chemical dosage and DOC removal efficiency.

Comparing the UV_{254} variation as shown in Fig. 4a, it is obvious that the concentration of organic matter with aromatic structure (HA in this case) decreased with increasing *p*-DADMAC dosage. In many studies, UV absorbance was used as a surrogate indicator for determining organic precursors (O'Melia et al., 1999; Singer and Bilyk, 2002). In this research, UV_{254} was also used as a supplementary index to determine the composition of organics in water. In order to determine the composition of organics in water treated by high polymer dose, UV_{254} is again used as an index, as shown in Fig. 4b. It can be observed that the reverse shows up when the concentration of DOC is already low in water treated by alum without polymer addition. It implies that if DOC is reduced to a low level, the addition of *p*-DADMAC must be controlled carefully for treating the water containing low level of DOC, otherwise, it might be useless and harmful.

3.3. Reduction of THM formation potential (THMFP)

Among three types of organic precursors, HA had the highest THM yield (110 μg THM/mg DOC), PHBA the second highest (60 μg THM/mg DOC) and TA the lowest at about 50 μg THM/mg DOC. HA contains many activating functional groups such as hydroxyl, carbonyl, and acryloxy etc. which will react with chlorine to form THM.

Chlorine demand and THMFP are both related to DOC concentration. Enhanced coagulation by alum plus *p*-DADMAC could reduce the chlorine demand. The THMFP and chlorine demand of raw, alum-, and alum *p*-DADMAC-treated waters for three different synthetic waters are compared and showed in Fig. 5. For HA and TA water, much less reduction of chlorine demand were observed for the water treated. However, the higher reduction in chlorine demand and THMFP was only found in the HA and TA water treated with alum plus *p*-DADMAC.

The THMFP results of HA water and treated water were shown in Table 2. For the most cases of HA, THMFP was found to decrease with increasing chemical dosage. If eliminating the data that were not able to reduce the turbidities to a level lower than 2 NTU, coagulation treatment at pH 5 could decrease THMFP by 85–94%, and 89–96% at pH 7. The results suggest that if strict standard (turbidity < 1 NTU) is adopted for treating high turbidity water in the future, high dosage of polymer is necessary to decrease THMFP effectively and, therefore, pH effect is not critical in this condition.

As the elimination based on residual turbidity standard, coagulation at pH 5 could reduce 67–86% of

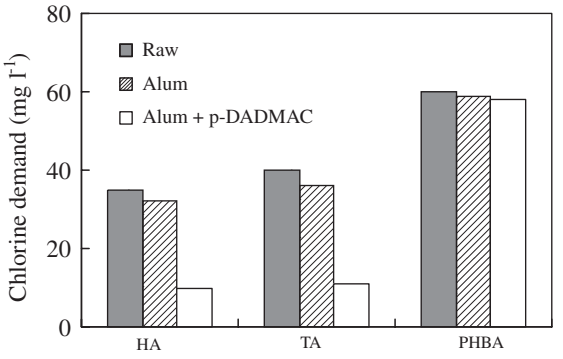

Fig. 5. Chlorine demand for raw, alum-, and alum + *p*-DADMAC-treated water for different source water (7.0 ± 0.7 mg l^{-1} DOC).

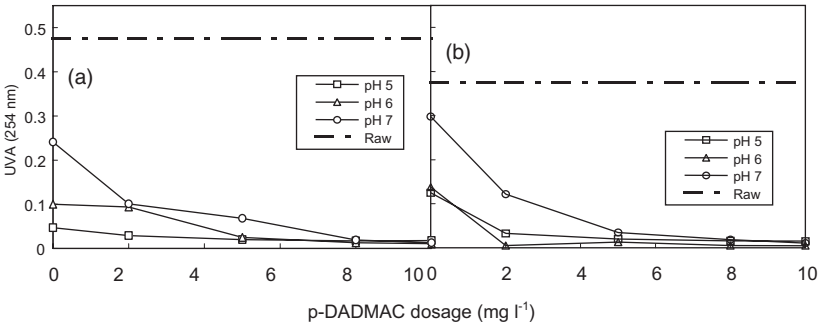

Fig. 4. UV_{254} (a) humic acid and (b) tannic acid as a function of *p*-DADMAC dosage at different pH (Alum dosage: 60 mg l^{-1}).

Table 2
Summary of THMFP percent removal in humic acid water samples treated by alum and alum plus *p*-DADMAC polymer

Applied dosage		pH 5				pH 6				pH 7			
Alum ($mg l^{-1}$)	*p*-DADMAC ($mg l^{-1}$)	TOC[a]	Tur[b]	THMFP ($\mu g l^{-1}$)	Percent decrease (%)	TOC[a]	Tur[b]	THMFP ($\mu g l^{-1}$)	Percent decrease (%)	TOC[a]	Tur[b]	THMFP ($\mu g l^{-1}$)	Percent decrease (%)
				1001				846				816	
20	0	+	+	898	10	+	+	843	0	+	+	666	18
20	2	+	+	784	22	+	+	848	0	+	+	846	–4
20	5	+	+	393	61	+	+	742	12	+	+	730	11
20	8	–	+	69	93	–	+	284	66	+	+	278	66
20	10	–	–	59	94	–	–	107	87	–	–	86	89
40	0	+	+	900	10	+	+	769	9	+	+	540	34
40	2	+	+	306	69	+	+	744	12	+	+	739	9
40	5	–	–	70	93		+	668	21	–	+	341	58
40	8	–	–	53	95	–	+	83	90	–	+	76	91
40	10	–	–	64	94	–	–	52	94	–	–	31	96
60	0	–	–	145	85	+	+	582	31	+	+	654	20
60	2	–	–	139	86	–	+	356	58	+	+	566	31
60	5	–	–	113	89	–	–	124	85	–	+	85	90
60	8	–	–	73	93	–	–	56	93	–	–	41	95
60	10	–	–	75	92	–	–	54	94	–	–	60	93

[a] If percent TOC removal > 35%; +: yes; –: no.
[b] If residual turbidity < 2 NTU; +: yes; –: no.

THMFP, 78–91% at pH 6, and 83–90% at pH 7. Low percent THMFP reduction at pH 5 is due to the poor performance of DOC removal caused by over-dosage of *p*-DADMAC. As a result, while treating TA water, higher pH will prevent over-dosage and lead to better THMFP reduction.

Fig. 6 further illustrated these relationships between THMFP and DOC for HA water and TA water. The linear relationship could be observed in both samples which was consistent with the findings suggested by other researchers (Page et al., 2002; Singer and Bilyk, 2002). The regression equations in Fig. 6a estimates that a 90 μg l^{-1} decrease in HM formation for every 1 mg l^{-1} decrease in DOC concentration (90 μg THM/mg DOC) and a 40 μg THM/mg DOC for HA and TA water, respectively, which are both higher than the result, 26 μg THM/mg DOC, proposed by Singer and Bilyk (2002). It could be explained by that the selected organic precursors in this research are more generative in formation of THM than the raw water from the river of United States.

The distribution of THMFP at various polymer doses is illustrated in Fig. 7 which indicated that the median THMFP decrease and the range of the measured THMFP data narrow with increasing polymer dose. This observation suggests that high dosage of polymer, *p*-DADMAC, should possess great performance in removing DOC for treating HA and TA waters.

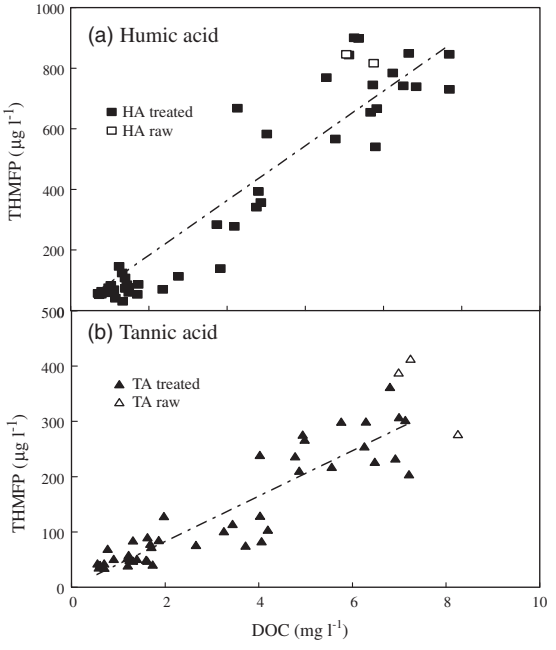

Fig. 6. Correlation between THMFP and DOC for (a) humic acid and (b) tannic acid.

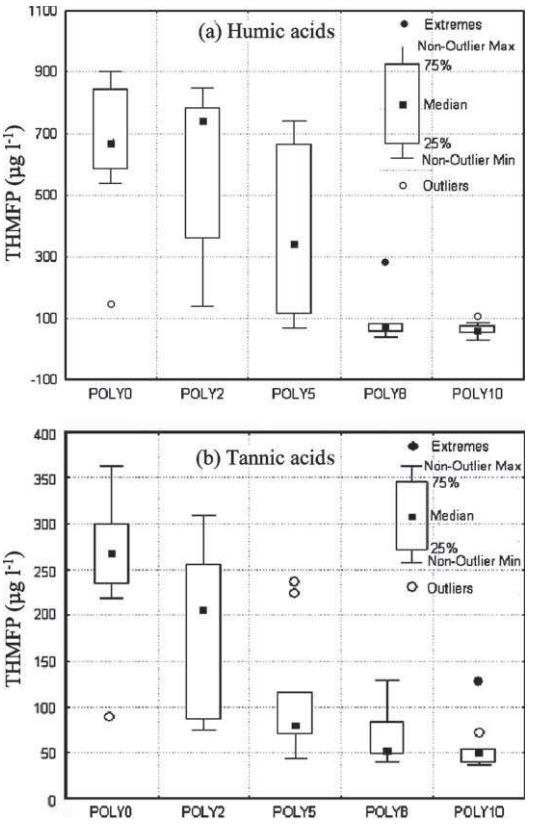

Fig. 7. Distribution of THMFP at various polymer doses (Alum dosage: 60 mg l^{-1}).

4. Conclusions

In this investigation, it was observed that at a specific pH (pH = 7) condition, the concentration of alum needed to decrease THMFP follows the order: HA > TA > PHBA, and acidic condition is conducive to alum coagulation, and is more effective with increasing alum dosage. Enhanced coagulation with the addition of a polymer, *p*-DADMAC, was found to be very effective in removing high MW of THM precursors, such as HA and TA, from the synthetic waters, and markedly reduced the alum dosages required for turbidity removal. However, the removal of low MW of THM precursors, such as PHBA, was found to be unfavorable to coagulation.

Residual TDOC concentration, UV absorbance, turbidity, THM formation potential, and chlorine demand in HA and TA waters, except for PHBA waters, were all substantially lower as a result of adding *p*-DADMAC as coagulant-aid in alum coagulation. The other two polymers, cationic PAM and non-ionic PAM, which had higher molecular weight but lower charge density than *p*-DADMAC, were not capable of removing effectively any of the parameters mentioned above. The results

implied that charge density was a very specific characteristic of polymer affecting the performance of coagulation process. While treating low turbidity water with *p*-DADMAC, its high charge density narrowed the optimum dosage and was impeditive to the performance of coagulation. As a result, using polymer to treat low turbidity water is not recommended.

References

Adin, A., Soffer, Y., Aim, R.B., 1998. Effluent pretreatment by iron coagulation applying various dose–pH combinations for optimum particle separation. Wat. Sci. Technol. 38, 27–34.

Anonymous, 1991. Final report on the assessment of polyacrylamide. J. Am. Coll. Toxicol. 10, 193–203.

APHA, 1995. Standard Methods for the examination of Water and Wastewater, 19th ed. American Public Health Association, Washington, DC.

AWWA, 1987. Standard for Poly(Diallydimethylammonium Chloride), AWWA B451-87. American Water Works Association, Denver, CO, USA.

Chang, E.E., Chaing, P.C., Chao, S.H., Liang, C.H., 1999. Effects of polydiallyldimethyl ammonium chloride coagulant on formation of chlorinated by products in drinking water. Chemosphere 39, 1333–1346.

Chang, E.E., Chiang, P.C., Ko, Y.W., Lan, W.H., 2001. Characteristics of organic precursors and their relationship with disinfection by-products. Chemosphere 44, 1231–1236.

Collins, M.R., Amy, G.L., Steelink, C., 1986. Molecular weight distribution, carboxylic acidity, and humic substances content of aquatic organic matter. Implications for removal during water treatment. Environ. Sci. Technol. 20, 1028–1032.

Divakaran, R., Pillai, V.N.S., 2001. Flocculation of kaolinite suspensions in water by chitosan. Wat. Res. 35, 3904–3908.

Exell, K.N., Vanloon, G.W., 2000. Using coagulants to remove organic matter. J. Am. Water Works Assoc. 92, 93–102.

Mallevialle, J., Bruchet, A., Fiessinger, F., 1984. How safe are organic polymers in water treatment. J. Am Water Works Assoc. 76, 87–93.

Manahan, S.E., 1994. Environmental Chemistry. Lewis Publishers, Chelesea MI, pp. 80–81.

Mustafa, M.B., Walker, H.W., 2001. Effect of natural organic coatings on the polymer-induced coagulation of colloidal particles. Colloids Surf. A 177, 215–222.

O'Melia, C.R., Becker, W.C., Au, K.K., 1999. Removal of humic substances by coagulation. Wat. Sci. Technol. 40, 47–54.

Owen, D.M., Amy, G.L., Chowdhury, Z.K., 1993. Characterization of Natural Organic Matter and its Relationship to Treatability. AWWA Res. Fund., Denver, CO, USA.

Page, D.W., van Leeuwen, J.A., Spark, K.M., Drikas, M., Withers, N., Mulcahy, D.E., 2002. Effect of alum treatment on the trihalomethane formation and bacterial regrowth potential of natural and synthetic waters. Wat. Res. 36, 4884–4892.

Ratnaweera, H., Gjessing, E., Oug, E., 1999. Influence of physical–chemical characteristics of natural organic matter (NOM) on coagulation properties: An analysis of eight Norwegian water sources. Wat. Sci. Technol. 40 (4–5), 89–95.

Seybold, C.A., 1994. Polyacrylamide review: Soil conditioning and environmental fate. Commun. Soil Sci. Plant Anal. 25, 2171–2185.

Singer, P.C., Bilyk, K., 2002. Enhanced coagulation using a magnetic ion exchange resin. Wat. Res. 36, 4009–4022.

White, M.C., Thompson, J.D., Harrington, G.W., Singer, P.C., 1997. Evaluating criteria for enhanced coagulation compliance. J. Am. Water Works Assoc. 89, 64–77.

ELSEVIER

Chemosphere 64 (2006) 1196–1203

CHEMOSPHERE

www.elsevier.com/locate/chemosphere

Relationship between chlorine consumption and chlorination by-products formation for model compounds

E.E. Chang [a,*], P.C. Chiang [b], S.H. Chao [a], Y.L. Lin [b]

[a] *Department of Biochemistry, Taipei Medical University, 250 Wu-Shin Street, Taipei 110, Taiwan*
[b] *Graduate institute of Environmental Engineering, National Taiwan University, 71 Chou-Shan Road, Taipei 106, Taiwan*

Received 10 May 2005; received in revised form 10 November 2005; accepted 10 November 2005
Available online 10 January 2006

Abstract

The objective of this research is to investigate the relationship between chlorine decay and the formations of disinfection by-products (DBP), including trichloromethane (TCM) and chloroacetic acid (CAA) in the presence of four model compounds, i.e., resorcinol, phloroglucinol, *p*-hydroxybenzoic acid, and *m*-hydroxybenzoic acid. The chlorine degradation in model compounds with OH and/or COOH functional groups were rapid after chlorination. The TCM yields of carboxylic group substituted compounds (3-hydroxybenzoic acid [3-HBA], 4-hydroxybenzoic acid [4-HBA]) were found to be lower than that of the *m*-dihydroxy substituted compounds. Phloroglucinol, with one more OH substitution group than resorcinol, tends to form significant amounts of CAA after chlorination. However, it was observed that with the COOH substitution of 3-HBA and 4-HBA tend to exhibit more CAA formation potential than resorcinol. The developed parallel second and first-order reaction model for chlorine demand has been successfully utilized for TCM, CAA and DBP formation modeling. A high correlation between CAA and TCM was observed for the model compounds.
© 2005 Elsevier Ltd. All rights reserved.

Keywords: Chlorine consumption; Resorcinol (R); Phloroglucinol (P); Hydroxybenzoic acid (HBA); Tichloromethane (TCM); Chloroacetic acids (CAA); Chlorine decay model

1. Introduction

After the humic fraction within nature organic matter (NOM) was identified as a major precursor for trihalomethanes (THM) formation (Rook, 1976), most researches have focused their research on the humic portion of the NOM for disinfection by-products (DBPs) formation. Marhaba and Van (2000) concluded that the hydrophilic acid fraction was the most reactive precursor to the THM formation; while the hydrophobic neutral fraction was related to the formation of HAA. Liang and Singer (2001) reported that hydrophilic carbon also plays an important role in DBP formation, especially for waters with low humic content. Recent studies indicate that all fractions of NOM contribute to the formation of DBP (Sinha, 1999; Chang et al., 2001; Gang et al., 2003). It appears that the properties of humic substances have molecular weights of several hundred or larger, with weakly acidic functional groups (such as carboxylic group), and phenolic group which cause different types and amounts of DBPs (Cook and Langford, 1998).

Several studies suggested that aliphatic carboxylic acids, hydroxybenzoic acids, phenols and pyrrole derivatives are reactive substrates of organic precursors for THMs formation (Norwood et al., 1980; Korshin et al., 1997). Rook (1976) postulated that the *m*-dihydroxy structure of resorcinol was the principal TCM precursor in aquatic humic materials and proposed a reaction mechanism. The reaction products, $CHCl_3$ and CCl_3COOH, were identified from the chlorination of resorcinol (Norwood et al., 1980). Chlorination could undergo electrophilic attack either at the chlorine atom (with displacement of hydroxyl,

* Corresponding author. Tel./fax: +886 2 2736 9236.
E-mail address: eechang@tmu.edu.tw (E.E. Chang).

0045-6535/$ - see front matter © 2005 Elsevier Ltd. All rights reserved.
doi:10.1016/j.chemosphere.2005.11.036

leading to chlorination) or at the hydroxyl group (with loss of chlorine). For example, *p*-hydroxybenzoic acid reacted rapidly to generate a mixture which is side-chain cleavage products of substitution and decarboxylation (Larson and Rockwell, 1979). Boyce and Hornig (1983) confirmed that the conversion of 1,3-dihydroxyaromatic precursors to THMs occurs in two stages. Extensive incorporation of halogen by electrophilic substitution and addition processes is followed by a complex series of hydrolysis and decarboxylation steps, which lead to TCM via carbon–carbon bond cleavage about the C_2 site of the aromatic ring.

In many research reports, mathematical models were suggested to predict THM formation of specific source water (Engerholm and Amy, 1983; Amy et al., 1987; Chang et al., 1996; Gang et al., 2002). Gang et al. (2002) constructed a mathematical model of chlorine decay to predict the THM formation. The authors (Gang et al., 2003) also indicated that the THM formation in fractionated NOM was a function of chlorine consumption. As the molecular weight of the fraction decreased, THM yield coefficients increased. Katz (1986) suggested that the total organic carbon (TOC) had a strong correlation with chlorine demand, particularly when turbidity was less than 20 NTU in the filtrate. The effect of chlorine demand on DBP formation is generally not well known because NOM is composed of many types of organics. Aromatics and humic substance strongly react with chlorine that could be responsible for the initial chlorine demand (Dotson and Helz, 1984).

Most organic matters contributing to major DBP precursors in source water of Taiwan are small compounds, with a molecular weight of less than 1 KDa which was measured by the ultrafiltration membranes (Chang et al., 2001; Chiang et al., 2002) However, only limited research has been done on DBPs formation with different functional groups of small molecular aromatic compounds. The objectives of this research were to: (1) develop the appropriate chlorine decay and DBP formation models for the selected four model compounds; (2) investigate the formation potential of trichloromethane (TCM) and chloroacetic acids (CAA) for the four model compounds; (3) evaluate the relationship between CAA/TCM and chlorine consumption with different functional groups of model compounds.

2. Material and methods

2.1. Sample preparation

Four model compounds with different functional groups of benzene i.e., carboxylic and phenolic groups were selected in this investigation to represent small molecular NOM. The four model compounds include phloroglucinol (1,3,5-trihroxybenzene), resorcinol (1,3-dihydroxybenzene), *m*-hydroxybenzoic acid (3-HBA), and *p*-hydroxybenzoic acid (4-HBA). The dissolved organic carbon (DOC) concentrations for model compounds, using de-ionized water (Milli-Q SP), were prepared and adjusted to approximately 3.0 (±0.2) mg/l as C. The characteristics of the model compounds are listed in Table 1.

2.2. Evaluation of Chlorine consumption

A 7-day chlorine consumption study was performed using 28 mg/l chlorine dosage (as Cl_2), about 9 times the DOC dosage, to determine the chlorine consumption, trichloromethane formation potential (TCMFP), and chloroacetic acid formation potential (CAAFP). Throughout these chlorination experiments, all samples were chlorinated by 13% free chlorine (sodium hypochlorite) stock solution and added phosphate buffer (pH 7.0). A blank sample was prepared using the same amount of deionized ultra filtered water, and chlorinated under the same conditions as the other samples. Samples were chlorinated in 6 liter glass bottles and then carefully transferred into 150 amber glass bottles with Teflon-lined caps. A separate bottle containing the four model compounds samples was used for each reaction kinetic test. There were 12 experimental data for 3-HBA, 4-HBA, resorcinol and phloroglucinol,

Table 1
Physical/chemical properties of model compounds

Model compound	Phloroglucinol	Resorcinol	3-HBA	4-HBA
Molecular formula	$C_6H_6O_3$	$C_6H_6O_2$	$C_7H_6O_3$	$C_7H_6O_3$
Molecular weight	126.11	110.11	138.12	138.12
Dissociation constant (pK_a)	pK_1 8.0 pK_2 9.2 pK_3 14	pK_1 9.30 p$K_2$11.06	pK_1 4.06 pK_2 9.92	pK_1 4.48 pK_2 9.32
Solubility in water	10 g/l (20 °C)	1000 g/l (20 °C)	slightly soluble (20 °C)	5000 mg/l (25 °C)
Structure	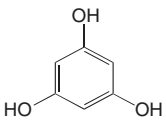	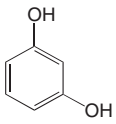	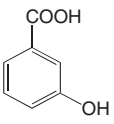	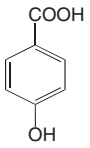
$SUVA_{254}$ (l mg^{-1})	0.67	0.47	0.73	11.8
Produced company	Across	Across	Across	Merck

respectively, obtained at the specific time intervals, i.e., 0.08, 0.17, 0.33, 0.50, 0.67, 0.83, 1, 3, 6, 24, 48 and 168 h during the reaction kinetic tests. The samples were kept headspace free in the dark at room temperature (25 ± 2 °C) until they were analyzed. Chlorine residual, DOC and UV adsorption were measured at different times for each bottle.

2.3. Analytical methods

Chlorine concentration was measured by *N*,*N*-diethyl-*p*-phenylenediamine (DPD) titration methods. DOC (TOC), UV_{254}, pH, and DBPFP analyses were conducted for each water sample. All analyses, unless otherwise noted, were performed according to the 19th edition of the Standards Methods (APHA, 1998). Water samples for DOC and UV analyses were conducted first by filtering through a prewashed 0.45 μm filter, and then the sample was analyzed by a TOC instrument (O.I. Corporation model 700) and UV spectroscopy (Hitachi U-2000). TCM and CAA (including mono-, di-, and tri-chloroacetic acids) were analyzed by HP 6890GC/ECD according to Standard Methods 6230D and USEPA methods 552.2, respectively. Duplicate analyses were performed on each sample, and the average was reported. If the difference between the two values was greater than 15%, a third analysis was performed, and the average of all three values was reported.

2.4. Models of chlorine decay and DBP formation

Owing to the unique characterization of the selected target compounds, many models developed in the literature (Gang et al., 2002, 2003) can not fit the experimental data well. As a result, the parallel first-order reaction model, which was originally derived by Gang et al. (2002) could be modified as the following:

$$\mathrm{NOM_R} + \mathrm{Cl_2} \xrightarrow{k_R} R - X \ \text{(rapid)} \tag{1}$$

$$\frac{dC_R}{dt} = -k_R C^n \tag{2}$$

$$\mathrm{NOM_S} + \mathrm{Cl_2} \xrightarrow{k_S} R - X \ \text{(slow)} \tag{3}$$

$$\frac{dC_S}{dt} = -k_S C \tag{4}$$

in which C_R is the chlorine concentration participating in a hypothetical separate rapid reaction; C_S is the chlorine concentration participating in a hypothetical separate slow reaction; R and X are chlorinated by-products; n and m are the order of the reaction with respect to the rapid and slow reactions, respectively.

The value of n and m are determined by the best fit as compared with the suggested reaction orders. Integrating these rate equations (Eqs. (2) and (4)) with $C_{R0} = fC_0$ and $C_{S0} = (1-f)C_0$, the chlorine concentration at any time is

$$C(t) = \left[-K_R \cdot t \cdot (-n+1) + f \cdot C_0^{-n+1}\right]^{\frac{1}{-n+1}} + \left[-K_S \cdot t \cdot (-m+1) + f \cdot C_0^{-m+1}\right]^{\frac{1}{-m+1}} \quad (n, m \neq 1) \tag{5}$$

$$C(t) = C_0 \cdot \left\{f \cdot e^{-K_R \cdot t} + (1-f) \cdot e^{-K_S \cdot t}\right\} \quad (n, m = 1) \tag{6}$$

in which $C(t)$ is the chlorine concentration at any time t (mg/l), C_0 is the initial chlorine concentration (dose), f is the fraction of the chlorine demand attributed to rapid reactions, k_R is the rate constant for rapid reactions, and k_S is the rate constant for slow reactions.

The coefficients (f, K_R, and K_S) obtained from the chlorine decay model (Eq. (5) or Eq. (6)) were used to predict the TCM, CAA, and DBP (TCM + CAA) formations. Eqs. (7)–(9) assume that the TCM, CAA and DBP formations are a function of chlorine consumptions with respect to the rapid and slow reactions:

$$\mathrm{TCM} = A(C_{R0} - C_R)^n + B(C_{S0} - C_S)^m \tag{7}$$

$$\mathrm{CAA} = C(C_{R0} - C_R)^n + D(C_{S0} - C_S)^m \tag{8}$$

$$\mathrm{DBP} = E(C_{R0} - C_R)^n + F(C_{S0} - C_S)^m \tag{9}$$

in which A and B are the TCM yield coefficient from the rapid and slow chlorine consumed, respectively; C and D are the CAA yield coefficients from the rapid and slow chlorine consumed, respectively; E and F are the DBP yield coefficients from the rapid and slow chlorine consumed, respectively.

The parameters n, m, f, k_R, ks and yield coefficients (A, B, C, D, E, F) were determined by non-linear regression software (SYSTAT 5.01).

3. Results and discussion

3.1. Chlorine demand and decay modeling

Fig. 1 shows the chlorine demand and residual chlorine associated with the hydroxybenzene and hydroxybenzoic acid during the chlorination process, respectively. It was observed that the chlorine consumption increased rapidly within the first 3 h and then gradually decayed after 3 h

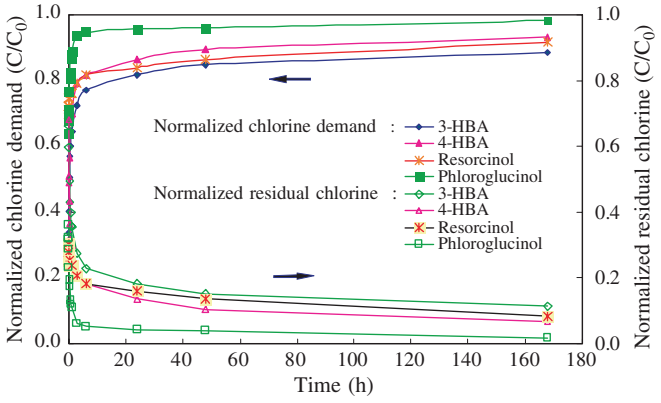

Fig. 1. Normalized chlorine demand and decay curves of model samples during the chlorination process.

of chlorination. Since the phenolates (dissociated form of phenols) from model compounds were responsible for the fast reaction with chlorine, all water samples consumed over 80% of the initial chlorine dose within the first 3 h, especially for the resorcinol, which had the highest chlorine consumption rate at 10 min.

The parallel second and first-order reaction model for chlorine demand derived in this study is the best fit as compared with the parallel first-order model (derived by Gang et al., 2002), *n*-order chlorine decay model, parallel second order and parallel first order and second order. Table 2 presents the chlorine decay constants and fitting parameters for the model compounds. The chlorine data of hydroxybenzene and hydroxybenzoic acid in Fig. 2 fit the model well, yielding the correlation coefficients of 0.985–0.991.

The constants of rapid decay rates ($K_R = 0.32$–$5.05\ l\ mg^{-1}\ h^{-1}$) in Table 2 were much higher than those of the slow decay rates ($k_S = 0.006$–$0.028\ h^{-1}$) for all model samples. The values of k_R for the hydroxybenzoic acids were much smaller than those of the hydroxybenzene samples. The proportion constants (f) shown in Table 2 ranged from 76% to 91% of the chlorine consumption. Differences in the reaction kinetics observed between these four compounds may be separated into two groups. For resorcinol and phloroglucinol, the chlorine consumptions were higher at first and increased gradually afterwards; whereas for 3-HBA and 4-HBA, chlorine consumptions were lower at first and increased rapidly afterwards.

Larson and Rockwell (1979) and Gallard and Gunten (2002) revealed that resorcinol, with two activating –OH groups, could release electrons rapidly, leading to the electrophilic addition and substitution reactions while chlorination was proceeding. Boyce and Hornig (1983) also pointed out that when both OH groups on an aromatic ring are located at an appropriated orientation to stabilize the transition state of the reaction through the donation of electron density, an electrophilic substitution mechanism could easily occur. These observations suggest that the aromatic carbon site adjacent to the C_1-hydroxyl group be inverted to electrophilic substitution by chlorine. However, phloroglucinol is highly symmetric and may form a resonance-stabilized intermediate because of three –OH groups. These three –OH groups may impede series of hydrolysis as well as decarboxylation with C–C bond cleavage on the aromatic ring resulting in a lower k_R value of phloroglucinol ($1.225\ l\ mg^{-1}\ h^{-1}$) than that of resorcinol ($5.051\ l\ mg^{-1}\ h^{-1}$).

As for hydroxybenzoic acids with moderately deactivating substituents (–COOH), the electron density on the benzene ring would be lowered during the ionization process of carboxyl group. The chlorination of carboxyl groups proceeds much slower than the chlorination of resorcinol and phloroglucinol, which is because that hydroxybenzoic acid reacts rapidly to give a decarboxylation product (Larson and Rockwell, 1979). As for the chlorine consumption rate between 3-HBA and 4-HBA, it was observed that there was a higher value for 4-HBA because the *p*-position of OH and COOH on the aromatic ring is more active than the *m*-position of OH and COOH which facilitates the chlorine reaction on hydroxybenzoic acid.

Table 2
Chlorine decay constants and fitting parameters of model compounds (chlorine dose = 28 mg/l)

Compounds	f	K_R ($l\ mg^{-1}\ h^{-1}$)	K_S (h^{-1})	R^2
3-HBA	0.760	0.319	0.006	0.995
4-HBA	0.819	0.328	0.008	0.998
Resorcinol	0.782	5.051	0.008	0.995
Phloroglucinol	0.913	1.225	0.028	0.985

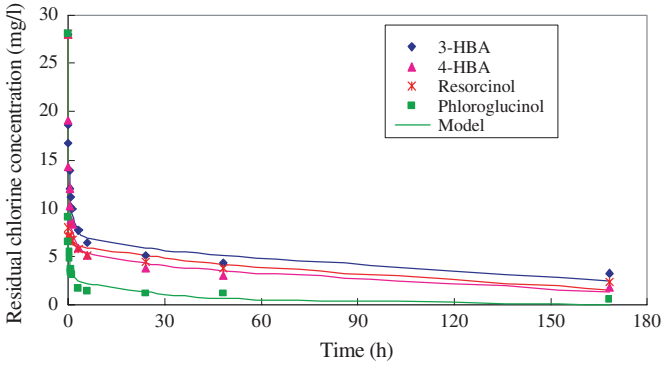

Fig. 2. The residual chlorine concentration and predictive data during the chlorination process.

3.2. TCM, CAA and DBP formation kinetics and modeling

Since the chlorine decay model was determined as the parallel second order (rapid reaction) and first order (slow reaction), the chlorine decay model could be simplified as:

$$C(t) = C_0 \cdot \left[\frac{f}{fC_0k_Rt+1} + (1-f)e^{-k_st}\right] \tag{10}$$

With the above observations, the TCM, CAA and DBP formation models could also be simplified as

$$\mathrm{TCM} = A\left\{fC_0 \cdot \left[1 - \frac{1}{fC_0k_Rt+1}\right]\right\}^n + B\left\{(1-f)C_0\left[1-e^{-k_st}\right]\right\}^m \tag{11}$$

$$\mathrm{CAA} = C\left\{fC_0 \cdot \left[1 - \frac{1}{fC_0k_Rt+1}\right]\right\}^n + D\left\{(1-f)C_0\left[1-e^{-k_st}\right]\right\}^m \tag{12}$$

$$\mathrm{DBP} = E\left\{fC_0 \cdot \left[1 - \frac{1}{fC_0k_Rt+1}\right]\right\}^n + F\left\{(1-f)C_0\left[1-e^{-k_st}\right]\right\}^m \tag{13}$$

The experimental data was inserted into the DBP formation model via Eqs. (11)–(13). Table 4 reveals correlation coefficients for TCM, CAA, and DBP formation model at different order of reaction. It was clearly observed that the parallel third and first order ($R(3,1)$) exhibits the

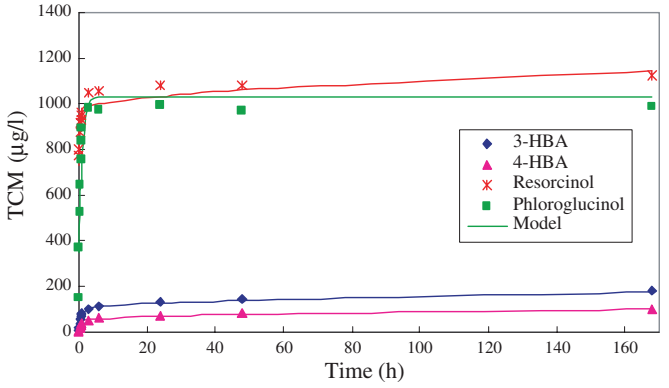

Fig. 3. The TCM formation and predictive data for model compounds during the chlorination process.

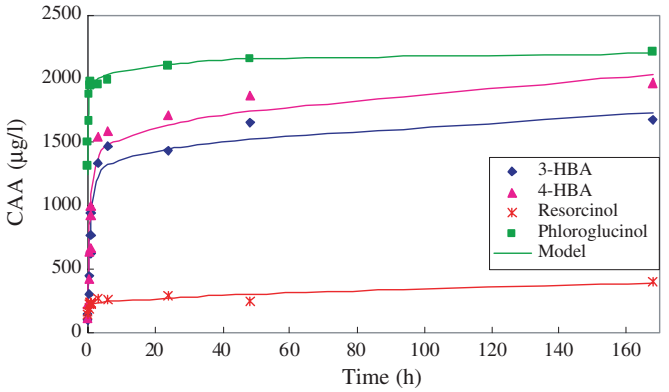

Fig. 4. The CAA formation and predictive data for model compounds during the chlorination process.

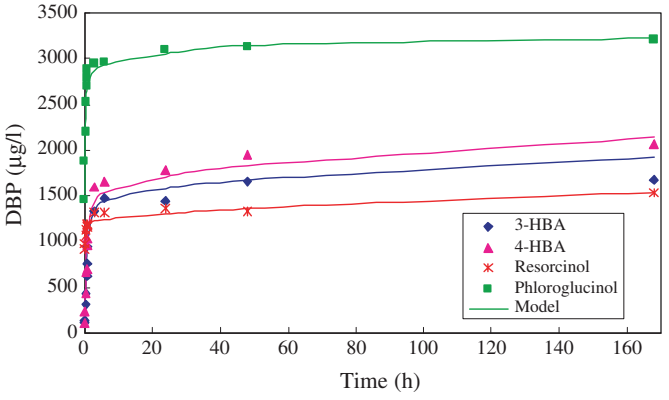

Fig. 5. The DBP formation and predictive data for model compounds during the chlorination process.

highest correlation coefficient (best fit) for the four model compounds with the exception of P for CAA model prediction. Figs. 3–5 show that the data fit the TCM, CAA and DBP formation model quite well, with correlation coefficients (0.854–0.996), which indicates that TCM, CAA and DBP formations were a function of chlorine consumption for the model compounds, which was consistent with other findings (Larson and Rockwell, 1979; Norwood et al., 1980; Boyce and Hornig, 1983).

The rate of $CHCl_3$ production and chlorine consumption varied with each model compound, however, the overall data showed two distinct patterns. The first pattern is exhibited by the *m*-dihydroxy substituted compounds and reflects a generally rapid and simultaneous exertion of both chlorine demand and TCM production (Figs. 1 and 3). The data suggests that this carbon between two hydroxyl groups should be responsible for TCM production (Larson and Rockwell, 1979; Rook, 1976).

The second pattern is demonstrated by the hydroxybenzoic acids data and indicates that TCM is a minor reaction product. The hydroxybenzoic acids pattern produces approximately 5–10-fold less chloroform formation potential than *m*-hydroxy substituted compounds (Table 3), although the chlorine demand remains relatively high. This phenomenon may be explained by the loss of a doubly activated carbon between two free hydroxyls in 3-HBA and 4-HBA.

Because of the hydroxy configuration, the molecule will probably undergo oxidative decarboxylation with substitution of chlorine in place of carboxyl (Larson and Rockwell, 1979), continuous chlorination and final cleavage could then occur at the chlorination site. The hydroxybenzoic acids pattern produces similar trichloromethane formation results. In addition to the chlorine demand for TCM production and oxidation, the evidence suggests that a portion of the chlorine demand is due to the incorporation of chlorine into non-$CHCl_3$ reaction products.

The chloroacetic acids (summation of mono-, di-, and tri-chloroacetic acid) were analyzed from the chlorination of model compounds as the disinfection by-products. In phloroglucinol, CAA formation rates also were initially rapid, corresponding with the rapid consumption of chlorine, followed by a slower, declining rate of production (Fig. 4). Above 90% CAA was generated within the first 3 h, as compared with the CAA formed at the end of reaction time—7 days. Christman et al. (1978) have noted that chlorination of resorcinol at high Cl_2/substrate ratios enhance-the accumulation of chlorinated acids, including chlorobutenedioic acid, dichloroacetic acid, and trichloroacetic acid etc. More electrophilic –OH groups of phloroglucinol have lower pK_a and higher $SUVA_{254}$ (Table 1) which yields approximately 5-fold CAA and 2-fold DBP (TCM and CAA) formation potential than resorcinol (Table 3). Further, existing –COOH substitution substances have lower pK_a values and generate more CAA as shown in Fig. 4. Therefore, the distribution of various species of chlorinated products also depends on the acidity (pK_a), $SUVA_{254}$, and characteristics of the substrate in solution (Trussell and Umphres, 1978; Peters et al., 1980; Gallard and Gunten, 2002).

The TCM (CAA) yield coefficient is defined as the ratio between the concentration (mg/l) of TCM (CAA) formed and the concentration of chlorine consumed (mg/l). Table 5 presents the TCM, CAA and DBP yield coefficients for

Table 3
TCM, CAA and DBP formation for model compounds treated by chlorine

Model compound	3-HBA	4-HBA	Resorcinol	Phloroglucinol
Initial concentration (mg-C/l)	3.0	3.0	3.0	3.0
Specific chlorine demand (mg Cl_2/mg-C)				
1 h	6.0	6.5	7.1	8.3
3 h	6.8	7.4	7.4	8.8
6 h	7.2	7.6	7.6	8.8
24 h	7.6	8.1	7.8	8.9
48 h	7.9	8.3	8.1	9.0
168 h	8.3	8.7	8.6	9.2
Specific TCM (μg TCM/mg-C)				
1 h	27	14	322	297
3 h	33	17	350	328
6 h	37	21	352	325
24 h	44	23	360	332
48 h	49	26	361	323
168 h	60	32	375	330
Specific CAA (μg CAA/mg-C)				
1 h	316	333	78	660
3 h	445	514	87	652
6 h	488	529	86	663
24 h	479	570	96	700
48 h	552	623	81	717
168 h	560	655	134	738
Specific DBP[a] *(μg DBP/mg-C)*				
1 h	343	347	400	958
3 h	477	531	437	980
6 h	525	550	437	988
24 h	523	593	456	1032
48 h	601	649	442	1041
168 h	620	687	509	1068

Chlorine dose = 28 mg/l as Cl_2.
[a] DBP = TCM + CAA.

Table 4
Correlation coefficients for TCM, CAA, and DBP formation models at different order of reaction

DBPs	Organics	R_i (n,m)[a]				
		R_1 (1,1)	R_2 (1.5,1)	R_3 (2,1)	R_4 (3,1)	R_5 (2,2)
TCM	3-HBA	0.885	0.947	0.994	0.996[b]	0.948
	4-HBA	0.585	0.918	0.979	0.991	0.913
	R	0.670	0.756	0.858	0.877	0.749
	P	0.556	0.658	0.808	0.860	0.714
CAA	3-HBA	0.724	0.817	0.927	0.958	0.858
	4-HBA	0.754	0.839	0.938	0.965	0.865
	R	0.759	0.789	0.836	0.854	0.810
	P	0.924	0.963	0.759	0.559	0.907
DBP	3-HBA	0.739	0.831	0.936	0.965	0.868
	4-HBA	0.759	0.843	0.940	0.966	0.868
	R	0.728	0.796	0.885	0.909	0.787
	P	0.790	0.902	0.997	0.959	0.954

[a] R_i (n,m) denotes the selected type of reaction order in which the n and m represent the order for rapid and slow reactions, respectively.
[b] The numerical values in the 'block' denote the correlation coefficients with the best fit representing the reaction order utilizes for model prediction.

model compounds at different order of reaction. In Table 5, it was observed that there were two distinct patterns, i.e., hydroxybenzoic acid (3-HBA and 4-HBA) and hydroxyl benzene (R and P), exhibited their respective reaction order (n,m) and DBP yield coefficient. Reckhow et al. (1990) also found that the specific DBP formation was related to the activated aromatic matter, whereas activated aromatic content was correlated with chlorine consumption. Gang et al. (2003) reported that there was no strong correlation between molecular weight and chlorine decay kinetics. With the above evidence, it suggests the amount of DBP generated be site-specific in practice, and the chlorine reacting mechanism be dependent on the nature of target compounds in principle. In this study, although these four small model compounds have their respective functional group reacted with chlorine to form DBP, the DBP formation is actually simulated by a chlorine demand model. The concept of DBP yield coefficient was useful for quantifying the difference in species production and evaluating the effect of organic precursor reduction.

3.3. Relationship between TCM and CAA

The specific chlorine demand (SCD) in Fig. 6 was defined as the ratio between the chlorine demand (mg/l) and the initial DOC concentration (mg/l) at the reaction times of 1, 3 and 168 h. In the first hour, the SCD and specific DBPFP (DBP formation potential/DOC concentration) of hydroxybenzenes are slightly higher than those of hydroxybenzoic acids, and the specific DBPFP of phloroglucinol was the highest among the four model compounds. However, no relationships between specific DBPFP and SCD of model compounds were observed based on the limited data collected at various times.

Fig. 7 shows the relationship between TCM and CAA formation potential of model compounds under different chlorination times (1, 3 and 168 h). After linear regression of experimental data, a high correlation between CAA and TCM concentration was observed. However, there are two patterns of DBP correlation based on the slopes of linear curves in Fig. 7. The hydroxybenzoic acids pattern produces a higher slope (>10) than that of the *m*-hydroxy substituted compounds (slope <1). These observations suggest that the aromatic carboxyl group has a strong correlation to the formation of CAA (Cook and Langford, 1998; Pomes et al., 1999). However, oxidative decarboxylation of dihydroxybenzoic acid was not observed which was consistent with the findings suggested by Norwood et al. (1980). Therefore, the formation of DBP is highly dependent on the nature of the organic matter.

4. Conclusions

This study shows that the four model compounds of small organic DBP precursors lead to high chlorine demand and high DBP formation potential. The chlorine degradation in model compounds with OH and/or COOH

Table 5
TCM, CAA and DBP yield coefficients for model compounds expressed as the best fit (referred to Table 4)

Organics	A	B	R^2	C	D	R^2	E	F	R^2
3-HBA	0.01	14.59	0.996	0.15	79.67	0.958	0.16	94.21	0.965
4-HBA	0.01	10.61	0.991	0.13	132.05	0.965	0.13	142.70	0.966
R	0.095	33.03	0.877	0.02	34.90	0.991	0.12	67.93	0.909
P	0.052	63.65	0.860	15.62	75.71	0.963	4.44	136.15	0.997

A: the TCM yield coefficient from the rapid chlorine consumption, B: the TCM yield coefficient from the slow chlorine consumption, C: the CAA yield coefficient from the rapid chlorine consumption, D: the CAA yield coefficient from the slow chlorine consumption, E: the DBP yield coefficient from the rapid chlorine consumption, F: the DBP yield coefficient from the slow chlorine consumption.

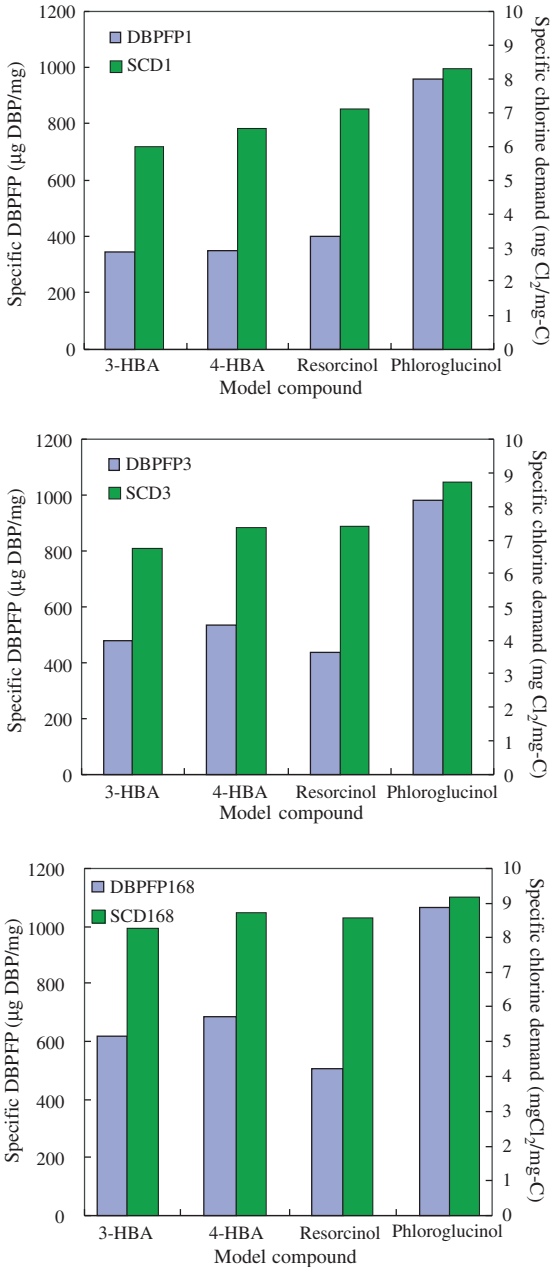

Fig. 6. Relationship between specific DBPFP and specific chlorine demand (SCD) for model compounds at reaction time of 1, 3 and 168 h, respectively.

functional groups were rapid after chlorination. It is noted that chlorination of model compounds at high Cl_2/sub-

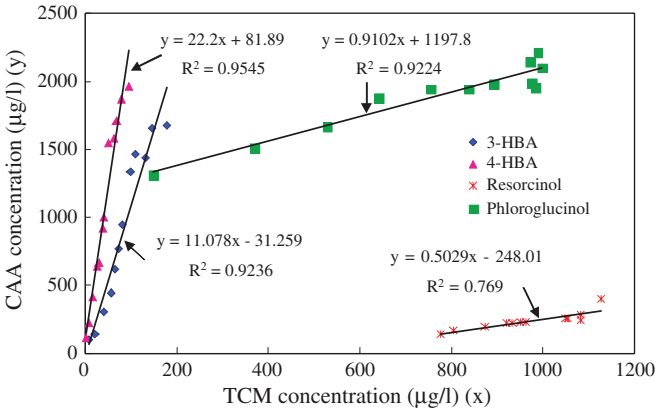

Fig. 7. Correlations between TCM and CAA concentration for model compounds.

strate ratios enhance the accumulation of chlorinated by-products including TCM and CAA. The rate of $CHCl_3$ production and chlorine consumption varied with each model compound, however, the overall data showed two distinct patterns. The first pattern exhibited by the hydroxybenzene reflects a generally rapid and simultaneous exertion of both chlorine demand and TCM production. The second pattern demonstrated by the hydroxybenzoic acids indicates that TCM is a minor reaction product. Further, the COOH substitution substances existed in the 3-HBA and 4-HBA compounds have lower pK_a values produced more CAAFP. CAA formation of model compounds shows a high correlation with TCM formation.

The parallel second and first-order reaction model for chlorine demand derived in this study is the best fit which can be utilized for TCM, CAA and DBP formation modeling. The parallel third order (rapid reaction) and first order (slow reaction) exhibits the highest correlation coefficient (best fit) for the four model compounds with the exception of P for CAA model prediction.

From this study, it may be concluded that the distribution of various species of chlorinated products depends on the acidity (pK_a), $SUVA_{254}$ and characteristics of the substrate in the solution. The formation of DBP is highly dependent upon the nature of the organic matter. Although these four small model compounds have their respective functional group reacted with chlorine to form DBP, the developed model in this investigation can be successful in predicting the DBP formation.

Acknowledgement

The authors express their thanks to the National Science Council, Taiwan, ROC (NSC 92-2211-E-038-001-) for its financial support of this study.

References

APHA, 1998. Standard Methods for the Examination of Water and Wastewater, 20th ed. American Public Health Association, Washington, DC.

Amy, G.L., Chadik, P.A., Chowdhury, Z.K., 1987. Developing models for predicting trihalomethane formation potential and kinetics. J. AWWA 79 (7), 89–97.

Boyce, S.D., Hornig, J.F., 1983. Reaction pathways of trihalomethane formation from the halogenation of dihydroxyaromatic model compounds for humic acid. Environ. Sci. Technol. 17 (4), 202–211.

Chang, E.E., Chiang, P.C., Chao, S.H., Lee, J.F., 1996. Effects of chlorination on THMs formation in raw water. J. Toxicol. Environ. Chem. 56, 211–215.

Chang, E.E., Chaing, P.C., Ko, Y.W., Lan, W.S., 2001. Characteristics of organic precursors and their relationship with disinfection by-products. Chemosphere 44 (5), 1231–1236.

Chiang, P.C., Chang, E.E., Liang, C.H., 2002. NOM characteristics and treatabilities of ozonation processes. Chemosphere 46 (4), 929–936.

Christman, R.F., Johnson, J.D., Haas, J.R., Pfaender, F.K., Liao, W.T., Norwood, D.L., Alexander, H.J., 1978. Natural and model aquatic humics: reactions with chlorine. In: Robert, L.J. et al. (Eds.), Water Chlorination: Environmental Impacts and Health Effects, vol. 2. Ann Arbor Science Publishers, Inc., Ann Arbor, MI.

Cook, R., Langford, C.H., 1998. Structural characterization of fulvic acid and humic acid using solid-state ramp-CP-MAS 13C nuclear magnetic resonance. Environ. Sci. Technol. 32 (6), 719–725.

Dotson, D., Helz, G.R., 1984Water Chlorination: Chemistry Environmental Impact and Health Effects, vol. 5. Lewis Publishers.

Engerholm, B.A., Amy, G.L., 1983. A predictive model for chloroform formation from humic acid. J. AWWA 75 (8), 418–423.

Gallard, H., Gunten, U.V., 2002. Chlorination of natural organic matter: kinetics of chlorination and of THM formation. Water Res. 36 (1), 65–74.

Gang, D.D., Segar, J.R., Clevenger, T.E., Banerji, S.K., 2002. Using chlorine demand to predict TTHM and HAA9 formation. J. AWWA 94 (10), 76–86.

Gang, D., Clevenger, T.E., Banerji, S.K., 2003. Relationship of chlorine decay and THMs formation to NOM size. J. Hazard. Mater. A 96 (1), 1–12.

Katz, E.L., 1986. The stability of turbidity in raw water and its relationship to chlorine demand. J. AWWA 78 (2), 72–75.

Korshin, G.V., Li, C.W., Benjamin, M.M., 1997. Monitoring the properties of natural organic matter through UV spectroscopy: a consistent theory. Water Res. 31 (7), 1787.

Larson, R.A., Rockwell, A.L., 1979. Chloroform and chlorophenol production by decarboxylation of natural acids during aqueous chlorination. Environ. Sci. Technol. 13 (3), 325–329.

Liang, L., Singer, P.C., 2001. Factors influencing the formation and relative distribution of haloacetic acids and trihalomethane under controlled chlorination conditions, in: Proceedings of the American Water Works Association and Water Quality Technology Conference, Tennessee, 11–15 November 2001.

Marhaba, T.F., Van, D., 2000. The variation of mass and disinfection by product formation potential of dissolved organic matter fractions along a conventional surface water treatment plant. J. Hazard Mater. 74 (3), 133–147.

Norwood, D.L., Johnson, J.D., Christman, R.F., Hass, J.R., Bobenrieth, M.R., 1980. Reactions of chlorine with selected aromatic models of aquatic humic material. Environ. Sci. Technol. 14 (2), 187–190.

Peters, C.J., Young, R.J., Perry, R., 1980. Factors influencing the formation of haloforms in the chlorination of humic substances. Environ. Sci. Technol. 14 (11), 1391–1395.

Pomes, M.L., Green, W.R., Thurman, E.M., Orem, W.H., Lerch, H.E., 1999. DBP formation of aquatic humic substances. J. AWWA 91 (3), 103–115.

Reckhow, D.A., Singer, P.C., Malcolm, R.L., 1990. Chlorination of humic materials: byproduct formation and chemical interpretations. Envrion. Sci. Technol. 24 (11), 1655–1664.

Rook, J.J., 1976. Haloforms in drinking water. J. AWWA 68 (3), 168–172.

Trussell, R.R., Umphres, M.D., 1978. The formation of trihalomethanes. J. AWWA 11, 604–612.

Sinha, S., 1999. Coagulability of NOM and its effects on formation of chlorination DBPs, Ph.D. dissertation, University of Colorado at Boulder, Colorado, 1999.

Reduction of Low-MW Model Compounds by Ozonation and O_3/UV Processes

E. E. Chang[*1]; P.C. Chiang[2]; and I Shu Li[2]

1. Department of Biochemistry, Taipei Medical University, 250 Wu-Shin Street, Taipei 110, Taiwan
2. Graduate institute of Environmental Engineering, National Taiwan University, 71 Chou-Shan Road, Taipei 106, Taiwan

* Corresponding Author

Phone: +886-2-2736-9236
FAX: +886-2-2736-9236
E-mail: **eechang@tmu.edu.tw**

Abstract: In this investigation, the low-molecular weight organic matters, such as resorcinol, phloroglucinol, and *p*-hydroxybenzoic acid, were selected as organic precursors during the ozonation and chlorination processes. The research work was focused on evaluating the effects of hydroxyl radical and ozone molecule on the reduction of organic precursors and DBP formation, and assessing the carcinogenic risk with respect to DBPFP between ozonation and O_3/UV processes. The two-stages ozone decomposition model, $[O_3]=[O_3]_0 \cdot \{F \cdot e^{-K_1 \cdot t} + (1-F) \cdot e^{-K_2 \cdot t}\}$, was developed throughout this investigation. In addition, a linear correlation between alkalinity and hydroxyl radical was found in the course of ozonation process. The destruction of organic precursors by hydroxyl radical exhibits better performance than that of by ozone. According to the risk assessment on the ozonation process, water samples treated by the O_3/UV and O_3 (pH 5) process exhibit the lower risk. Therefore, both the

O_3/UV and ozonation processes with proper operation can reduce the organic precursors thereby providing the safe drinking water.

CE Database subject headings: low-molecular organic precursors, hydroxyl radical, inhibitor, DBPFP, ozonation, O_3/UV process, risk assessment

Introduction

In conventional water treatment, the use of chlorine for disinfection is quite popular in the world. Residual chlorine in the finished water is essential to ensure the safe drinking water without microorganism contaminants in the water distribution system. However, chlorine reacts with natural organic matters (NOMs) in water generating disinfection by-products (DBP). Among these DBP, trihalomethanes (THM) and haloacetic acids (HAA) are commonly found and investigated, which have been confirmed to be carcinogenic to human beings.

The dominant organic precursors of THM formation in the water environment would be aquatic NOMs, mainly consist of humic substance (Bocye et al., 1983; Rook, 1976). However, aquatic humic substances are complicated by its uncertain chemical structure. Many studies have focused on the reaction of chlorine with simple organic species in humic substance. It had been reported that aliphatic carboxylic, hydroxybenzoic acid, phenol, and pyrrole nitrogen derivatives were the main functional groups observed in the model compounds such as resorcinol, phloroglucinol, and *p*-hydroxybenzoic acid (Richardson et al., 1999; Bocye et al., 1983). Moreover, these simple organic matters are characterized as low-molecule DBP precursors, which are not effectively removed by the traditional water treatment processes (Chang, 2005).

In order to reduce the THM and HAA formation in the chlorination process, ozonation process could be introduced prior to the chlorination process for the purpose of reducing DBP precursors. Recently, ozone and other advanced oxidation processes (AOP), such as O_3/UV process, have been investigated to reduce total organic carbon (TOC) concentration and trihalomethane formation potential (THMFP) in source water (Amirsaedari et al., 2000; Chin and Bérubé, 2005). Ozonation process is caused by its autocatalytic self-decomposition and other complex reactions including direct (ozone) and indirect (hydroxyl radical) ozone reactions, which are affected by different pH levels (Westerhoff et al., 1998; Daniel et al., 1999; Von Gunten, 2003). At high pH, ozone reacts with hydroxyl ions (OH^-) as a catalyst and yields many kinds of free radical such as $\cdot OH$, $O_2^{-\cdot}$, and $HO_2^{-\cdot}$ etc., which is also called the indirect ozonation. However, there are inhibitors including *tert*-butanol, *p*-chlorobenzoate, carbonate, and bicarbonate ions, which would limit and inhibit the hydroxyl radical formation resulted in reducing the performance of ozonation (Jan et al., 1998; Fernando, 2004). The mechanism of hydroxyl radical formation in the O_3/UV process can be expressed as follows: (Mirat and Vasistas, 1987)

$$O_3 + H_2O + h\nu \rightarrow H_2O_2 + O_2$$

$$H_2O_2 + h\nu \rightarrow 2(\cdot OH)$$

On the other hands, many studies were also conducted to investigate the disinfection by-products formation during the ozonation process including aldehyde, ketones, ketoaldehydes, carboxylic acids, aldo acids, keto acids, hydroxyl acids, esters, and alkanes (Miltner et al., 1992; Schechter and Singer, 1995; Richardson et al., 1999). Among these by-products, aldehyde is mostly concerned and investigated because of its harmful and carcinogenic to human beings.

Therefore, the objectives of this research were intended to (1) determine the

hydroxyl radical formation in ozone and O_3/UV processes, (2) evaluate the effects of hydroxyl radical and ozone molecule on the reduction of organic precursor and the removal of DBP formation concentration, (3) understand the inhibition of alkalinity on indirect ozonation process and (4) assess the difference and carcinogenic risk in DBP formation during chlorination process followed by the ozonation or O_3/UV processes. In this investigation, the low-molecular weight organic matters, such as resorcinol, phloroglucinol, and *p*-hydroxybenzoic acid, were selected as organic precursors with high DBP formation potential during the ozonation and chlorination processes.

Materials and Methods

Sample Preparation

The characteristics of the selected model compounds including resorcinol (R), phloroglucinol (P), and *p*-hydroxylbenzoic acid (PHBA) are listed in Table 1. The experimental synthetic water was composed of total organic carbon (TOC) 3.0 ± 0.3 mg/L for R, P, PHBA and were prepared with de-ionized water (Milli-Q SP). All chemicals for experimental analysis were prepared with de ionized water (Milli-Q SP).

Experimental Procedures

A glass reactor with an operation volume 5.0 L and free space 0.5 L was employed for ozonation process shown in Figure 1. It was equipped with a water jacket to maintain a constant temperature, 25 ^{o}C. Ozone was generated by bubbling oxygen in an ozone generator (Model SG-01A, Sumitomo, Tokyo, Japan).

In the ozonation experiments, ozonated water was first prepared. Five liter of water was placed in the reactor and controlled at 25 ^{o}C. Ozone gas was then introduced into the water through a bubble diffuser at bottom of the reactor for 2 hours until reaching an equilibrium concentration. The saturated ozone concentration in aqueous solution is about 18 mg/L. By adding the selected compounds of alkalinity and different pH levels changes the experimental conditions (pH 5, 7 and 9) and maintains 40 minutes reaction time to determine TOC, UV_{254}, and aldehyde concentration. An additive of alkalinity in ozonation is prepared by $NaHCO_3$ at 60 mg/L as $CaCO_3$. In the preliminary test, the selected compounds is substituted for blank water in the experiment and takes sample with specific reaction time until 40 minutes to determine concentration of alkalinity, dissolved ozone, hydroxyl radical, and hydrogen peroxide.

Chlorination process is to evaluate the chlorine demand and chlorination by-products formation in the chlorination followed by the ozonation process. A 7-days chlorine demand study was introduced by 10mg/L chlorine dose to determine the chlorine consumption, trichloromethane formation potential (THMFP), and chlorinated haloacetic acid formation potential (HAAFP). Throughout these chlorination experiments, all samples were chlorinated by 13% free chlorine (sodium hypochlorite) stock solution and add phosphate buffer (pH 7.0). Samples were chlorinated in 300 mL glass bottle and kept headspace free in the dark at room temperature (25±2 ^{o}C) until 168 hours.

Analytical Methods

Dissolved ozone concentrations were determined by the indigo method (method 4500-O_3, standard method 19th edition). The TOC analysis (O. I. Analytical) was done by the UV-persulfate technique using the infrared carbon dioxide analyzer and

calibrated with the potassium hydrogen phthalate standard. The UV_{254} were analyzed by UV-visible spectrophotometer (UV-1601, SHIMADZU) after filtering through a 0.45 μm filter. The determination of hydrogen peroxide was performed by a spectrophotometric method using DPD (N,N-diethyl-p-phenylene- diamine) (Bader, 1988). The hydroxyl free radical is analyzed by a fluorometric method (Karin, 2002). Chlorine concentration was determined by DPD (N,N-diethyl-p-phenylene- diamine) titration methods. All analyses, unless otherwise noted, were performed according to the 19th edition of the standard method (APHA, 1998).

Aldehyde including formaldehyde, acetaldehyde, glyoxal, and methyl glyoxal were derivatized to the corresponded oximes by *o*-(2,3,4,5,6 penta-fluorobenzyl)-hydroxylamine (PFBHA), which were microextracted with hexane and then analyzed in a GC/ECD system (Trace GC). THMs were analyzed in a GC/ECD system with purge and trap injection (HP 6890 series). The column in GC is a fused silica capillary column (method 6232, standard method 19th edition). HAAs were determined by a liquid-liquid extraction procedure (extracting with methyl tert-butyl ether) in a GC/ECD system, in accordance with USEPA methods 552.2.

Results and Discussion

This study of ozonation and O_3/UV processes is divided into two phases. The preliminary test was performed to investigate the effects of hydroxyl radical and alkalinity on ozonation. Further, this study was focused on ozonation (O_3/UV) of organic precursors and ozonation by-products formation.

Ozonation Process at Different pH Levels

In a batch reactor, ozonation mechanism changes at different pH levels. At pH 5 (acidic condition), ozone self-decomposition reaction is the predominant reaction. This reaction mechanism may be described by the first-order model (Slawomir et al., 1999) shown in Eq (1), and is called direct reaction. At pH 7 (neutral condition) and pH 9 (basic condition), ozone decomposes rapidly to form hydroxyl radical, and is called indirect reaction.

$$-r_{O_3} = \frac{d[O_3]}{dt} = K_D[O_3] \quad (1)$$

In Figure 2, it was observed that ozone decomposition rate increases with increasing pH. There are more hydroxyl ions (OH^-) at high pH, which promotes ozone decomposition reaction to form hydroxyl radical (Staehelin and Hoigné, 1982). At pH 5, ozone self-decomposition reaction results in high ozone concentration. Further, the highest ozone decomposition rate is at pH 9 and the order of ozone decomposition rate at different pH levels is O_3 (pH 9) > O_3 (pH 7) > O_3 (pH 5).

As shown in Figure 2, the ozone decomposition reaction may be divided into two stages at pH 5, 7 and 9. Ozone decomposes fast in the first stage (rapid reaction), but the decomposition curve trends smoothly in the second stage (slow reaction). According to the Slawomir study (1999), the theory of ozone decomposition reaction follows the first-order model, but the simple kinetics equation (Eq (1)) does not completely describe the ozone decomposition in the both stages. The kinetic constants of the both stages are obviously different as indicated by the slop of the curve shown in Figure 2. The designation K_1 and K_2 represents the kinetics constants for the rapid and slow reactions in this study, respectively. In order to mathematically model the experimental data of ozone decomposition reaction in two stages, the ozone decomposition reaction was modified as：

$$[O_3] = [O_3]_0 \cdot \{F \cdot e^{-K_1 \cdot t} + (1-F) \cdot e^{-K_2 \cdot t}\} \quad (2)$$

Where $[O_3]$ is the ozone concentration at time t (mg/L); $[O_3]_0$ is the initial ozone concentration; *F* is the fraction of the ozone consumption attributed to rapid reaction; K_1 is the first-order rate constant for the rapid reaction (min^{-1}); and, K_2 is the first-order rate constant for the slow reaction (min^{-1}). The parameters *F*, K_1, and K_2 were determined by non-linear regression software (SYSTAT 5.01). Because the almost ozone decomposes in the rapid reaction at pH 9, the difference between rapid and slow reactions is insignificant. Therefore, the fraction of the ozone consumption attributed to the rapid reaction, *F*, at pH 9 is equal to 1, which indicates that there is only K_1 rate constant existed in the modified model.

The kinetic constants for these two stages at pH 5, 7, and 9 are listed in Table 2. The higher correlation coefficients (R^2) shown in Table 2 indicate that Equation 2 expresses the ozone decomposition reaction very well. Because the ozone consumption lacks the slow reaction at pH 9, the modified model based on rapid and slow reactions shows the worse correlation coefficient (R^2) than that at pH 7. Figure 2 also presents the ozone decomposition reaction and predictive data at different pH levels, in which the dashed lines and solid lines denote the predictive data determined by the Slawomir model and modified model, respectively. As shown in Table 2, the value of K_1 increases with increasing pH value, which indicates ozone molecules decompose more rapidly in the beginning at high pH level than that at low pH level. Besides, the fraction of the ozone consumption attributed to rapid reaction, *F*, also increases with increasing pH value. The slow reaction rate shown in Figure 2 varies smoothly, but the value of K_2 also increases with increasing pH.

The formation concentration of hydroxyl radical at pH 7 and 9 is shown in Figure 3. According to Figure 3, hydroxyl radical formation is more significant at pH 9 than

pH 7, which indicates that more hydroxyl ions (OH^-) would promote more hydroxyl radical formation, and also affect ozone decomposition rate. High pH increases the ozone decomposition rate as well as the hydroxyl radical formation.

Figure 4 presents linear correlation between ozone and hydroxyl radical concentration at pH 7 and 9 at different ozonation time. Since the high OH^- concentration at pH 9 decomposes ozone completely to form more hydroxyl radical, the residual ozone concentration shown in the y-intercept (O_3) is close to zero. However, the occurrence of less hydroxyl radical formation and high ozone concentration at pH 7 resulted in producing a residual ozone concentration of 15 mg/L as shown in the y-intercept (O_3). The above evidence suggests that the main oxidants in ozonation at pH 7 are both ozone molecules and hydroxyl radicals.

Effect of Alkalinity on Ozonation

To simulate nature water quality in this experiment, alkalinity is prepared by adding $NaHCO_3$ at 60 mg/L as $CaCO_3$. Correlation of the residual alkalinity ratio and hydroxyl radical concentration during the ozonation process was shown in Figure 5. The [Alkalinity/$Alkalinity_0$] represents the ratio between the residual alkalinity and the initial alkalinity. Alkalinity at pH 7 and 9 decreases rapidly in the beginning and remains constant afterwards. It was reported that the hydroxyl radical reacts with carbonate and bicarbonate ions to lead to the alkalinity decrease at pH 7 and 9. The reducing degree of alkalinity has a strong correlation with the presence of hydroxyl radical concentration, i.e., pH 9 > pH 7. In Figure 5, alkalinity concentration decreases as hydroxyl radical increases, and maintains constant once the hydroxyl radical disappears. Therefore, the hydroxyl radical is one of the most important chemical elements affecting the alkalinity concentration during the ozonation process.

Further evidence of the effect of alkalinity on ozonation is illustrated in Figure 6, which presents the relationship between hydroxyl radical exposure and alkalinity reduction. In this study, the exposure represents the multiplication between reactant ($\cdot$OH) concentration and reaction time. The high exposure (10^{-3} mg/L $\times$ min) of hydroxyl radical leads to low alkalinity ratio, which is expressed by the empirical formula: $Y = -0.0006X + 0.8786$ (X: hydroxyl radical exposure; Y: alkalinity/alkalinity$_0$) as shown in Figure 6. Based on the empirical formula, the hydroxyl radical exposure during the ozonation process could be easily interpreted by the reduction of alkalinity.

O_3/UV Process

The photolysis of aqueous ozone (O_3/UV process), called the advanced oxidation processes (AOPs) is commonly used in water and wastewater treatment plants. Figure 7 shows the measured concentration of dissolved ozone and hydroxyl radical during the ozonation and O_3/UV processes. The O_3/UV process is operated at 30 Watts (UV light intensity). With increasing illumination time by UV light, the ozone concentration decreases rapidly and forms more hydroxyl radical in a batch reaction.

The difference in hydroxyl radical formation between indirect ozone process and O_3/UV process was clearly shown in Figure 3. The hydroxyl radical formation concentration in O_3/UV process is about 0.02 mg/L at 1 minute reaction which is much higher than that at pH 9 (0.007 mg/L). Moreover, the order of hydroxyl radical formation concentration is $\cdot$OH (O_3/UV)>$\cdot$OH (pH 9)>$\cdot$OH (pH 7), and the effect of alkalinity on hydroxyl radical formation is not significant once the pH value is held constant. Table 3 summaries the experimental data for the ozone, hydroxyl radical, and hydrogen peroxide concentration in the ozonation and O_3/UV processes.

Ozonation of Organic Precusors

Figure 8 presents the results of TOC removal efficiency in the ozonation and O_3/UV processes. The removal efficiency of TOC in the batch ozonation is below 6 %. This evidence suggests that the electrophilic character of ozone could only oxidize and destroy a small amount of the aromatic structure and unsaturated bond of organic matter without mineralizing the organic carbon to form carbon dioxide as well as the destruction by hydroxyl radical. Therefore, the reduction of these organic precursors in the ozonation process is very limited. The removal efficiency of TOC for three model compounds was found to be over 40 % in the O_3/UV process, which suggests that the higher hydroxyl radical exposures (O_3/UV) could effectively reduce the TOC concentration. The effect of alkalinity on removal of TOC was presented in Figure 8 which indicates that the natural inhibitor (alkalinity) could be negligible because of the insignificant removal efficiency of TOC in ozonation.

Organic compounds with aromatic structures or conjugated double bonds would absorb light in the ultraviolet wavelength range, commonly 254 nm (UV_{254}). SUVA is defined as a ratio between the ultraviolet absorbance (UV_{254}) and the concentration of TOC in water, i.e., UV_{254} (m^{-1})/TOC (mg/L). The change of the value of SUVA is shown in Figure 9. The most aromatic structure and conjugated double bonds are destroyed by ozone and hydroxyl radical resulting in the high UV_{254} decrease, which results in the low value of SUVA. According to an Edzwald and Van (1990) study, when the value of SUVA is smaller than 2, the composition in the sample is mostly non-humics, low hydrophilic materials, and low molecular weight. In other words, the sample contains relatively small amount of aromatic moieties. Therefore, the lower SUVA after the ozonation and O_3/UV processes indicates that ozone and hydroxyl radical can effectively destroy the aromatic structure and also reduce chlorinated

by-products formation potential (Rook, 1976). As shown in Figure 9, the difference of SUVA for the three model compounds is insignificant, because of their similar benzene structure, to which the attack of ozone following Crigee mechanism and the nonselective reactivity of hydroxyl radical result in having similar TOC and UV_{254} removal.

Formation of Ozonation by-Products

According to a Glaze study (1986), the ozonation by-products include aliphatic aldehyde, hydrogen peroxide, organic peroxide, and saturated carboxylic acid. Among them, aldehyde is the most concerned because of its harmful to human health. Aldehyde consists of formaldehyde, acetaldehyde, glyoxal, and methyl glyoxal that are commonly found and investigated in ozonation process. Figure 10 shows the formation of the ozonation by-product (aldehyde) for resorcinol at different levels of pH and alkalinity treated by the ozonation and O_3/UV processes. In this study, the principal aldehyde formation is formaldehyde, especially at high pH. For instance, at pH 9 the ratio of formaldehyde in aldehyde formation is up to 70 %, while at pH 7 is 50 %, and pH 5 is 39 % in resorcinol. This formation suggests that hydroxyl radical (formed at pH 9) could destroy organic compound and generate shorter chain by-products such as formaldehyde than ozone molecule (formed at pH 5). In general, the order of the aldehyde formation concentration is O_3 (pH 9) > O_3 (pH 7) > O_3 (pH 5). Similar observations for phloroglucinol and *p*-hydroxybenzoic acid were also found in this study.

As shown in Figure 10, the addition of alkalinity would decrease the aldehyde concentration in the indirect ozone process. The phenomenon conforms to the above-mentioned findings, which states that alkalinity could reduce hydroxyl radical

concentration to inhibit oxidation reaction and result in less aldehyde formation. In the O_3/UV process, the higher hydroxyl radical exposure reduces TOC by 40 % and further oxidization results in lowering aldehyde concentration to 2 μg/L. In summary, the order of aldehyde formation with respect to the ozonation process is O_3 (pH 9; Alk=0) > O_3 (pH 9; Alk =60) > O_3 (pH 7; Alk=0) > O_3 (pH 7; Alk=60) > O_3 (pH 5) > O_3/UV. It was thus concluded that the ozone and hydroxyl radical could break the aromatic structure and destroy organic precursors in the ozonation process.

Formation of Chlorination by-Products

Among the chlorine demands for these three model compounds, resorcinol is the lowest. It could be explained that the two activating –OH groups in resorcinol are situated at vicinal position to stabilize the transition state of the reaction through the donation of electron density. Therefore, the electrophilic addition and substitution reactions by chlorine easily occurs, which leads to low chlorine demand (Boyce and Hornig, 1983). However, the symmetric structure for phloroglucinol flanked with three –OH groups may form a resonance-stabilized intermediate, which could confine the hydrolysis and decarboxylation with C–C bond cleavage on the aromatic structure and result in more chlorine demand (Chang et al., 2006). For *p*-hydroxybenzoic acid, the moderately deactivating group (–COOH) would lower the electron density on aromatic structure, but not for the symmetric structure such as phloroglucinol. Therefore, the order of chlorine demand is strictly depended upon the physical and chemical property of the model compounds and followed by P > PHBA > R. In this investigation, the destruction of organic precursors by hydroxyl radical results in the higher chlorine consumption than ozone molecular during the chlorination process,

and the inhibition of alkalinity would increase the chlorine consumption. The detailed experimental data are listed in Table 4.

Chlorination of natural organic matter results in the formation of various chlorination disinfection by-products (DBP). Among all DBP, the THM and HAA are considered as the principal disinfection by-products which cause public health concerns for safe drinking water. The comparison of specific DBP formation potentials (DBPFP) and DBP yield coefficient (*D*) between the ozonation and O_3/UV processes are also shown in Table 4. As mentioned earlier, the ozone and hydroxyl radical could change the properties in the three model compounds by destroying the aromatic structure, which leads to more reduction of chlorine demand and DBPFP. In the O_3/UV process, the 40% TOC reduction performed by the hydroxyl radical would also enhance the reduction of DBPFP. Therefore, the reduction of DBPFP by the O_3/UV process is much higher than that by the ozonation process. The relationship between DBP formation and chlorine demand could be evaluated by the DBP yield coefficient (*D*). Table 4 shows the values of *D* in different processes. The order of *D* is similar to the order of DBPFP as O_3/UV system < < ozonation.

Risk Assessment between Ozonation and O_3/UV Process

In this study, it was found that ozonation of organic precursors is successful in reducing the chlorination by products, especially at pH 5 for the ozonation and the O_3/UV processes. However, it is noted that there are other DBPs such as aldehyde would be occurred in the course of ozonation. Therefore, it is required to have a further risk assessment to determine if the ozonation process is appropriate based on the carcinogenic DBPs concerns. The THMs, HAAs and aldehyde are considered

carcinogenic substances by USEPA and its carcinogenic risk can be determined by the following equation:

$$Carcinogenic\ \ risk = CDI \times SF \tag{4}$$

Where chronic daily intake (CDI) is the quantity of ingestion (mg/kg-day), and slope factor (SF) is the carcinogenic slope factor $(mg/kg\text{-}day)^{-1}$. The value of CDI is calculated based on the assumption that one person drinks 2 liters of water per day, with an average weight of 70 kilogram. The value of SF is varied with different carcinogenic substances, which represents the slope of diagram of dose-response relationship. According to toxicity data of DBP and aldehyde proposed by USEPA, the value of SF is 4.4×10^{-3} for chloroform, 4×10^{-3} for HAA, and 0.08 for formaldehyde. The final carcinogenic risk is assumed to be the sum of these three carcinogenic substances and listed in Table 5.

According to Table 5, the lowest carcinogenic risk is in the O_3/UV process and the order of carcinogenic risk is O_3/UV << O_3 (pH 5) < O_3 (pH 7; Alk=60) < O_3 (pH 7; Alk=0) < O_3 (pH 9; Alk=60) < O_3 (pH 9; Alk=0). Therefore, both the ozonation with proper operation and O_3/UV processes can reduce the organic precursors and provide safer drinking water. Further, the O_3/UV process is considered as the appropriate treatment technology for reducing DBPs and aldehyde formation under the conditions operated in this investigation.

Conclusions

The ozone decomposition mechanism changes at different pH levels. There are more hydroxyl ions (OH^-) at high pH, which promotes ozone decomposition reaction to form hydroxyl radical. A modified ozonation decomposition model, $[O_3] = [O_3]_0 \cdot \{F \cdot e^{-K_1 \cdot t} + (1-F) \cdot e^{-K_2 \cdot t}\}$, is developed in this investigation. The model can

predict the ozone decomposition reaction more accurately than that by the first order model (Slawomir et al., 1999).

The fluorescence method was introduced to analyze hydroxyl radical level in the indirect ozone process and O_3/UV processes. It was observed that the amount of hydroxyl radical exposure in the O_3/UV process was much higher than in the indirect ozone process. In the presence of alkalinity, the inhibition is significant and the linear correlation between alkalinity and hydroxyl radical exposure was revealed which might have insight into the effect of alkalinity on inhibition of hydroxyl radical. Consequently, more reduction of TOC and DBP in the O_3/UV process would be observed.

In ozonation, the chlorine demand increases with decreasing pH and increasing alkalinity. It is concluded that hydroxyl radical can more strongly destroy the organic precursors resulted in reducing chlorine consumption than ozone molecule. Moreover, the destruction of organic precursors by hydroxyl radical exhibits higher DBP formation potential than that by ozone molecule, and the inhibition of alkalinity in hydroxyl radical results in less DBP formation. In the ozonation process, the aldehyde concentration increases with increasing pH, which indicates that the hydroxyl radical increases both chlorination by-products and aldehyde formation. According to the risk assessment in ozonation process, water samples treated by the O_3/UV and O_3 (pH 5) process exhibit the lower risk. Therefore, both the ozonation and O_3/UV processes with proper operation can reduce the organic precursors thereby providing the safe drinking water.

Acknowledgments

The authors express their thanks to the National Science Council, Taiwan, ROC (NSC

94-2211-E-038-001-) for its financial support of this study

References

Amirsaedari, Y., Yu, Q., and Williams, P. (2000). "Effect of ozonation and UV irradiation with direct filtration and disinfection by-product precursors in drinking water treatment." *Environmental Science and Technology*, 22, 1015-1023.

Bader, H., Sturzenegger, V., and Hoigne, J. (1988). "Photometric method for the determination of low concentration of hydrogen peroxide by the peroxidase catalyzed oxidative of N,N-Diethyl-p-phenylenediamine (DPD)." *Water Research,* 22(9), 1109-1115.

Boyce, S.D., and Horning, J. F. (1983). "Reaction pathways of trihalomethane formation from the halogenation of dihydroxyaromatic model compounds for hunic acid." *Environmental Engineering,* 124(1), 16-24.

Chang, E.E., Chiang, P.C., Tang, W.Y., Chao, S.H., and Hsing, H.J. (2005). "Effects of polyelectrolytes on reduction of model compounds via coagulation." *J. Chemosphere*, 58, 1141-1150.

Chang, E.E., Chiang, P.C., Chao, S.H., and Lin, Y. L. (2006). "Relationship between chlorine consumption and chlorination by-products formation for model compounds." *J. Chemosphere* (in press)

Chin, A., and Bérubé, P.R. (2005). "Removal of disinfection by-product precursors with ozone-UV advanced oxidation process." *Water Research*, 39, 2136-3144.

Daniel, U., Peter, M. H., Graham, A.G., Dennis, M. and Franklyn, S. (1999). "Modeling enhanced coagulation to improve ozone disinfection." *J. Am. Water Works Assoc.*, 91(3), 59-73.

Edzwald, J.K. and Tobiason, J.E. (1999). "Enhanced coagulation: US requirements and a broader view." *Water Science and Technology*, 40(9), 55-62.

Fernando, J. and Beltrán (2004). “Ozone Reaction Kinetics for Water and Wastewater Systems” Lewis Publishers, New York Washington, D.C.

Glaze, W. H. (1986). "Chemistry of Ozone, By-products, and Their Health Effects, In Ozonation: Recent Advances and Research Needs.” *AWWARF*, Denver, Colo., Jun.

Jans, U. and Hoigne, J. (1998). “Activated carbon black catalyzed transformation of aqueous ozone into OH-radicals.” *Ozone Science &. Engineering*, 20, 67-89.

Karin, T. and Stefan, O. (2002). “Detection of hydroxyl radicals produced by wood-decomposing fungi.” *FEMS Microbiology Ecology,* 40, 13-20.

Miltner, R. J., Shukairy, H. M., and Summers, R. S. (1992). “Disinfection by-products formation and control by ozonation and biotreatment.” *J. Am. Water Works Assoc.* 11, 83.

Richardson, S.D., Thruston, Jr A.D., Caughran, T.V., Chen, P.H., Collette, T.W., and Floyd, T.L. (1999). “Identification of new ozone disinfection by-products in drink water.) *Environmental Science & Technoogy*, 33, 3368-3377.

Rook J. J. (1976). “Haloforms in drinking water.” *J. Am. Water Works Assoc.* 68 (3) 168.

Schechter, D. S., and Singer, P. (1995), “Formation of aldehydes during ozonation.” *Ozone Science &. Engineering* 17, 45-68.

Slawomir, W. H., William, D. B., and Leo, C. F. (1999). “Variability of ozone reaction kinetics in batch and continuous flow reactors.” *Water Research*, 33, 2130-2318.

Staehelin, S. and Hoigné, J. (1982). “Decomposition of ozone in water: rate of initiation by hydroxide ions and hydrogen peroxide.” *Environmental Science & Technology*, 16, 666-681.

von Gunten, U. (2003). “Ozonation of drinking water: Part I. Oxidation Kinetics and

product formation." *Water Research*, l.37, 1443-1467.

Westerhoff, P., Alken G.,, Amy, G., and Debroux, J. (1998). "Relactionships between the structure of natural organic matter and its reactivity towards molecular ozone and hydroxyl radicals." *Water Research*, 33, 2265-2276.

Website: http://www.epa.gov/iris/index.html.

Website: http://toxnet.nim.nih.gov

Table 1 Summary of the physical/chemical properties for organic compounds

Organic Compounds	Resorcinol	Phloroglucinol	*p*-hydroxybenzoic acid
Molecular Formula	$C_6H_6O_2$	$C_6H_6O_3$	$C_7H_6O_3$
Molecular Weight	110.11	126.11	138.12
Structure	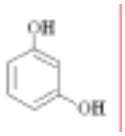	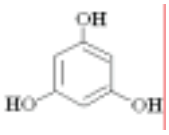	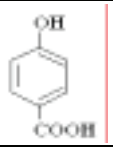
Boiling Point (℃)	280	-	211
Melting Point (℃)	177	218.5	214.5
Density/Specific Gravity	1.27	1.46	1.44
Dissociation Constants	pK = 9.30	pK = 8.45	pK = 4.54
Octanol Water Partition Coefficient	pK_{ow} = 0.80	pK_{ow} = 0.16	pK_{ow} = 1.58
pH	5.2	-	2.4
Solubility	0.717 g/L	10.6 g/L	5 g/L
Vapor Density (air = 1)	3.79	4.3	4.8
Vapor Pressure (mmHg)	4.89×10^{-4}	1.6×10^{-4}	8.2×10^{-5}
Produced Company	ACROS	ACROS	ACROS

Reference: U.S. National Library of Medicine. http://toxnet.nim.nih.gov

Table 2 Ozone decomposition constants for parallel first-order reaction at different pH levels

pH	*F*	K_1	K_2	R^2
5	0.534	0.005	0.158	0.999
7	0.787	0.256	0.011	0.999
9	1	2.643	-	0.963

Table 3 Summary experimental data for ozonation and O_3/UV processes

	ozonation					**O_3/UV**
	[a]Alkalinity = 0			**[a]Alkalinity = 60**		**pH 5**
	pH 5	**pH 7**	**pH 9**	**pH 7**	**pH 9**	
[b]ozone exposure	425.4	194.2	154.7	17.8	5.3	97.5
[c]·OH exposure	0	2.6	0.9	18.7	14.5	77.9
[d]H_2O_2 (Maximum conc.)	14.1	1.1	-	1.4	-	-

[a] unit of alkalinity ：mg/L as $CaCO_3$

[b] unit of ozone exposure: mg/L×min

[c] unit of ·OH exposure: 10^{-3} mg/L×min

[d] unit of H_2O_2 concentration: μM (Analysis method(Bader, et al., 1988))

Table 4 Comparisons of chlorine consumption, specific DBP, and DBP yield coefficient for three model compounds

Organic	Ozonation					O_3/UV
	Alkalinity = 0			Alkalinity = 60		pH 5
	pH 5	pH 7	pH 9	pH 7	pH 9	
	[a]Chlorine consumption (mg Cl_2/mg C)					
R	2.0	1.5	1.3	1.6	1.3	5.2
P	2.0	1.5	1.3	1.6	1.3	5.1
PHBA	2.0	1.5	1.2	1.6	1.3	5.2
	[b]Specific DBP (μg DBP /mg C)					
R	23.6	98.6	220	88.5	154	7.3
P	18.2	98	232	85	170	7.2
PHBA	22.3	107	247	91.9	165	10.7
	[c]*D* (μg DBP /mg Cl_2)					
R	12.4	64.1	173.9	53.4	115	1.4
P	8.8	63.3	190	52.2	130	1.4
PHBA	11.2	69.7	201	56.3	124	2.1

[a]Chlorine consumption (mg Cl_2/mg C) = chlorine consumption after 168 hours / Residual TOC (mg/L) after ozonation

[b]Specific DBPFP: DBPFP (μg/L) / Residual TOC (mg/L) after ozonation

[c]D: DBPFP (μg/L) / Cl_2 demand (mg/L) after 168 hours

Table 5 The carcinogenic risk for THM, HAA and aldehyde in different treatment processes

Organics		Carcinogenic risk					
		Ozonation					O_3/UV
		Alkalinity = 0			Alkalinity = 60		pH 5
		pH 5	pH 7	pH 9	pH 7	pH 9	
R	THM	7×10^{-7}	4×10^{-6}	1×10^{-5}	3×10^{-6}	8×10^{-6}	6×10^{-7}
	HAA	2×10^{-7}	1×10^{-6}	1×10^{-5}	9×10^{-7}	5×10^{-6}	6×10^{-9}
	aldehyde	3×10^{-6}	7×10^{-6}	1×10^{-5}	5×10^{-6}	6×10^{-6}	7×10^{-7}
	Risk	$\mathbf{4\times10^{-6}}$	$\mathbf{1\times10^{-5}}$	$\mathbf{3\times10^{-5}}$	$\mathbf{9\times10^{-6}}$	$\mathbf{2\times10^{-5}}$	$\mathbf{1\times10^{-6}}$
P	THM	1×10^{-7}	3×10^{-6}	2×10^{-5}	2×10^{-6}	1×10^{-5}	4×10^{-7}
	HAA	2×10^{-7}	1×10^{-6}	1×10^{-5}	9×10^{-7}	5×10^{-6}	6×10^{-9}
	aldehyde	6×10^{-6}	7×10^{-6}	9×10^{-6}	5×10^{-6}	5×10^{-6}	5×10^{-7}
	Risk	$\mathbf{6\times10^{-6}}$	$\mathbf{1\times10^{-5}}$	$\mathbf{4\times10^{-5}}$	$\mathbf{8\times10^{-6}}$	$\mathbf{2\times10^{-5}}$	$\mathbf{1\times10^{-6}}$
PHBA	THM	1×10^{-6}	3×10^{-6}	2×10^{-5}	2×10^{-6}	8×10^{-6}	6×10^{-7}
	HAA	3×10^{-7}	3×10^{-6}	1×10^{-5}	2×10^{-6}	6×10^{-6}	3×10^{-8}
	aldehyde	6×10^{-6}	7×10^{-6}	1×10^{-5}	5×10^{-6}	5×10^{-6}	5×10^{-7}
	Risk	$\mathbf{7\times10^{-6}}$	$\mathbf{1\times10^{-5}}$	$\mathbf{4\times10^{-5}}$	$\mathbf{9\times10^{-5}}$	$\mathbf{2\times10^{-5}}$	$\mathbf{1\times10^{-6}}$

Reference : www.epa.gov/iris/index.html.

Figure Captions

Fig. 1. The experimental apparatus of the ozone batch reactor

Fig. 2. The ozone decomposition and predictive decay model at different pH levels

Fig. 3. The difference in hydroxyl radical between ozonation and O_3/UV processes

Fig. 4. The relationship between ozone and hydroxyl radical concentration at pH 7 and 9 in the ozonation process

Fig. 5. Correlation of residual alkalinity ratio and hydroxyl radical concentration during the ozonation process

Fig. 6. The correlation between hydroxyl radical exposure and residual alkalinity ratio at pH 9

Fig. 7. The measured concentration of dissolved ozone and hydroxyl radical during the O_3/UV process

Fig. 8. Removal of TOC at various levels of pH and alkalinity for three model compounds treated by the ozonation and O_3/UV processes

Fig. 9. SUVA measured at various levels of pH and alkalinity for model compounds treated by the ozonation and O_3/UV processes

Fig. 10. The formation of aldehyde for resorcinol at various levels of pH and alkalinity treated by the ozonation and O_3/UV processes

Fig. 1.

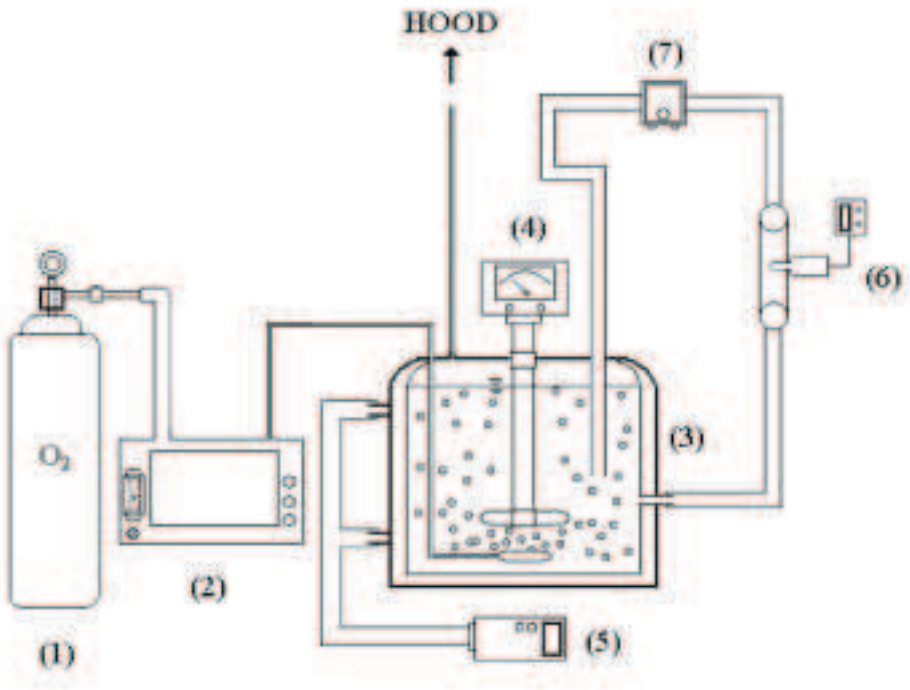

(1) oxygen cylinder

(2) Ozone generator

(3) Batch reactor

(4) 6-bladed-disk turbine

(5) Thermostat

(6) pH meter

(7) Pump

Fig. 2.

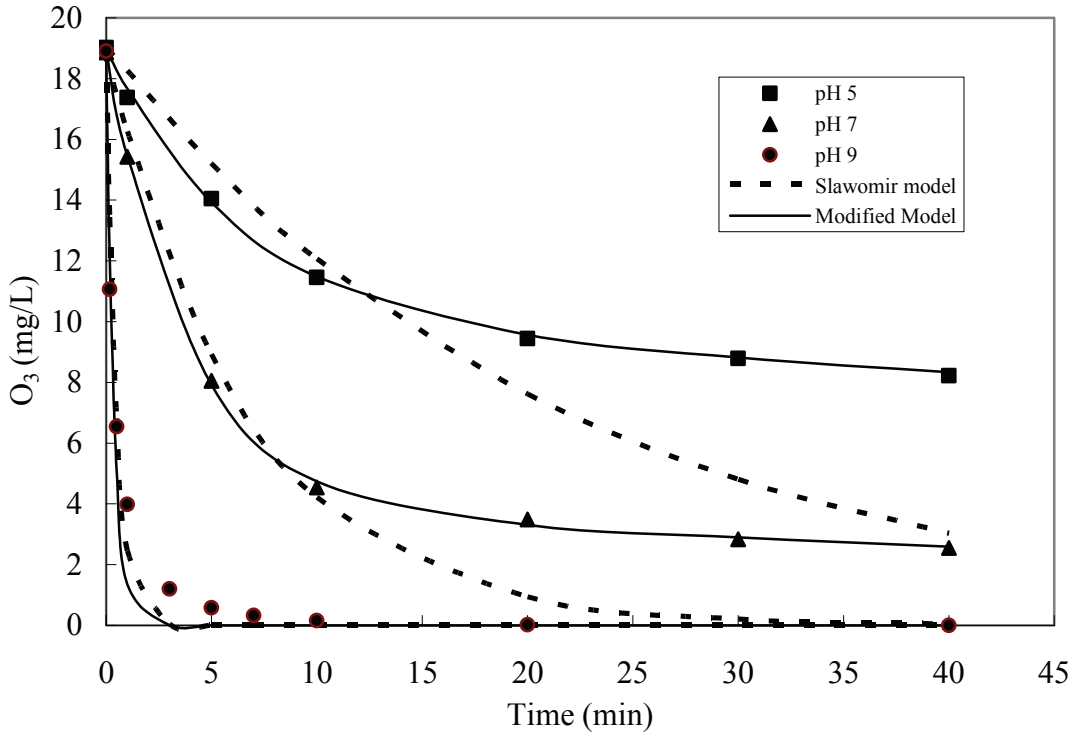
20
18
16
14
12
10
8
6
4
2
0
O_3 (mg/L)
0
5
10
15
20
25
30
35
40
45
Time (min)
pH 5
pH 7
pH 9
Slawomir model
Modified Model

Fig. 3.

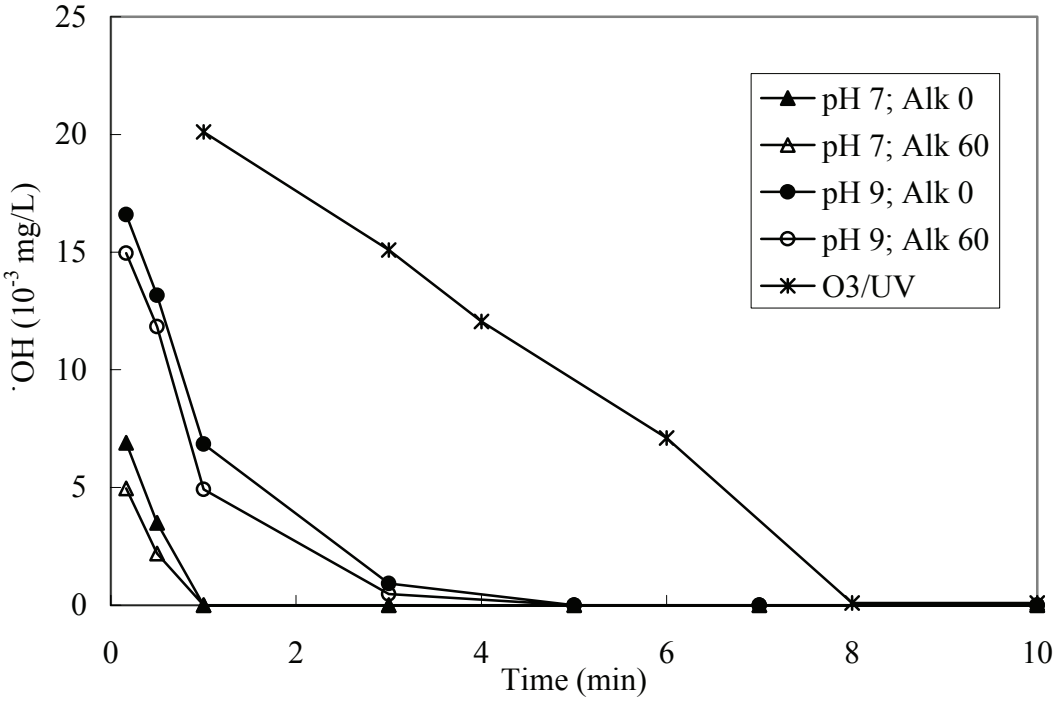
25
20
15
10
5
0
·OH (10-3 mg/L)
0
2
4
6
8
10
Time (min)
pH 7; Alk 0
pH 7; Alk 60
pH 9; Alk 0
pH 9; Alk 60
O3/UV

Fig. 4.

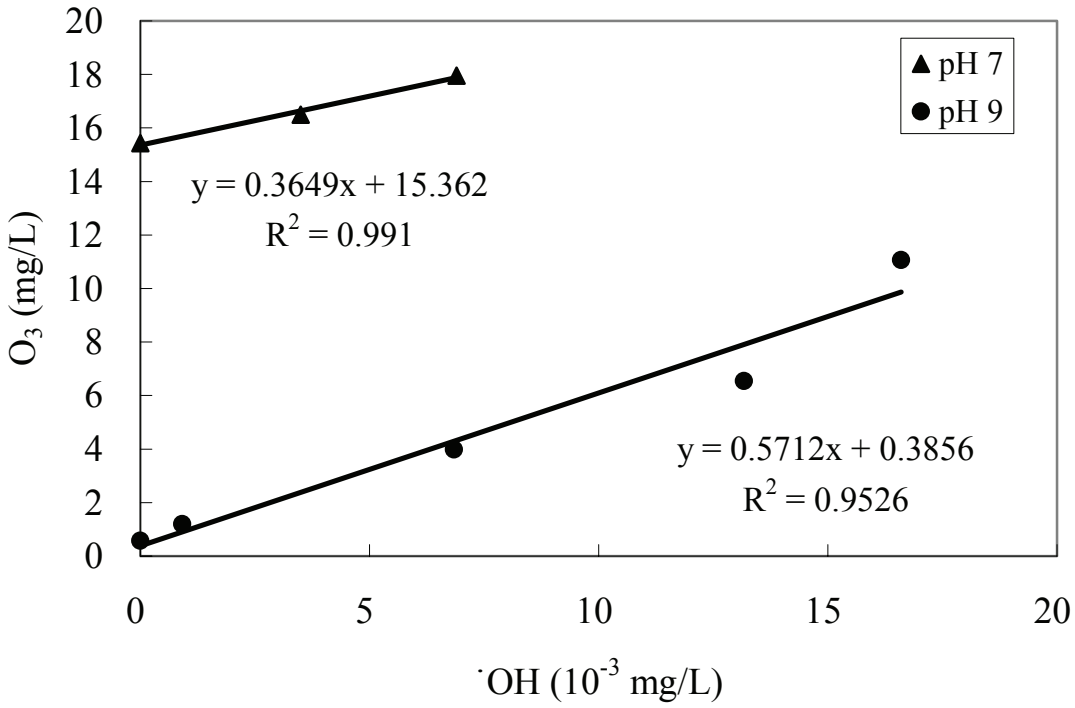
20
18
16
14
12
10
8
6
4
2
0
0
5
10
15
20
O3 (mg/L)
·OH (10-3 mg/L)
pH 7
pH 9
y = 0.3649x + 15.362
R2 = 0.991
y = 0.5712x + 0.3856
R2 = 0.9526

Fig. 5.

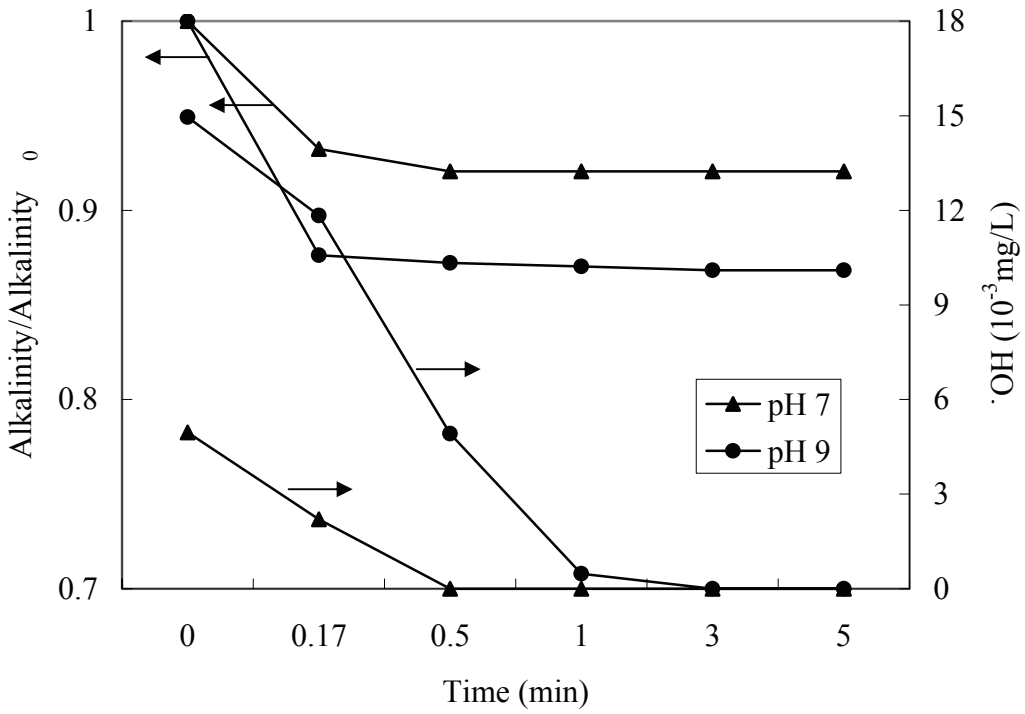
1
0.9
0.8
0.7
Alkalinity/Alkalinity 0
18
15
12
9
6
3
0
·OH (10-3mg/L)
pH 7
pH 9
0
0.17
0.5
1
3
5
Time (min)

Fig. 6.

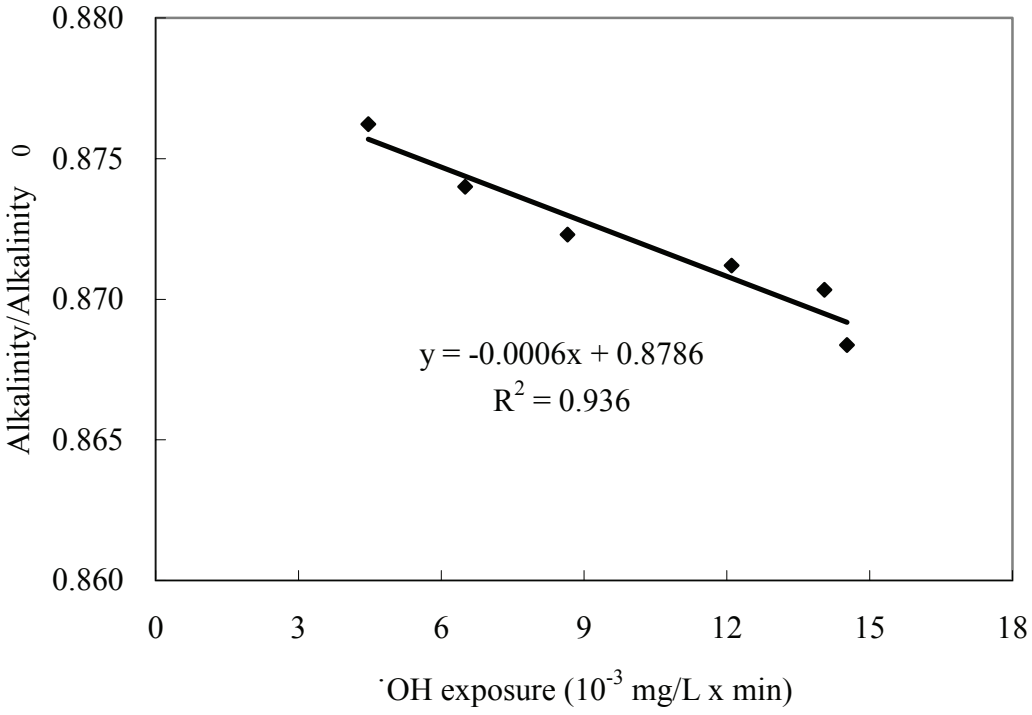
0.880
0.875
0.870
0.865
0.860
Alkalinity/Alkalinity 0
y = -0.0006x + 0.8786
R2 = 0.936
0
3
6
9
12
15
18
·OH exposure (10-3 mg/L x min)

Fig. 7.

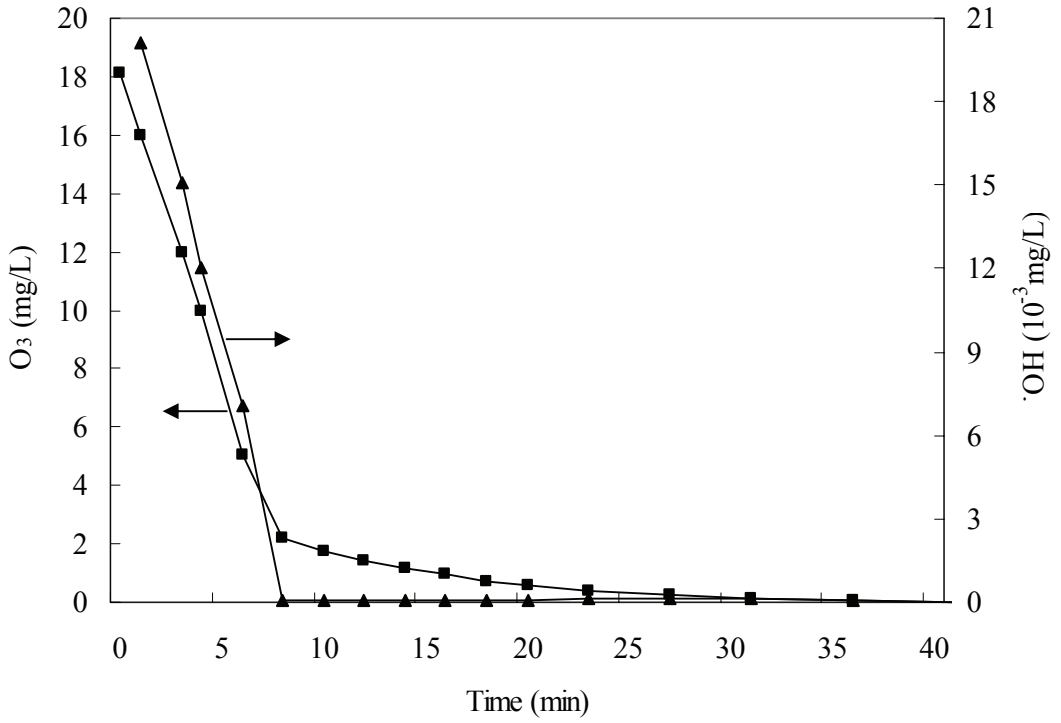
20
18
16
14
12
10
8
6
4
2
0
O3 (mg/L)
21
18
15
12
9
6
3
0
·OH (10-3 mg/L)
0
5
10
15
20
25
30
35
40
Time (min)

Fig. 8.

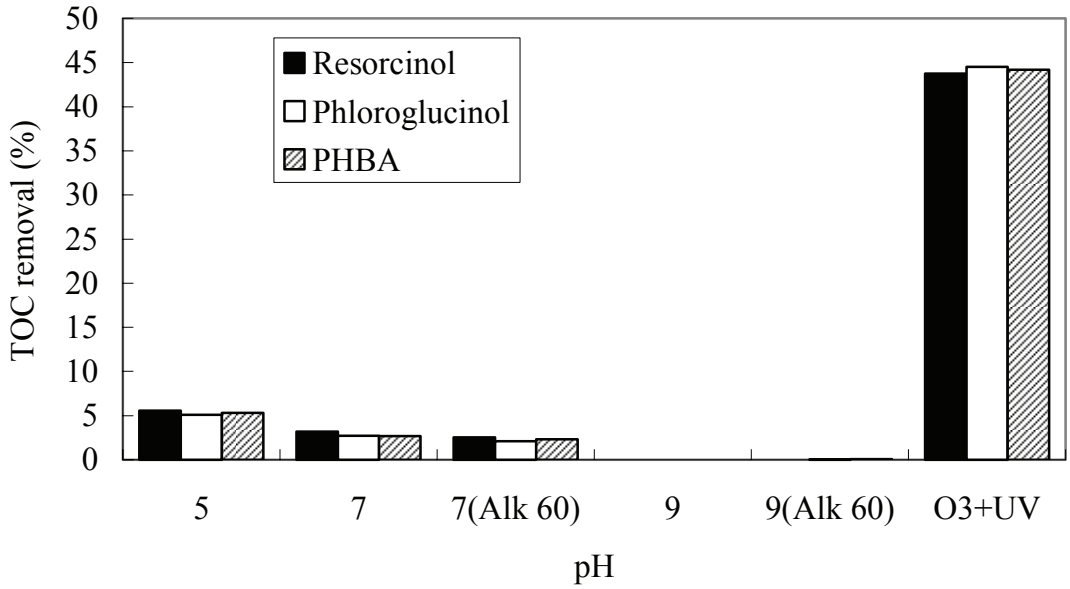
50
45
40
35
30
25
20
15
10
5
0
TOC removal (%)
Resorcinol
Phloroglucinol
PHBA
5
7
7(Alk 60)
9
9(Alk 60)
O3+UV
pH

Fig. 9.

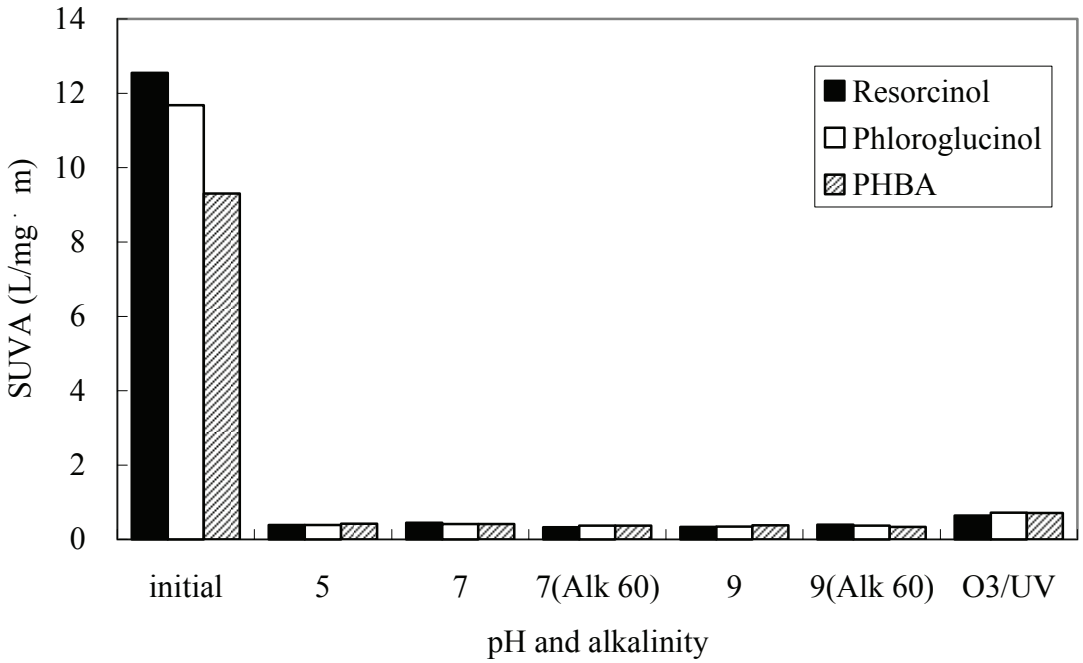
14
12
10
8
6
4
2
0
SUVA (L/mg · m)
Resorcinol
Phloroglucinol
PHBA
initial
5
7
7(Alk 60)
9
9(Alk 60)
O3/UV
pH and alkalinity

Fig. 10.

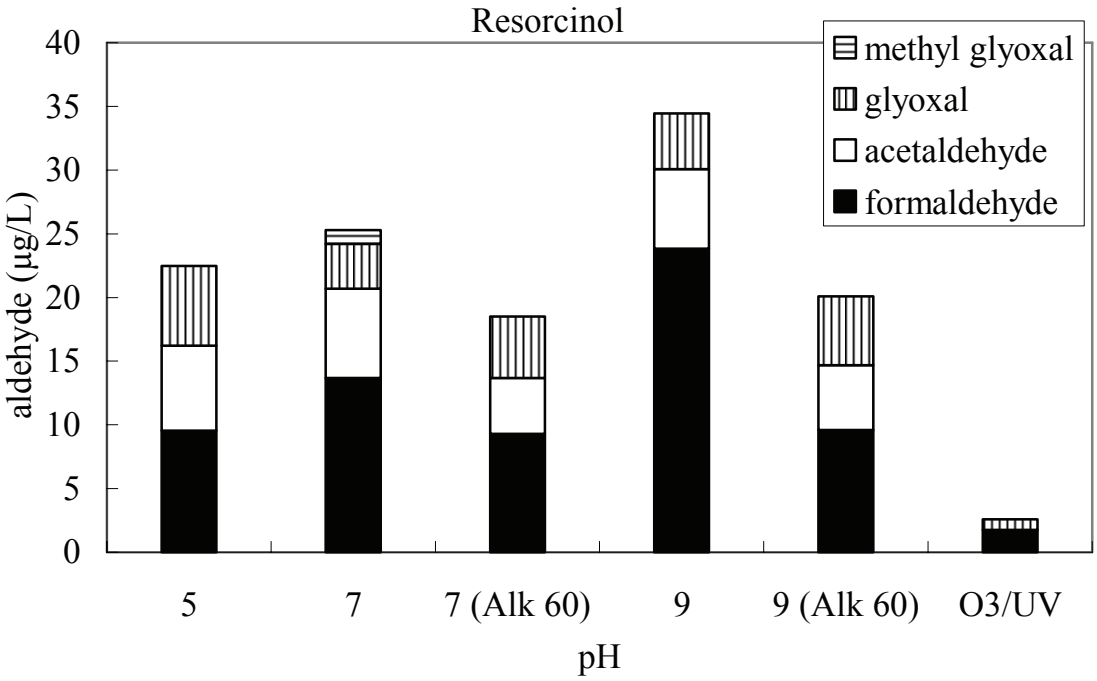
Resorcinol
methyl glyoxal
glyoxal
acetaldehyde
formaldehyde
aldehyde (µg/L)
40
35
30
25
20
15
10
5
0
5
7
7 (Alk 60)
9
9 (Alk 60)
O3/UV
pH